Pergamon

Progress in Oceanography 41 (1998) 1–68

Progress in Oceanography

"Great Salinity Anomalies" in the North Atlantic

Igor M. Belkin[a,b,*], Sydney Levitus[a], John Antonov[a,c], Svend-Aage Malmberg[d]

[a]*Ocean Climate Laboratory, National Oceanographic Data Center, National Oceanic and Atmospheric Administration, E /OC5, 1315 East-West Highway, Silver Spring, MD 20910-3282, USA*
[b]*Shirshov Institute of Oceanology, Russian Academy of Sciences, 36 Nakhimovsky Prospekt, Moscow 117851, Russia*
[c]*University Corporation for Atmospheric Research, P.O. Box 3000, Boulder, CO 80307, USA*
[d]*Marine Research Institute, Skúlagata 4, P.O. Box 1390, 121, Reykjavik, Iceland*

Abstract

We revisited the "Great Salinity Anomaly" of the 1970s (GSA'70s; Dickson et al., 1988) and documented the newly identified "Great Salinity Anomaly" of the 1980s (hence termed GSA'80s), both propagated around the North Atlantic in a similar fashion. The advective mechanism, initially proposed to explain the observed sequence of low-salinity, low-temperature events during the GSA'70s, apparently holds also for the GSA'80s. The latter was successively observed in the West Greenland Current (1982), the Labrador Current (1983), the Flemish Pass (1984), near the Charlie-Gibbs Fracture Zone (1984–1985), in the Rockall Channel (1985), south of Iceland (1985–1988), in the North Sea (1986–1987), Norwegian Sea (1987–1988), Barents Sea (1988–1989) and Iceland Sea (1989–1990). The advection speed of the GSA'80s seems to be greater than the one of the GSA'70s: The 1980s anomaly reached the Barents Sea 6 to 7 years after peaking in the West Greenland Current, while the 1970s anomaly traveled the same route in 8 to 10 years. These anomalies, however, seem to be of different origin. The GSA'70s was apparently boosted remotely, by a freshwater/sea ice pulse from the Arctic via Fram Strait. Consequently, the GSA'70s was accompanied by a large sea ice extent anomaly in the Greenland and Iceland Seas, which propagated into the Labrador Sea. In contrast, the GSA'80s was likely formed locally, in the Labrador Sea/Baffin Bay mainly because of the extremely severe winters of the early 1980s, but supplemented with a possible contribution of the Arctic freshwater outflow via the Canadian Archipelago (facilitated by strong northerly winds) which would have enhanced stability and ice formation. This anomaly was also associated with a positive sea ice extent anomaly in the Labrador Sea/Baffin Bay which,

* Corresponding author. Present address: Graduate School of Oceanography, University of Rhode Island, 215 South Ferry Road, Narragansett, RI 02882, USA.

PII: S0079-6611(98)00015-9

however, had no upstream precursor in the Greenland Sea. Thus the GSAs are not necessarily caused solely by an increased export of freshwater and sea ice from the Arctic via Fram Strait. These results are corroborated by the early 1990s data when a new fresh, cold anomaly was formed in the Labrador Sea and accompanied by a large positive sea ice extent anomaly. The harsh winters of the early 1990s were, however, confined to the Labrador Sea/Baffin Bay area while the atmospheric and oceanic conditions in the Greenland, Iceland, and Irminger Seas were normal. The Labrador Sea/Baffin Bay area appears therefore to play a key role in formation of GSAs as well as in propagation of the GSAs formed upstream. A likely contribution of the enhanced Canadian Archipelago freshwater outflow to the GSA formation also seems to be significant. *Two major modes* of the GSA origin are thus identified, *remote* (generated by an enhanced Arctic Ocean freshwater export via either Fram Strait or the Canadian Archipelago) and *local* (resulting from severe winters in the Labrador Sea/Baffin Bay). Both modes should be taken into account to model decadal variability of the coupled ocean–ice-atmosphere system in the North Atlantic/Arctic Basin.

Contents

1. Introduction

The "Great Salinity Anomaly" of 1968–1982 (GSA'70s hereafter) was one of the most remarkable and well-documented decadal-scale events of the 20th century in the North Atlantic. According to Dickson et al. (1988), minima in salinity (and temperature) time series observed successively around the northern North Atlantic during this period could be accounted for by advection of a fresh (and cold) anomaly along main ocean currents as shown in Fig. 1 (Ellett and Blindheim, 1992, Fig. 6). The anomaly was first observed in 1965–1971 northeast of Iceland (Malmberg, 1969, 1973), then in 1969–70 in the West Greenland Current (Buch, 1985; Buch and Stein, 1987), in 1971–72 near Labrador (Trites, 1982) and Newfoundland (Keeley, 1982), in 1972 at Ocean Weather Station (OWS) "Bravo" in the Labrador Sea (Lazier, 1980), in 1974–1975 at OWS "C" ("Charlie") near the Charlie-Gibbs Fracture Zone (Dickson et al., 1988), in 1975 in the Rockall Channel (Ellett, 1979; Ellett and MacDougall, 1983), in 1976 in the Faroe-Shetland Channel (Dooley et al., 1984; Martin et al., 1984) and south of Iceland (Malmberg, 1984a, 1985), in 1977–78 in the Norwegian Sea (Gammelsrød and Holm, 1984), in 1978–1979 south of Spitsbergen (Dickson and Blindheim, 1984), and eventually back to the Greenland and Iceland Seas in 1981–83 (Farrelly et al., 1985; Malmberg, 1986).

The ***advective*** explanation of salinity changes recorded in various basins of the North Atlantic was suggested first by Ellett (1980, 1982), Lazier (1980), Taylor and Stephens (1980), Taylor (1983). Northward propagation of anomalous TS-conditions (minima in both T and S) in the Norwegian Atlantic Current was implied by Gammelsrød and Holm (1984) and traced by Dickson and Blindheim (1984) northward up to the Barents Sea and Spitsbergen. The consistent pattern of the GSA'70s advection around the northern North Atlantic, elaborated in detail by Dickson et al. (1988), has been widely accepted by the oceanographic community.

Nonetheless, ***alternative*** hypotheses have been put forward to account for the observed phenomena. For example, Ellett and MacDougall (1983), Dooley et al. (1984), and Martin et al. (1984) suggested that the temporal TS-variability observed west of Britain might be caused by a conjectural large-scale eastward shift of water masses, i.e. a 300-km eastward shift of the Polar Front. Pollard and Pu (1985) assumed increased in situ surface moisture flux (i.e. increased excess of precipitation over evaporation) as the primary cause of local freshening. Hansen and Kristiansen (1994) suggested that the simultaneous salinity variations observed in different water

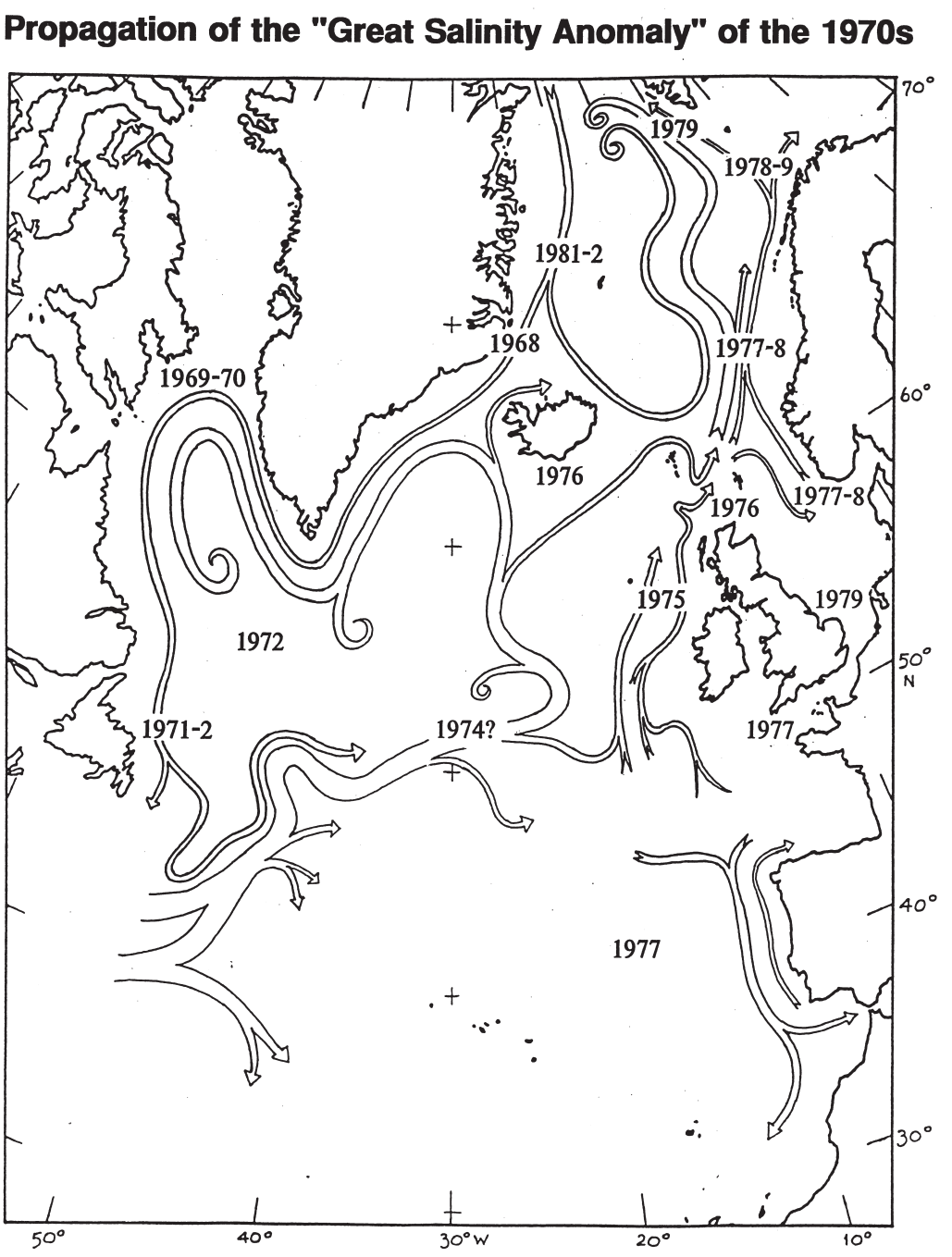

Fig. 1. A scheme by Ellett and Blindheim (1992, Fig. 6) showing transit dates for the minimal values of the "Great Salinity Anomaly" of the 1970s (by Dickson et al., 1988). The Krauss (1986) scheme of circulation has been modified in the Northeast Atlantic by Ellett and Blindheim (1992) after Meincke (1986) and others.

masses around Faroe Islands could be only explained by the changing dynamical balance of the currents transporting these water masses.

The descriptive works by Dickson et al. (1988) and other researchers have stimulated search for interactions between the northern North Atlantic and the Arctic Ocean (Mysak et al., 1990; Mysak and Power, 1992; Mysak, 1995; Serreze et al., 1992) as well as modeling efforts (Delworth et al., 1993, 1997; Häkkinen, 1993, 1995; Mysak, 1995; Weaver and Hughes, 1992; Weaver, 1995; Wohlleben and Weaver, 1995; Holland et al., 1995). The modeling studies seem to be especially important in the light of the findings by Deser and Blackmon (1993), Kushnir (1994), and Reverdin et al. (1997) who demonstrated the leading role of the decadal/interdecadal scales in the overall variability of the ocean.

Observations and models have shown that the GSA'70s is unlikely to be a unique phenomenon although perhaps its magnitude was exceptional. When additional repeat observations along standard sections and at standard stations extended time series into the 1990s, another large TS-anomaly, of the 1980s (hence termed "GSA'80s"), became evident (Fig. 2). As for the previous anomaly, the GSA'80s is much better defined in the salinity time series compared to the temperature series. The series show that a well-ordered sequence of salinity minima occurred around the subpolar gyre. The pattern emerges of a conspicuous fresh, cold anomaly being advected by the West Greenland Current (1982) and the Labrador Current (1983–1984) into the central North Atlantic (1984–1985) and thence to the Northeast Atlantic (1985–1986) into the North Sea (1987–1988), the Norwegian Sea (1987–1988), the Barents Sea (1989), and then back to North Icelandic waters (1989–1990). In addition, retrospective analyses have shown that similar anomalies had occurred in the past, so that the emergence of large salinity anomalies (usually associated with temperature anomalies) appears to be more or less regular phenomena. For example, several authors commented on distinct TS-minima in time series across the North Atlantic observed about a decade before and after the GSA'70s (Myers et al., 1989; Ellett and Blindheim, 1992; Drinkwater, 1994); quasi-decadal *temperature* oscillations were identified at OWS "C" and have been shown to be part of a basin-wide feature (Levitus et al., 1994, 1995).

In this paper we present a detailed description of the GSA'80s, compare it with the preceding similar anomaly, GSA'70s, and draw some general inferences. The paper's structure is as follows. Data sources of the time series used in the analysis are characterized in Section 2. An elaborated scenario of the GSA'80s advection around the northern North Atlantic is presented in Section 3. Most important problems related to GSAs such as their origin, propagation, longevity, salt budget, recurrence, regularity, deep-water impact, long-term variability etc. are discussed in Section 4. Main results and ramifications are summarized in Section 5.

Our task is facilitated by the fact that now we have at hand two similar events, studied in detail, instead of the single (GSA'70s) event available to Dickson et al. (1988) and other earlier researchers. We also draw on latest results of modeling and statistical analysis of long-term variability of the ocean–ice-atmosphere system obtained by the mid-1990s.

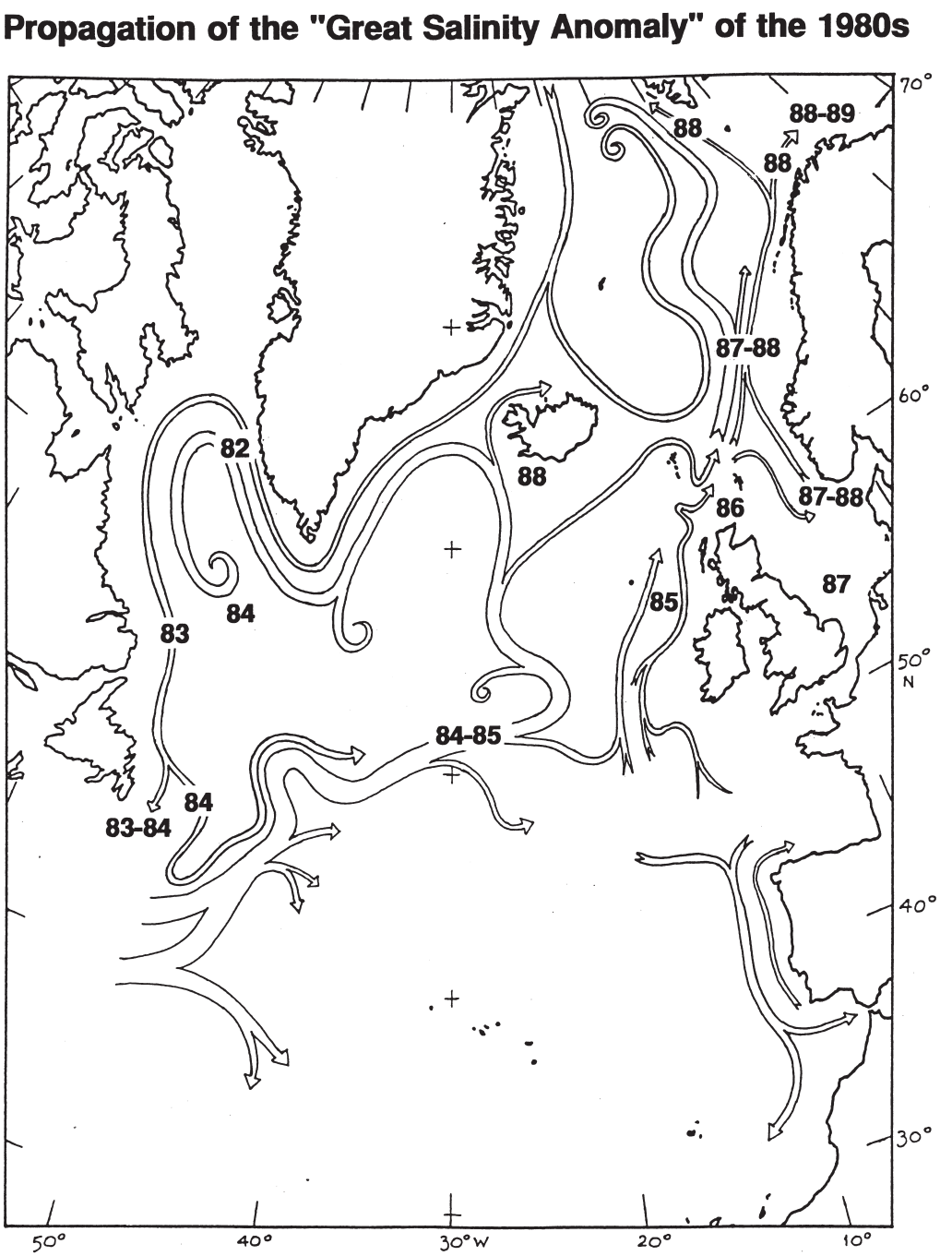

Fig. 2. Propagation of the “Great Salinity Anomaly” of the 1980s based on the transit dates for the minimal salinities. The circulation scheme by Ellett and Blindheim (1992, Fig. 6) was used to ensure easy comparison with Fig. 1.

2. Data

Published time series of temperature, T, and salinity, S, extending up to 1995, were used to describe the GSA'80s. To illustrate its propagation (Fig. 2) we have used the current pattern scheme previously utilized to show advection of the GSA'70s (Fig. 1) since this schematic was also found to be consistent with the new data as well. Using the extended time series we will also comment on similar decadal-scale anomalies observed before and after the GSA'80s, including anomalies of the late 1950s, 1970s, and early 1990s. A pattern of repeated decadal-scale advective events emerges from this study. However, the events (anomalies) are not necessarily of the same nature or structure, therefore much can be gained from their comparative study.

Locations of sections and stations used in this work are shown in Fig. 3 accompanied by Table 1 which provides coordinates and references to sources of the data. References are given to the time series data presented and analyzed at appropriate places in the text. Table 2 provides additional information about Russian standard sections in the Central North Atlantic.

3. Advection of the "Great Salinity Anomaly" of the 1980s around the northern North Atlantic

3.1. North Icelandic waters

In a series of papers of the 1990s, S.-A. Malmberg advanced the idea that the very first signatures of the GSA'80s may have appeared in the late 1970s in North Icelandic waters (Malmberg and Kristmannsson, 1992, Fig. 4; Malmberg and Blindheim, 1993, 1994; Malmberg et al., 1994, Fig. 5; Malmberg et al., 1996, Fig. 5). Indeed, the years of 1976–1979 featured very low salinities in the East Icelandic Current, apparently derived from its principal source, the East Greenland Current. The TS-characteristics of the East Icelandic Current in 1976–1979 were of a polar current rather than an Arctic current as usual (Malmberg and Svansson, 1982; Malmberg, 1984a, b; a review of Atlantic, Polar, Arctic, and Shelf water mass definitions can be found in Hopkins, 1991). These conditions could be responsible, in particular, for the "small salinity anomaly" in the Arctic Intermediate Water found in the late 1980s south of Iceland and in the Greenland–Iceland Seas (Malmberg et al., 1990; Bjarni Sæmundsson GSP Group, 1991; Malmberg and Kristmannsson, 1992). The Arctic conditions (T = 1°–3°C, S = 34.5–34.8) observed north of Iceland in 1981–1983 are considered to be a signature of the return of the previous anomaly, GSA'70s (Malmberg, 1986; Malmberg and Kristmannsson, 1992; Malmberg and Blindheim, 1994).

The idea of the GSA'80s formation north of Iceland in the late 1970s, however meets serious objections. First of all, a large-scale negative salinity anomaly is expected to be accompanied by a large positive sea ice extent anomaly (e.g., GSA'70s) because surface freshening enhances stability and ice formation

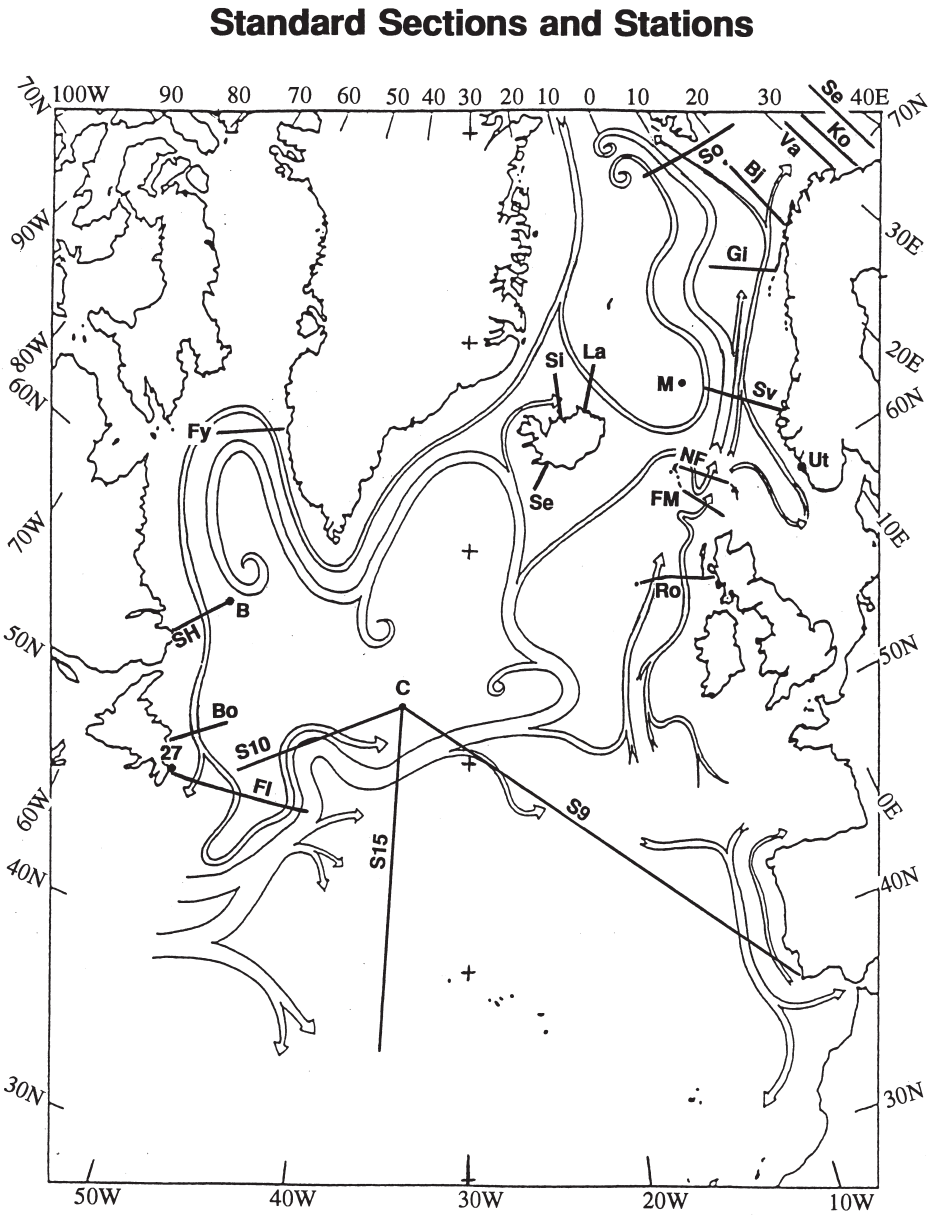

Fig. 3. Standard sections and stations used in this work overlayed on the circulation scheme by Ellett and Blindheim (1992, Fig. 6). Coordinates of these sections and stations are given in Table 1.

Table 1
Standard sections and stations

Code	Section/Station Name	Location	Reference
Icelandic Waters:			
Si	Siglunes-N	66°16'N, 18°50'W–68°00'N, 18°50'W	ICES (1997)
La	Langanes-NE	66°37'N, 14°16'W–68°00'N, 12°40'W	ICES (1997)
Se	Selvogsbanki-SW	63°41'N, 20°41'W–63°00'N, 21°28'W	ICES (1997)
Labrador Sea and Grand Banks of Newfoundland:			
Fy	Fylla Bank	63°57'N, 52°22'W–63°12'N, 59°10'W	Stein (1988); ICES (1997)
SH	Seal Island/Hamilton Bank	53°14'N, 55°39'W–55°04'N, 52°30'W	Stein (1988); ICES (1997)
Bo	Bonavista	48°44'N, 52°58'W–50°00'N, 49°00'W	Stein (1988); ICES (1997)
Fl	Flemish Cap	47°00'N, 52°02'W–47°00'N, 42°00'W	Stein (1988); ICES (1997)
27	Station 27	47°33'N, 52°35'W	ICES (1997)
B	OWS "B" ("Bravo")	55°47'N, 51°53'W	ICES (1997)
Central North Atlantic:			
C	OWS "C" ("Charlie")	52°45'N, 35°30'W	ICES (1997)
S10	S10	49°04'N, 48°07'W–52°24'N, 36°41'W	Present work
S15	S15	36°30'N, 35°00'W–52°00'N, 35°00'W	Present work
S9	S9	52°45'N, 35°30'W–37°11'N, 09°13'W	Present work
Northeast Atlantic:			
Ro	Malin Head-Rockall (MR)	56°40'N, 06°08'W–57°35'N, 13°38'W	ICES (1997)
NF	Nolso-Flugga (FS)*	62°00'N, 06°12'W–60°56'N, 01°00'W	ICES (1997); *Faroe-Shetland
FM	Fair Isle-Munken (FIM)*	60°10'N, 03°44'W–61°12'N, 06°22'W	ICES (1997); *Shetland-Faroe
Ut	Utsira	59°17'N, 05°02'E	ICES (1997)
Norwegian, Barents, and Greenland Seas:			
M	OWS "M" ("Mike")	66°00'N, 02°00'E	ICES (1997)
Sv	Svinøy-NW	62°22'N, 05°12'E–64°40'N, 00°00'E	ICES (1997)
Gi	Gimsøy-NW	68°24'N, 14°05'E–70°24'N, 08°12'E	ICES (1997)
Bj	Bjørnøya (Bear Island)-S	70°30'N, 20°00'E–74°15'N, 19°10'E	ICES (1997)
Va	Vardø-N	70°30'N, 31°13'E–76°30'N, 31°13'E	ICES (1997)
Ko	Kola-N	69°30'N, 33°30'E–79°30'N, 33°30'E	Loeng et al. (1992)
Se	Semøyene (Sem Islands)-N	69°05'N, 37°20'E–76°30'N, 37°20'E	ICES (1997)
So	Sørkapp-W	76°20'N, 05°00'E–76°20'N, 25°00'E	Dickson and Blindheim (1984)

Table 2
Russian standard sections* in the Central North Atlantic (after Belkin and Levitus (1996), Table 1)

Section	Total number of repeat transects along the section	No. of stations	Years
S2	42	946	1975–85
S5	20	275	1975–85
S9	86	2303	1976–85
S10	25	248	1975–84
S13	14	175	1981–85
S14	9	85	1982–85
S15	17	461	1982–85

*All these sections are shown in Fig. 10. Sections S9, S10, and S15 are also shown in Fig. 3.

(Malmberg, 1969; Marsden et al., 1991; Section 4.2). Contrary to what would then be expected, the late 1970s featured only a moderate sea ice extent in the Greenland and Iceland Seas (Chapman and Walsh, 1993, Fig. 7; Agnew, 1993, Table 1; Section 4.2). Secondly, the time interval between the suggested appearance of the GSA'80s north of Iceland (1976–1979) and its observation off West Greenland (1982; Section 3.2) is too long. To arrive in North Icelandic waters in 1976–1979, the anomaly should have appeared in the East Greenland Current (located upstream) earlier, about 1975–1978, i.e. 4 to 7 years before 1982 when the GSA'80s actually peaked in the West Greenland Current off the Fylla Bank (Section 3.2). Given the swiftness of the East and West Greenland Currents, where drift velocities of surface buoys reach 70 cm/s (Krauss, 1995), such slow movement of the GSA'80s seems highly unlikely. Indeed, the GSA'70s covered the same distance in just 1 to 2 years (Dickson et al., 1988).

3.2. West Greenland Current

Fylla Bank (West Greenland Current, ~64°N) (Stein, 1988; Buch and Stein, 1987, Figs 2–7; Myers et al., 1989, Fig. 2a; Myers et al., 1990b, Fig. 4; Hovgård and Buch, 1990, Fig. 3.2; Drinkwater, 1994, Figs 20–21; Stein, 1995b, Figs 11–13; Stein, 1996a, Fig. 9–10). The exact timing of either the arrival of the GSA'80s to the Fylla Bank, or its local formation there, is difficult because the different time series imply different years, 1982 or 1983. Some of the time series (e.g. those observed in October–November) are deemed unreliable because of the fresh water outflow from Godthåb Fjord (Buch, 1982). According to the most detailed data by Buch and Stein (1987), Figs 2–4, July time series, the GSA'80s peaked over Fylla Bank in 1982, which seems consistent with the dating from annual summaries by Drinkwater (1994), Figs 20–21, as shown in Fig. 4, whereas the mid-June T-series by Hovgård and Buch (1990), Fig. 3.2, autumn TS-series by Stein (1995b), Figs 11–12 and June T-series by Stein (1996a), Fig. 9 show that the GSA'80s peaked in 1983.

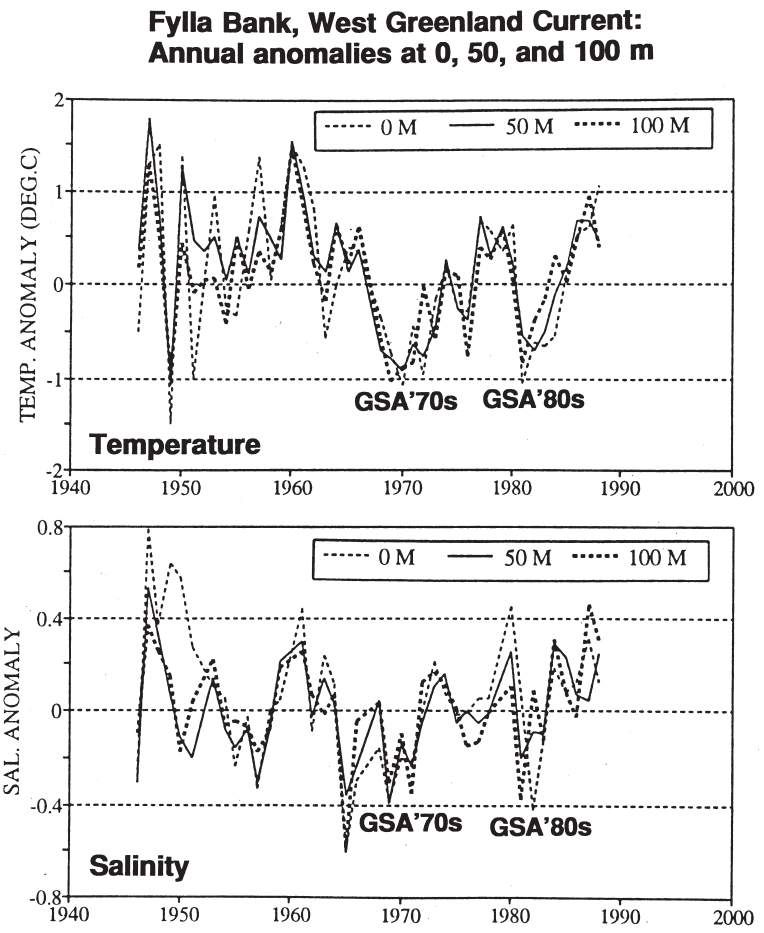

Fig. 4. Annual anomalies of temperature (top) and salinity (bottom) at 0, 50, and 100 m over Fylla Bank, West Greenland Current (Drinkwater, 1994, Figs 20 and 21)

3.3. Offshore Labrador Current and central Labrador Sea

The Labrador Current consists of inshore and offshore branches with high mean currents and relatively low variability (Narayanan et al., 1996). These branches are considered separately, in this section the offshore branch, and in the next section the inshore branch. Water properties of the Labrador Current and the Labrador Shelf are determined by a combination of atmospheric forcing and advection from West Greenland (Drinkwater, 1994, p.7). Therefore, time series for Fylla Bank are significantly correlated with those farther downstream, as far as the Grand Banks area, with a lag of about 1 to 2 years (e.g., Myers et al., 1989). The longest time series are available along the Seal Island line off Labrador and Bonavista line off Newfoundland (Stein, 1988; ICES, 1997).

Seal Island-Hamilton Bank (Labrador Current, ~53–55°N) (Fig. 5, modified after Myers et al., 1989, Fig. 2b; Stein, 1988). At 50 m, the minimum of 1972 is well-defined, while the minimum of 1984 is less pronounced though distinct (as well as the minimum of 1959–61).

OWS "Bravo" (central Labrador Sea, 55°47'N, 51°53'W). We do not show any figures for "Bravo", because this Ocean Weather Station was withdrawn from service in 1974, and the 1964–1974 data were presented and analyzed by Lazier (1980). The data have been augmented by Myers et al. (1990b) with the data from the Seal Island line Stations 10–12, which are close to "Bravo", thus substantially improving the temporal resolution prior to 1964 and extending the "Bravo" time series up to 1987. Myers et al. (1990b) have illustrated salinity time series for the 500–2000 m layer (their Fig. 3a) in which the anomalies of the '70s and '80s are ill-defined, except for a sharp drop of S500 in 1972; only the minimum of 1958–1959 is clearly seen.

Even though the OWS "Bravo" is located in the center of the Labrador Sea, the station is not isolated from the sea's periphery, particularly, from the Labrador Current, as a result of the lateral offshore advection from the current into the sea's interior (Reynaud et al., 1995; Loder et al., 1998); therefore the OWS "Bravo" can be considered representative for the entire sea.

Central Labrador Sea (Fig. 6, modified after Lazier (1995), Fig. 7). The salinity of the Labrador Sea in the 0–250 m layer decreased from 1976 to 1984 when it reached its absolute minimum (34.35 psu) (Lazier, 1995). The minimum may have occured before 1984 and been even more pronounced since the Lazier (1995) time series has no data between the cruises of 1981 and 1984 (Lazier, 1988, Fig. 2). The previous low-S anomaly in the Labrador Sea detected in the OWS "Bravo" data (Lazier, 1980) peaked in 1970–71 (Fig. 6).

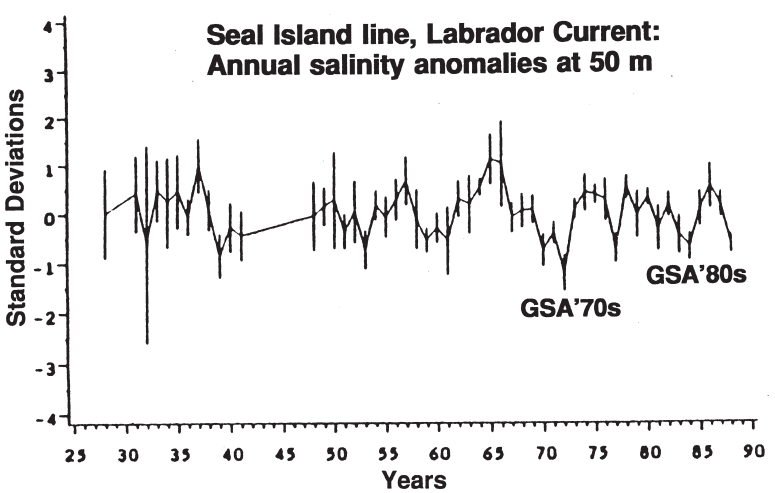

Fig. 5. Annual salinity anomalies (standard deviations) for the Seal Island line, Labrador Current, at 50 m, stations 2 through 6 (Myers et al., 1989, Fig. 2b). Vertical lines show 95% confidence limits.

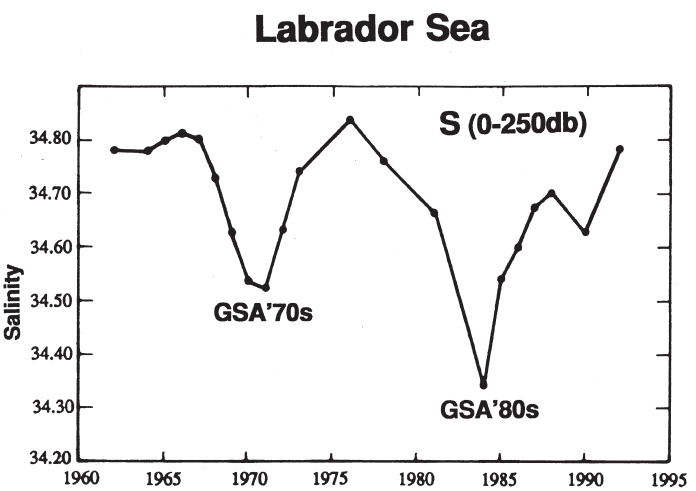

Fig. 6. Area-averaged salinity of the central part of the Labrador Sea in the 0–250 m layer (Lazier, 1995, Fig. 7).

3.4. Inshore Labrador Current

Station 27 (inshore Labrador Current, off St. John's, Newfoundland) (Myers et al., 1990a, Fig. 3; Petrie et al., 1992, Figs 3–4; Drinkwater, 1994, Figs 22–23; Drinkwater et al., 1995, Figs 18–19; Mertz and Myers, 1994, Figs 2 and 4; Hutchings and Myers, 1994, Fig. 4). Station 27 (47°33'N, 52°35'W, 176 m depth) has the longest and most complete TS-time series on the NW Atlantic shelf (Umoh et al., 1995). The station is located just 5 km from the coast. Therefore, the long-term advective signal (the subject of this study) might be thought to be contaminated by runoff, orographic winds and other processes because of its proximity to the coast. However, interannual salinity variability on the Newfoundland Shelf measured at Sta. 27 is neither correlated with interannual variability in runoff into Ungava Bay, nor with ice-melt in Hudson Bay (Myers et al., 1990a). Hence, the long-term signal measured at Sta. 27 is not apparently significantly contaminated by processes related to inland waters. Advection by the Labrador Current seems to be critically important on the longer time scales, from interannual to decadal (Umoh et al., 1995). The long-term variability observed at Sta. 27 is thus determined largely by remote long-term variations in the Labrador Current and in the West Greenland Current.

The GSA'80s arrived at Sta. 27 in 1983 and persisted for two years according to *non-smoothed* monthly data by Petrie et al. (1992, Fig. 3) (Fig. 7). It should be noted that the *smoothed* data presented by Petrie et al. (1992), Fig. 4, Drinkwater (1994), Figs 22–23 (Fig. 8), Drinkwater et al. (1995), Figs 18–19, and Mertz and Myers (1994), Figs 2 and 4 are biased to 1984–1985 being the time period of the GSA'80s.

The GSA'70s timing also differs according to the non-smoothed data series versus the smoothed series; being 1970 versus 1971, respectively; except for the annual upper layer salinity data presented by Drinkwater (1994), Fig. 23, which shows the

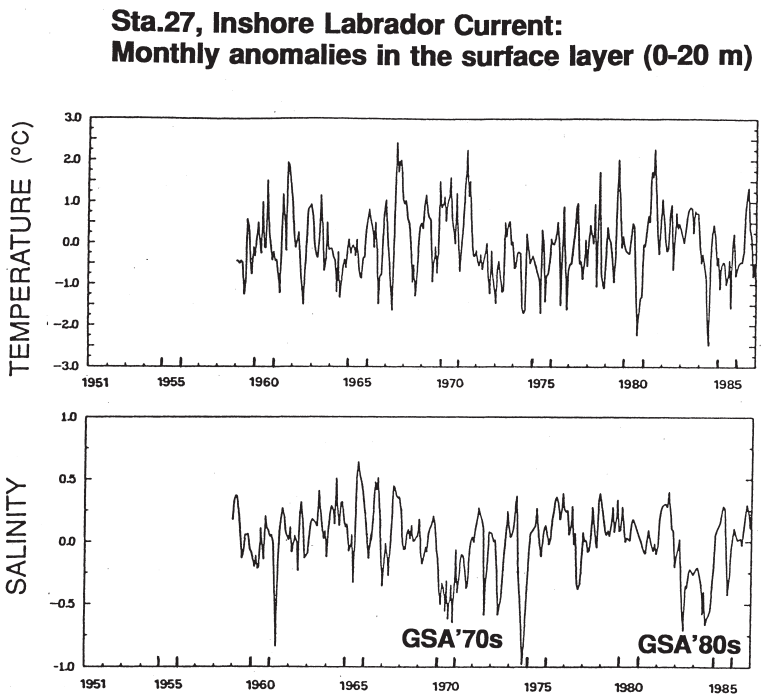

Fig. 7. Monthly anomalies of temperature (top) and salinity (bottom) in the surface layer (0–20 m) at Station 27, the inshore Labrador Current (Petrie et al., 1992, Fig. 3).

GSA'70s in 1970 (Fig. 8)). As noted above, we always prefer dating based on original data, which has not been low-pass filtered.

The Drinkwater (1994) data (Fig. 8) also show a pronounced minimum in 1991, which may have signalled the arrival of the next "great salinity anomaly", of the 1990s.

3.5. Grand Banks of Newfoundland and Flemish Cap

The Flemish Cap section (Fig. 9, modified after Myers et al. (1989), Fig. 2b; Stein, 1988). The 1984 S-min at 50 m is pronounced, as well as the earlier S-min of 1971. This section is extremely important for monitoring the outflow from the Labrador Sea because the section crosses the Flemish Pass, the main offshore conduit for the Labrador Current.

It is worth noting that during the passage of GSA'80s, the temperature at Flemish Cap (Ellett and Blindheim, 1992, Fig. 13, from data of Trites and Drinkwater, 1990) decreased to its minimum in 1985 (for the 1972–1989 series), almost coinciding in time (and seemingly associated) with the salinity minimum of 1984 along the Flemish Cap line. We note also that the thermal manifestation (negative temperature anomaly) of the previous salinity anomaly (GSA'70s) at Flemish Cap was indistinct.

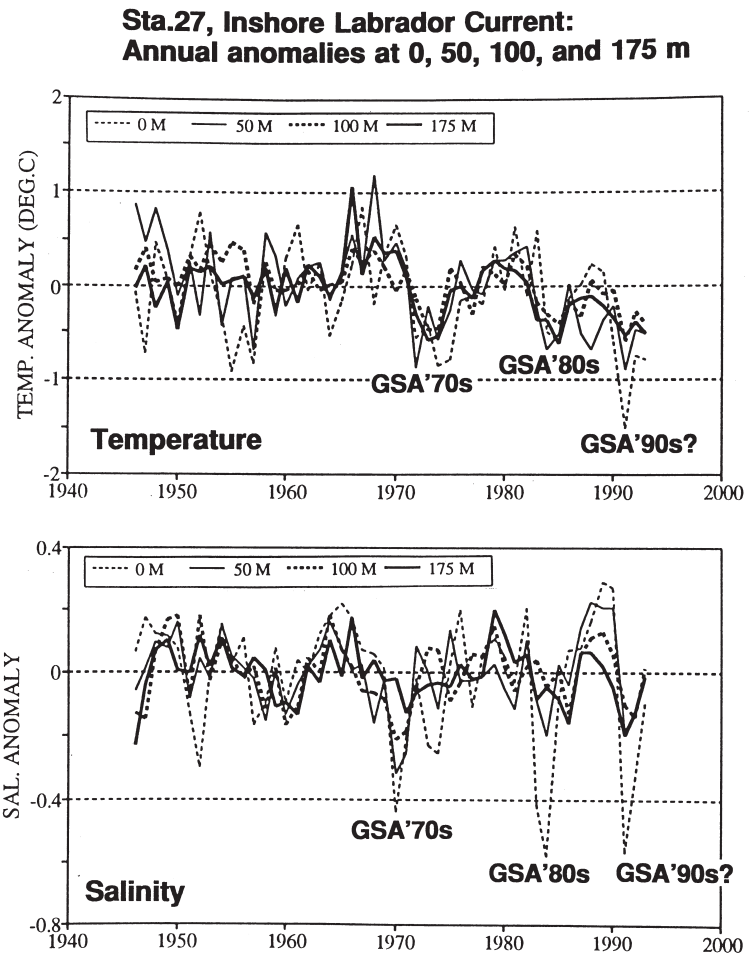

Fig. 8. Annual anomalies of temperature (top) and salinity (bottom) at 0, 50, 100, and 175 m at Station 27, the inshore Labrador Current (Drinkwater, 1994, Figs 22–23).

3.6. North Atlantic Current near the Charlie-Gibbs Fracture Zone

The Russian data set of repeated transects along standard lines occupied since 1971 in the DIGMA program (this Russian acronym stands for "Long-term Investigation of Hydro-Meteorological Anomalies" or LIHMA) represents the main source of regular data in the Central North Atlantic (for reviews of Russian works in the North Atlantic see, for example, Baranov, 1991; Lappo et al., 1995). To study long-term variability of the North Subarctic Front (NSAF), associated with the northernmost branch of the North Atlantic Current (NAC), Belkin and Levitus (1996) have contoured and analyzed 213 repeated transects along seven standard sections, namely, S13, S10, S14, S15, S5, S9, and S2 (Fig. 10, from Belkin and Levitus (1996), Fig. 1). Below

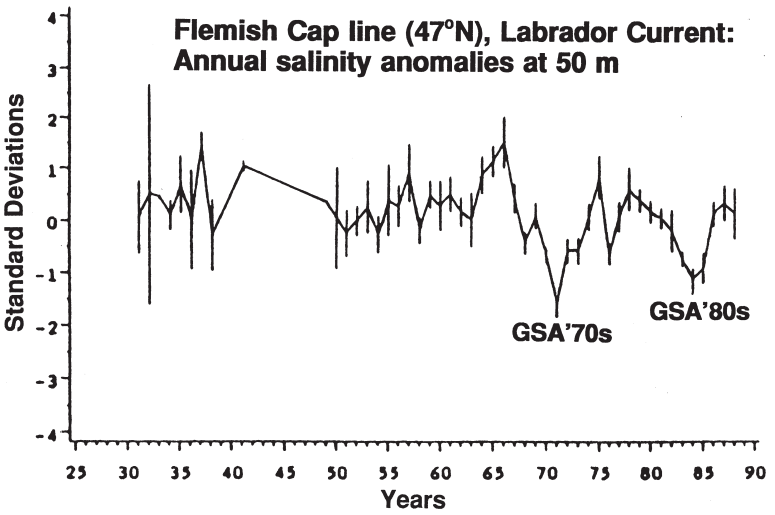

Fig. 9. Annual salinity anomalies (standard deviations) for the Flemish Cap line, Labrador Current, at 50 m (Myers et al., 1989, Fig. 2b). Vertical lines show 95% confidence limits.

we present time series from three of these standard sections: S10, S15, and S9. The oblique section S10 spans a quasi-stationary meander of the NAC termed the "Northwest Corner" by Worthington (1976), p. 27 and studied by Lazier (1994), thus crosses the SAF twice. Downstream of the Northwest Corner the SAF bifurcates (Fig. 10) into the North and South SAF (SSAF), both of which are crossed by section S15 along 35°W.

The LIHMA data: **Section S10** (SW of OWS 'C'; Fig. 11), **Section S15** (S of OWS 'C'; Fig. 12), **Section S9** (SE of OWS 'C'; Fig. 13). During 1976–1985, as a part of the above-mentioned Russian LIHMA program, approximately 120 repeat transects were occupied along these three standard lines which extend from OWS 'C' to the southwest, south, and southeast. The transects were analyzed by Belkin and Levitus (1996) to describe the North Subarctic Front (NSAF) and to study its decadal variability. Of the three standard lines, Section S9 was occupied more frequently and systematically than others. The salinity time series for the cold side of the NSAF along this line (Fig. 13) revealed a sharp drop in early 1984, allowing Belkin and Levitus (1996) to date precisely the arrival of GSA'80s to Section S9. The low-S anomaly persisted here at least through 1985. The corresponding temperature time series also shows a noticeable decline in 1984–85 (Belkin and Levitus, 1996, Fig. 6b). Transects across the NSAF along sections S10 and S15 occupied in the 1980s confirm that a steep decrease in salinity occurred in 1984 (Figs. 11 and 12).

OWS "C" ("Charlie"; 52°45'N, 35°30'W) (Fig. 14). The station was located near the Charlie-Gibbs Fracture Zone where the North Subarctic Front (sometimes called the "Polar Front") associated with the northern branch of the North Atlantic Current crosses the Mid-Atlantic Ridge. Fig. 14 shows monthly and yearly means of T and S at 200 m for 1964–1990. Each monthly mean value (open symbols) has

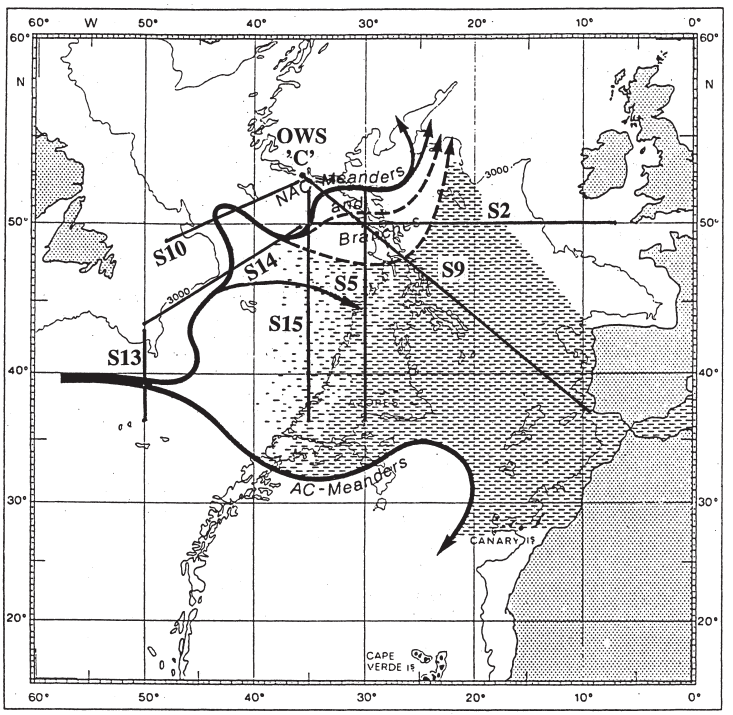

Fig. 10. Currents of the central North Atlantic. The base map by Sy (1988) shows the North Atlantic Current (NAC), with its transient branches (broken lines); the Azores Current (AC), and the Mediterranean Water tongue (hatched) (reprinted from Deep-Sea Research, vol. 35, A. Sy, Investigation of large-scale circulation pattern in the central North Atlantic: the North Atlantic Current, the Azores Current, and the Mediterranean Water plume in the area of the Mid-Atlantic Ridge, pp. 383–413, copyright© 1988, with kind permission from Elsevier Science Ltd, The Boulevard, Langford Lane, Kidlington, 0X5 1GB, UK). Added is the eastward branch of the NAC along ~46°N (Dietrich et al., 1975; I.M. Belkin, unpublished manuscript, 1993). Numbered solid lines show standard sections occupied by Russian research vessels (Table 2) and analyzed by Belkin and Levitus (1996).

been computed as an average of available daily means. Yearly values (solid symbols) are the averages of the available monthly means (the months with observations are shown in the lower panel of the figure). No restrictions have been applied to the number of observations per day or the number of days in a month with data to compute daily or monthly means, respectively. The computations for 1964–1973 are based on the NODC Station Data file only (the MBT data are not used). The 1975–1985 data are based on the daily means provided by GOIN (State Oceanographic Institute, Moscow), the data for 1986, 1989, and 1990 are based on observations digitized by ICES, and the data for 1987 and 1988 are based on the monthly means published by GOIN.

The time series of temperature and salinity at OWS "C" exhibit a strong decadal-scale signal and a decreasing multi-decadal trend (Fig. 14), both features were identified in temperature series alone by Levitus et al. (1994) and Levitus et al. (1995)

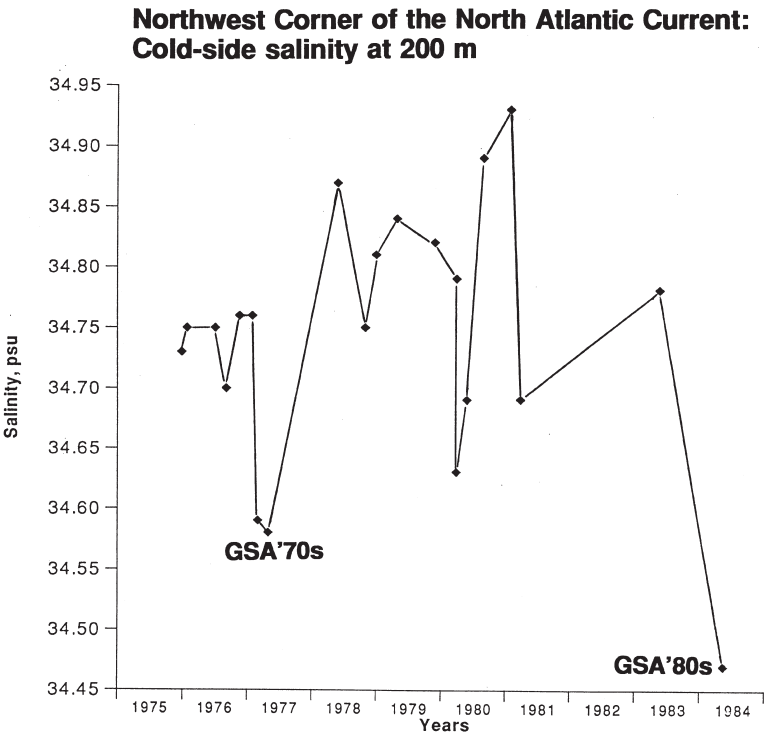

Fig. 11. Salinity at the 200-m depth, at the cold side of the North Subarctic Front (associated with the northernmost branch of the North Atlantic Current), along the S10 section across the Northwest Corner.

(also briefly noted in T-S-time series by Dooley (1992)). The cold, fresh anomalies of the mid-1970s and mid-1980s are conspicuous. Unfortunately, there was a ~18-month time break in the observations at OWS "C", so the timing of GSA'70s can only tentatively be determined as 1975 (by the salinity). The timing of GSA'80s can be reliably determined as 1985 (by the salinity).

3.7. Irminger Current

Selvogsbanki, Station 5 (S-5, Irminger Current south of Iceland) (Malmberg and Kristmannsson, 1992, Figs 11b and 12)). South of Iceland, at S-5, the GSA'70s peaked in 1976, a year (or less) after it peaked near OWS "C". The GSA'80s peaked at S-5 in 1985-1988, one-to-three years after the 1984–1985 minimum near OWS "C". The difference in time lag may have been caused either by a shift in the currents pattern or by the supposedly more sluggish circulation in the 1980s. The latter anomaly was well-defined only in subsurface layers (100–400 m) (Fig. 15; also Malmberg and Kristmannsson, 1992, Table 6), while the earlier one was identifiable in the surface layer as well (Malmberg, 1985, Fig. 9; Dickson et al., 1988, Fig. 14).

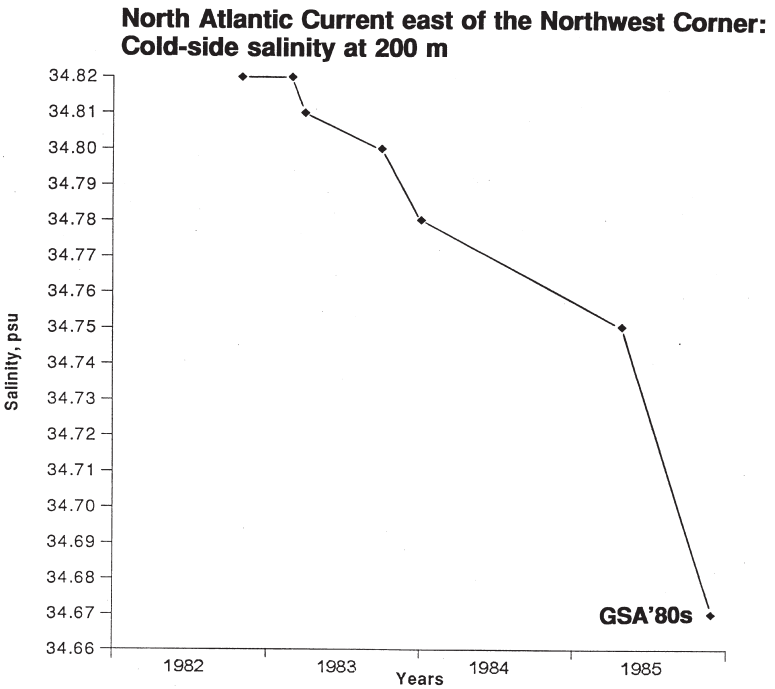

Fig. 12. Salinity at the 200-m depth, at the cold side of the North Subarctic Front (associated with the northernmost branch of the North Atlantic Current), along the S15 meridional section (35°W) east of the Northwest Corner.

3.8. Rockall Channel

Here we discuss the data presented by Ellett and Blindheim (1992), Fig. 16, Ellett (1994), Figs 3 and 5, and Ellett (1995), Fig. 4; the surface TS-data have been published by Ellett and Jones (1994).

The GSA'80s reached the Rockall Channel in early 1985 and persisted there for at least 4 years, up to mid-1989 (Fig. 16). Two other minima are conspicuous in the data set, one in 1975 (GSA'70s) and another in 1981, the latter being noted by Ellett and Blindheim (1992). The arrival time to Section S9 was determined reliably as early 1984, one can conclude that the time lag between the S9 and Rockall Channel events is about 1 year. This estimate is close to the time lag of 9 months between the passage of GSA'70s through OWS "C" (still uncertain because of the 18-month gap in the data for 1974–1975) and its arrival at the Rockall Channel in the fall of 1975 (Fig. 16), as determined by Dickson et al. (1988).

Winter anomalies of surface salinities (Fig. 17, bottom) also show a conspicuous minimum in 1976 (GSA'70s) and a less pronounced minimum in 1986–1987 (GSA'80s). The temperature minima of 1974–1975 and 1987 that can be attributed to GSA'70s and GSA'80s respectively, can be seen, especially in mean winter (January–March) anomalies (Fig. 17, top, solid line).

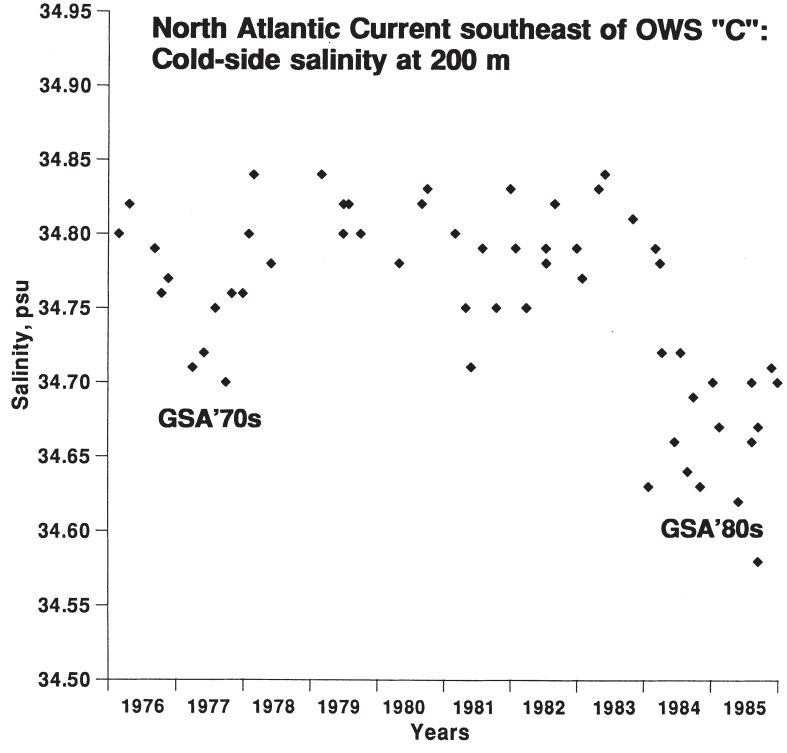

Fig. 13. Salinity at the 200-m depth, at the cold side of the North Subarctic Front (associated with the northernmost branch of the North Atlantic Current), along the S9 section southeast of OWS “C” (Belkin and Levitus, 1996, Fig. 6c).

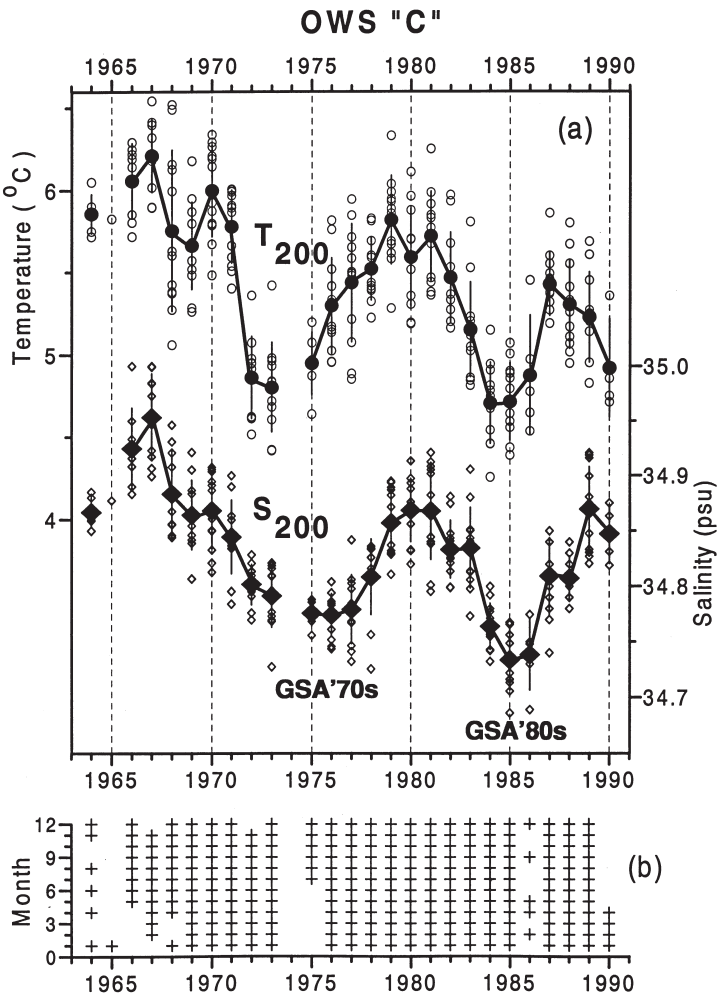

Fig. 14. (a) Temperature (circles) and salinity (diamonds) at the 200-m depth at Ocean Weather Station "C" (52°45'N, 35°30'W). Open (solid) symbols show monthly (annual) means. Bars show standard deviations about annual means. (b) Availability of monthly means.

In the deep salinity data (Fig. 18), the GSA'70s is discernable down to at least 1000 m (with a minimum in 1977–1978), whereas the GSA'80s is just discernible at 500 m as a slight decrease in 1987. It should be noted, however, that these data are the anomalies from the means for 1975–1978 (Ellett, 1994), the time of the GSA'70s passage through the Rockall Channel, hence an anomaly *per se*. It is unclear also if the S500 decrease in 1989 (Fig. 18) could be accounted for by the GSA'80s. According to Ellett (1994), the general trends at this depth (occupied by Eastern North Atlantic Water, ENAW) are largely similar to the winter surface time series (Fig. 17). The latter series, however, does not reveal a sharp S0 drop in late

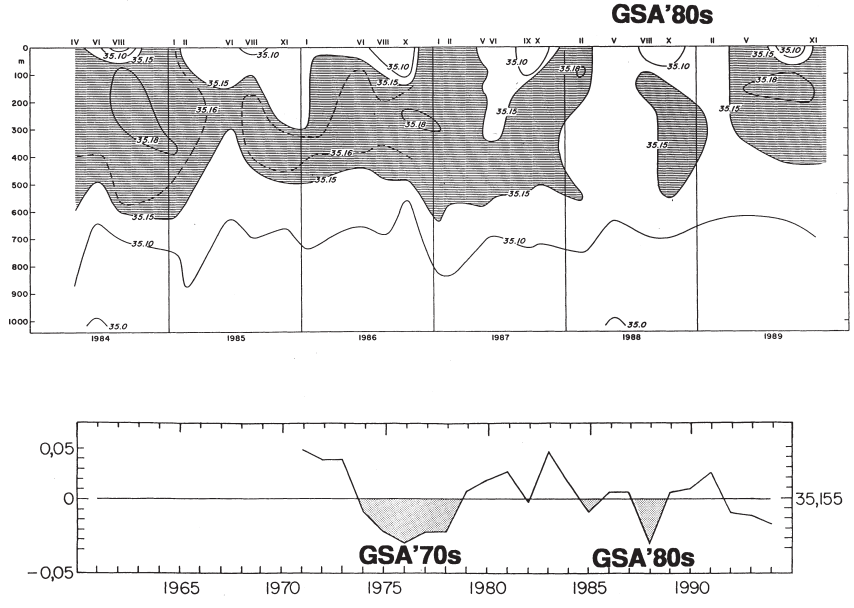

Fig. 15. Salinity isopleths (top) and salinity deviations at 100 m (bottom) at station S-5 in the Selvogsbanki section across the Irminger Current south of Iceland (adapted from Malmberg and Kristmannsson (1992), Figs 11b and 12)).

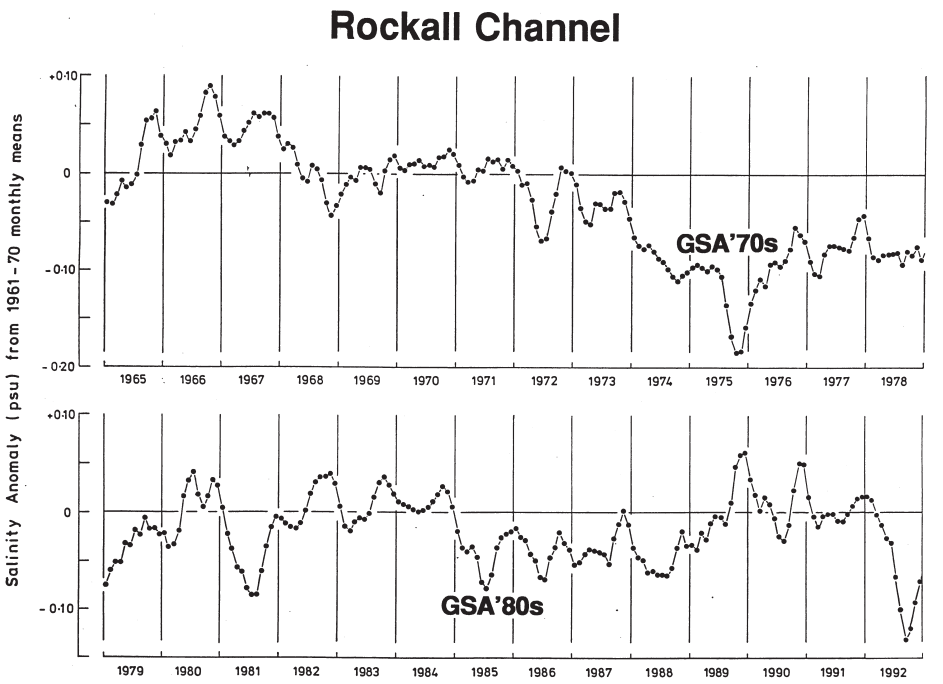

Fig. 16. Running three-monthly means of monthly surface salinity anomalies (psu) from 1961–1970 means for the Rockall Channel, 1965–1992 (Ellett, 1996, personal communication; the 1965–1990 time series published by Ellett and Blindheim (1992), Fig. 16).

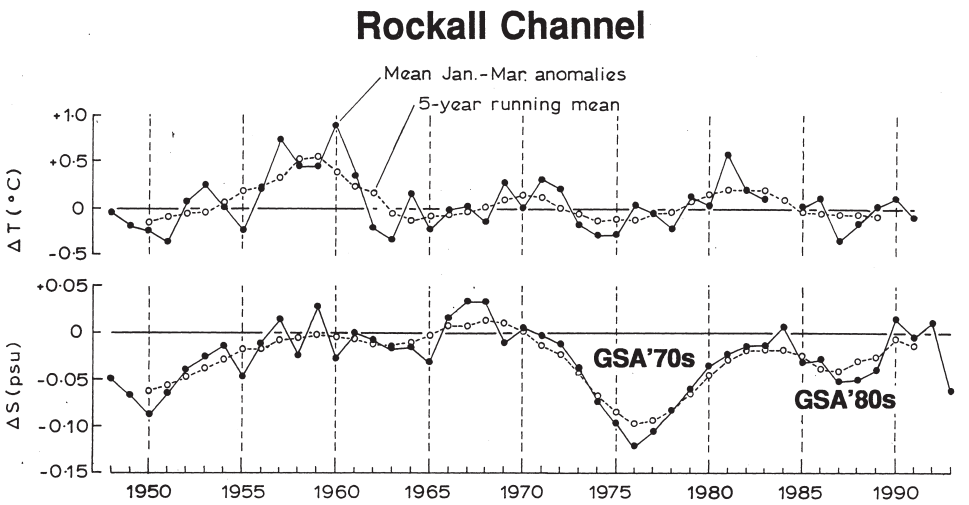

Fig. 17. Winter (January–March) anomalies from 1961–1970 means of surface temperature (°C; above) and salinity (psu; below) in the central Rockall Channel (Ellett, 1994, Fig. 3; Ellett, 1995, Fig. 4).

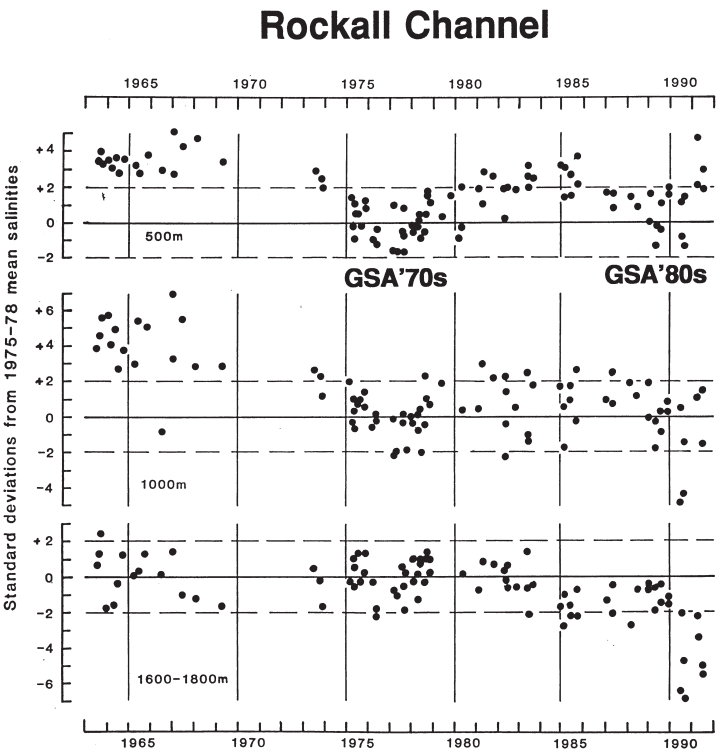

Fig. 18. Salinity anomalies (standard deviations) from 1975–1978 means in the central Rockall Channel at three depths (Ellett, 1994, Fig. 5).

1980s (analogous to the observed S500 drop in 1989), as might be expected based on the similarity between time series at 0 m and 500 m, the ENAW depth; instead, the winter surface time series (Fig. 17) features the steep *increase* in 1990 noted by Ellett (1994). We thus conclude that the S500 drop of 1989 is a forerunner of the abrupt freshening of the deeper layers observed in 1990 (Fig. 18).

3.9. Faroe-Shetland Channel

Repeat observations in the Faroe-Shetland Channel (FSC) were begun in 1893 along two survey lines, Nolso-Flugga section and Fair Isle-Munken section (Turrell, 1995, personal communication 1997). The FSC is the confluence and the conduit for several water masses such as North Atlantic Water (NA), Modified NA (MNA), Arctic Intermediate Water (AI), and Norwegian Sea Deep Water (NSDW); definitions for these water masses have been reviewed by Hopkins (1991). The salinity time series for North Atlantic Water (Fig. 19 (Turrell, 1995, Fig. 3)) reveals two conspicuous minima, in 1908, and in 1975–78 (GSA'70s). The minimum which may correspond to GSA'80s is distinct although less pronounced than GSA'70s. The time series constructed for different water masses in FSC allowed an alternative expla-

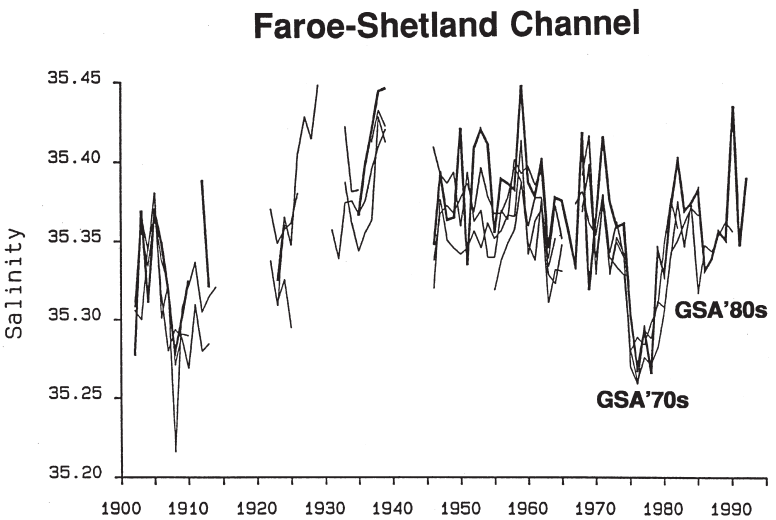

Fig. 19. Salinity (psu) of North Atlantic water derived from observations along the two standard Faroe-Shetland Channel sections. Thin multiple lines are derived from Martin (1976), Walsh and Martin (1986), Martin (1993), and Dooley et al. (1984). Heavy solid line derived from the Turrell (1995) recalibrated data set. Adapted from Turrell (1995), Fig. 3.

nation of GSA'70s to be put forward (Hansen and Kristiansen, 1994), which may be correct at least locally, and which may also be correct as to GSA'80s (see a discussion in Section 4.13). The *surface salinity* time series for the Faroe-Shetland Channel constructed by Reverdin et al. (1994), Section 8.1, also reveals two conspicuous minima, around 1910 and in the late 1970s (GSA'70s), and a few less distinct minima, including the one in the late 1980s, presumably associated with the GSA'80s.

3.10. English Channel

According to Dickson et al. (1988), p.121 and Fig. 15, the GSA'70s peaked in the English Channel in 1977, based on the salinity record for the Seven Stones Lightvessel (Western Approaches to the Channel, 50°04'N, 06°04'W). The signal is strong enough, and the timing is consistent with the GSA'70s propagation hypothesis; however, the question remains as to the advection path of any NAC anomaly supposedly entering the Channel. The problems is, there is no current branch of the NAC which could transport the NAC anomalies directly to the English Channel, according to various circulation schematics (e.g. Krauss, 1986, Fig. 19; Turrell and Shelton, 1993, Fig. 3.4; Otto and Van Aken, 1996, Fig. 1). Geostrophic transport estimates by Arhan et al. (1994), p.1311 for the Bord-Est quasi-meridional hydrographic section between 60° and 20°N offshore of the European and African continental slopes show that the NAC quasi-zonal transport north of 45°N in the upper layer (with the potential density $\sigma_\theta < 27.25$), which totals 3.4 Sv, may contribute

1.0 Sv to the northward Slope Current, but most of it (2.4 Sv) feeds a southward transport off the Iberian Peninsula. In the same time, even long-term average temperature and salinity maps show warm and salty offshore oceanic waters spreading to the English Channel and the Strait of Dover, eventually penetrating the North Sea. This eastward spreading is apparently wind-driven, with its TS-characteristics derived mainly from the northward Slope Current. How could the GSAs join (and, possibly, cross) the Slope Current still remains to be seen. Dickson et al. (1988) did not find any sign of the GSA'70s in salinity time series in the Eastern Channel, and in the southern North Sea (Southern Bight and German Bight); they concluded that "in these inner parts of the shelf, the signal has been overwhelmed by the local inputs" (*ibid*., p.121). The GSAs, however, still could reach the southern North Sea from the north, if facilitated by the northerly winds, as can be inferred from recent results of Corten and Van de Kamp (1996) discussed in the next section.

3.11. North Sea

Oceanic anomalies can penetrate the North Sea proper via two pathways, northern and southern. In the north, oceanic anomalies enter the North Sea directly with the Norwegian Trench Atlantic Inflow, and the East Shetland Atlantic Inflow, the Fair Isle Current and its extension, the Dooley Current (Turrell, 1992a, b; Turrell et al., 1996), whereas the southern pathway, through the English Channel and the Strait of Dover, is an indirect one (as shown in the previous section) and is, perhaps, less important.

Oceanic anomalies could ultimately reach (and circulate through) the Skagerrak before leaving the North Sea via the Norwegian Coastal Current; the GSA'70s was actually observed in the Skagerrak in the late 1970s (Svendsen and Danielssen, 1995; Danielssen et al., 1996).

Advective low-frequency salinity signals of GSAs are contaminated in the North Sea by river runoff and precipitation, whose role in the freshwater/salinity balance of the semi-enclosed marginal sea may be significant and should be taken into account. The western North Sea salinity is affected by river runoff from Scotland and England; the southern North Sea is influenced by discharge of Schelde, Maas, Rhine, Ems, Weser, and Elbe; the eastern North Sea receives freshwater from the Baltic Sea and with the Norwegian river runoff (a summary of the North Sea freshwater fluxes can be found in Otto et al. (1990), p. 177, Table 1-II).

The southern North Sea is sporadically inundated by inflows of warm, salty Atlantic Water through the Strait of Dover caused by persistent southerly winds. Such inflows can dramatically alter TS- and ecological characteristics of the southern North Sea (e.g., Corten and Van de Kamp, 1996). It is also possible that in the southern North Sea such high-salinity inflows from the south can completely obliterate any low-salinity advective signals arriving via the northern entrance. The latest high-salinity inflow occurred in 1989–1991, penetrating the North Sea from both the south and the north (Heath et al., 1991; Ellett and Turrell, 1992; Becker and Dooley, 1995).

When, however, the southerlies slacken, the GSAs signals from the north can

reach the Southern Bight; as can be inferred from the results of Corten and Van de Kamp (1996), who have shown that TS-variability and abundance of southern species in the southern North Sea are correlated with the occurrence of southerly winds over The Netherlands. Therefore we suggest that the arrival of the low-salinity anomaly of 1987 in the southern North Sea (Fig. 20c, Fig. 20d, modified after Corten and Van de Kamp (1996, Figs 4, 5 and 7)) might have resulted from the then-prevailing northerlies helping the GSA'80s to reach the Southern Bight from the north, rather than via the English Channel.

Svendsen and Magnusson (1992) found that the main subsurface inflow of the Atlantic Water (AW) to the North Sea is best represented by areal spread of the mean (50–200 m) salinity greater than 35.1. They found also that "the pulsation of the AW outside the North Sea (probably through the Faroe-Shetland Channel, FSC) seems to have a significant influence on the transport into the North Sea" (*ibid.*, p.155). Figures 20a and 20b (Svendsen and Magnusson, 1992, Fig. 4) show long-term variability of different TS-indices of the Atlantic Water's areal spread. Both GSA'70s and GSA'80s are evident in time series of all six indices.

Utsira (Norwegian Coastal Current, 59°17'N) (Fig. 21 (Ellett and Blindheim, 1992, Fig. 19)). Although oceanic waters can penetrate the North Sea via several

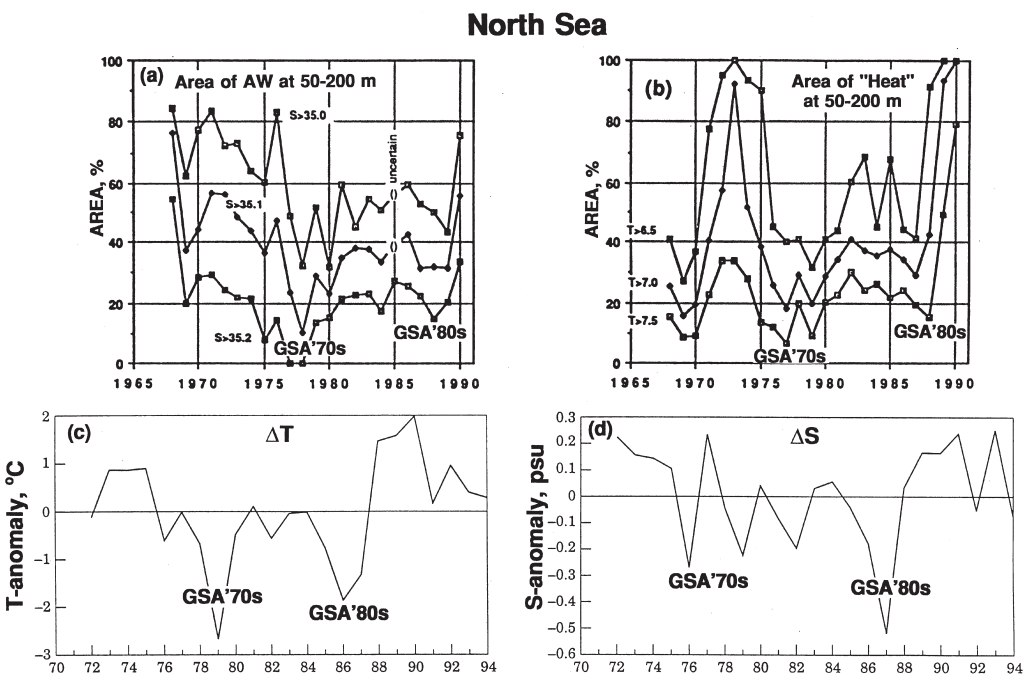

Fig. 20. GSAs in the North Sea. (a) Fraction of the area north of 57°N in the North Sea, at the 50–200-m depth, covered by Atlantic Water (AW) with mean S > 35.0, 35.1, and 35.2. (b) As in (a) but with mean T > 6.5°C, 7.0°C, and 7.5°C (Svendsen and Magnusson, 1992, Fig. 4). (c) Average T-anomalies in February for ICES Stations 1–6, southern North Sea. (d) As in (c) but for S (Corten and Van de Kamp, 1996, Figures 4–5).

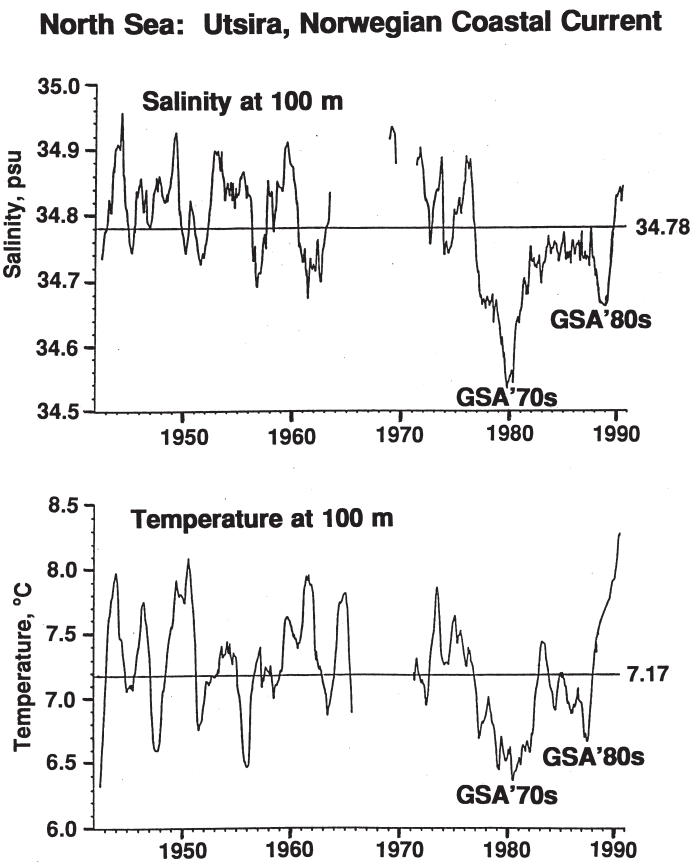

Fig. 21. Temperature and salinity at 100 m at Utsira, Norwegian Coastal Current (Ellett and Blindheim, 1992, Fig. 19; Blindheim, 1996, personal communication).

pathways as discussed above, there is only one exit for the waters from the North Sea, the Norwegian Coastal Current (NCC). Monitoring the NCC is, therefore, of great importance. The coastal Norwegian station Utsira is ideally located for this purpose. Advection of the GSA'80s through Utsira can be identified by the 1988–1989 minimum in surface temperature and salinity time series (Fig. 21). Commenting on the series, Ellett and Blindheim (1992), p. 27–28 noted that "no signal of the "Great Salinity Anomaly" (of the 1970s) was seen and a longer low temperature and salinity period occurred between 1977 and 1982." Their statement implies that this relatively cold and fresh 5-year period is too long to be considered as a manifestation of the GSA'70s. However, even brief inspection of low-S/low-T events associated with the GSA'70s (as well as GSA'80s) shows that in any particular place the anomalies typically persisted for about 2 to 4 years, so that the 5-year time span is not prohibitively long for such anomalies. In fact, it is the 1-year time span of GSA'70s in the Rockall Channel that should be considered exceptionally short. Therefore we

believe that the 5-year low-S/low-T period at Utsira was caused by the propagation of GSA'70s that arrived there in 1977 (about one year after passing through the Rockall Channel) and peaked in 1980.

3.12. Norwegian Sea

OWS "M" ("Mike"; 66°N, 2°E), southern Norwegian Sea (Fig. 22 (Gammelsrød et al., 1992, Figs 3–4)). At 50 m, the GSA'80s can be reliably distinguished only in the salinity time series as a sharp decline in 1986–1987 persisting through 1990. This anomaly is noticeable also in the density series as a gradual decrease in late 1980s. The GSA'70s, however, is distinct in temperature also which peaked in 1979–1980. This anomaly was especially strong in salinity, with a pronounced minimum in 1977–1978.

Isopleth diagrams for the upper 1000 m (Gammelsrød et al., 1992, Fig. 4) (not shown) reveal the thickness (vertical extent) of GSA'70s (and, likely, of GSA'80s

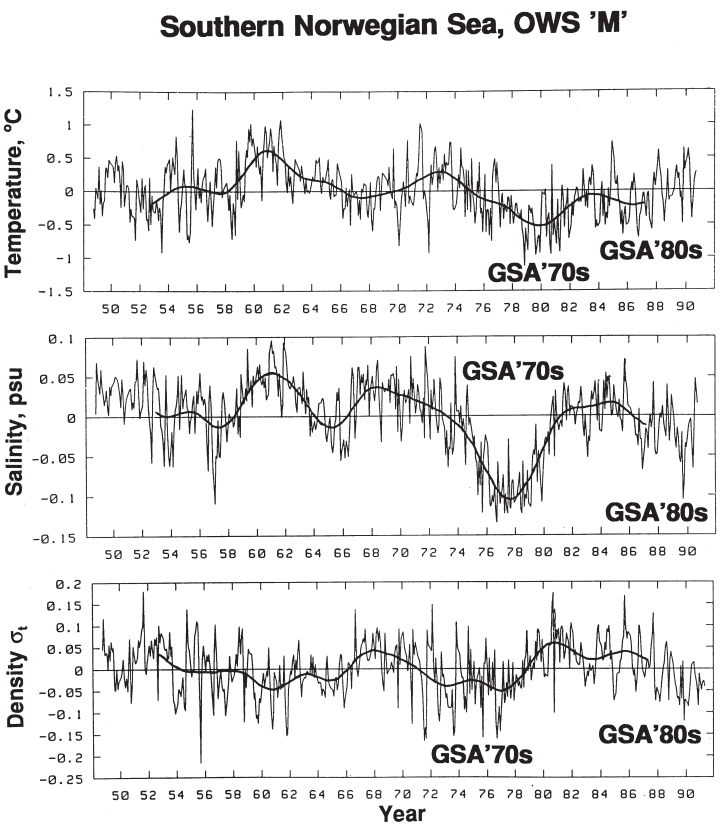

Fig. 22. Monthly mean anomalies of temperature (a), salinity (b), and density σ_t (c) at 50 m at OWS "M", southern Norwegian Sea (Gammelsrød et al., 1992, Figures 3–4).

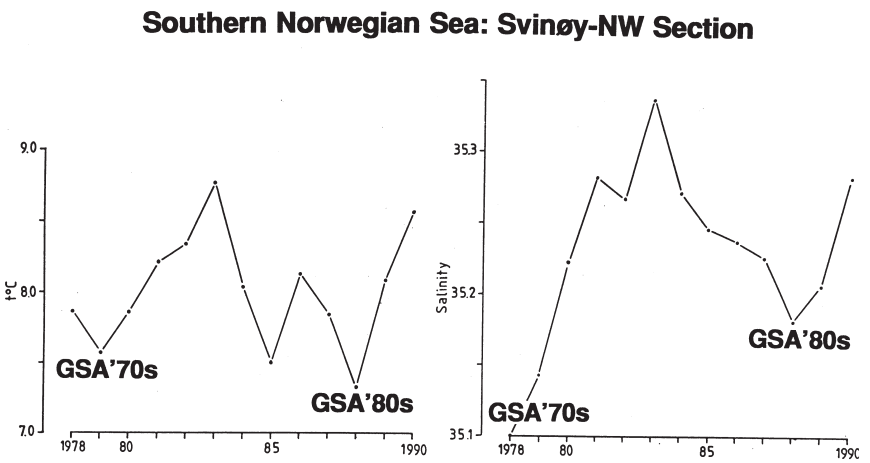

Fig. 23. Summer temperature (a) and salinity (b) in the 50–200 m layer on the Svinøy-NW section, southern Norwegian Sea (Loeng et al., 1992, Fig. 4a).

as well) to be about 500 m. The diagrams demonstrate also that the anomalies first appeared in the surface layers, so the time lag increased with depth.

The anomaly of '70s at OWS 'M' was unusual in that the salinity was clearly leading, not the temperature, as commonly found elsewhere. The cause of this peculiarity is unknown.

Svinøy-NW, Norwegian Atlantic Current, southern Norwegian Sea (Fig. 23 (Loeng et al., 1992, Fig. 4a)). The summer salinity of the 50–200 m layer reached a minimum in 1988 (GSA'80s). The timing of the temperature signal is ambiguous: it has two minima, in 1985 and 1988. The GSA'70s is evident as a salinity minimum in 1978 (or earlier) and a temperature minimum in 1979.

Gimsøy-NW, Norwegian Atlantic Current, northern Norwegian Sea (Fig. 24

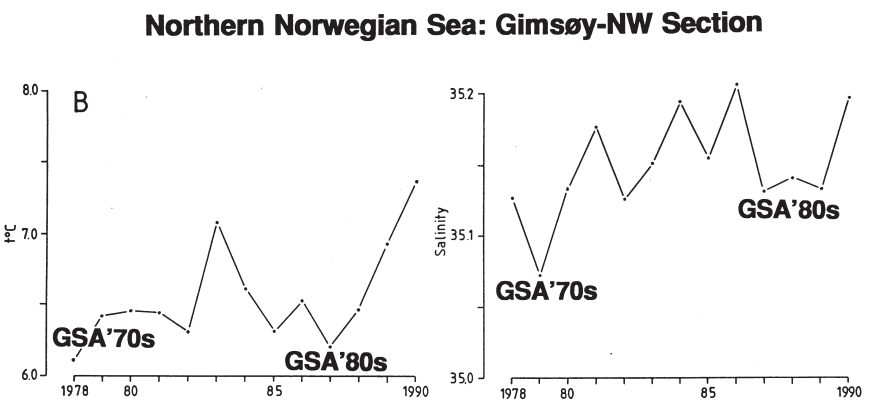

Fig. 24. Summer temperature (a) and salinity (b) in the 50–200 m layer on the Gimsøy-NW section, northern Norwegian Sea (Loeng et al., 1992, Fig. 4b).

(Loeng et al., 1992, Fig. 4b)). The salinity minimum associated with GSA'80s occurred in 1987–89, while the temperature minimum occurred in 1985–1987. Once again, as it was often observed elsewhere, the temperature signal preceeds the salinity signal. The GSA'70s is evident as a temperature minimum in 1978(?) and the salinity minimum in 1979.

3.13. Barents Sea

Fugløya-Bjørnøya (Bear Island), western Barents Sea (Fig. 25 (Loeng et al., 1992, Fig. 3a)). Both anomalies, of '70s and '80s, are clearly seen in the time series of temperature and salinity anomalies for the subsurface layer (50–200 m). The

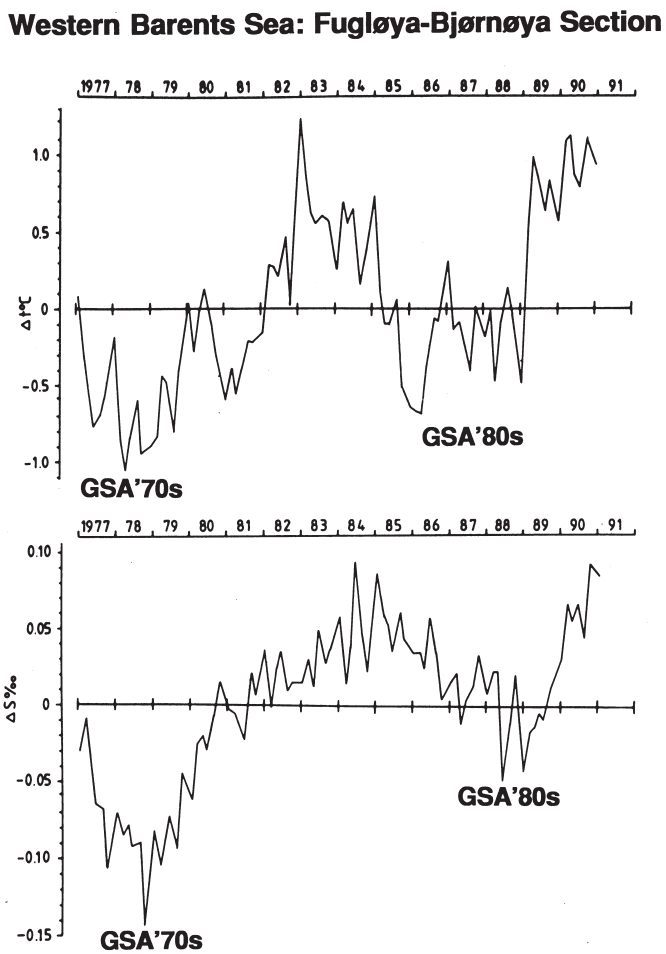

Fig. 25. Temperature (a) and salinity (b) anomalies in the 50–200 m layer on the Fugløya-Bjørnøya (Bear Island) section, western Barents Sea (Loeng et al., 1992, Fig. 3a).

GSA'70s reached its extremum in 1978 (the salinity minimum was observed in late 1978 (Loeng et al., 1992)). The GSA'80s, dated by the salinity, peaked in 1988; its timing in the temperature record being ambiguous, although both T and S increased sharply in 1989.

Vardø-N, central Barents Sea (Fig. 26 (Loeng et al., 1992, Fig. 3b)). Along this section, the pattern was similar to the previous one: The GSA'70s and GSA'80s are pronounced in both T and S, although these decadal–scale anomalies are defined better in the salinity series than in the temperature. The GSA'70s peaked in 1979 (the salinity minimum occurred about six months later than along the previous section (Loeng et al., 1992)). The GSA'80s peaked in the winter of 1988–1989. Again, dating using the salinity anomaly is quite unambiguous, whereas the temperature series is more complicated.

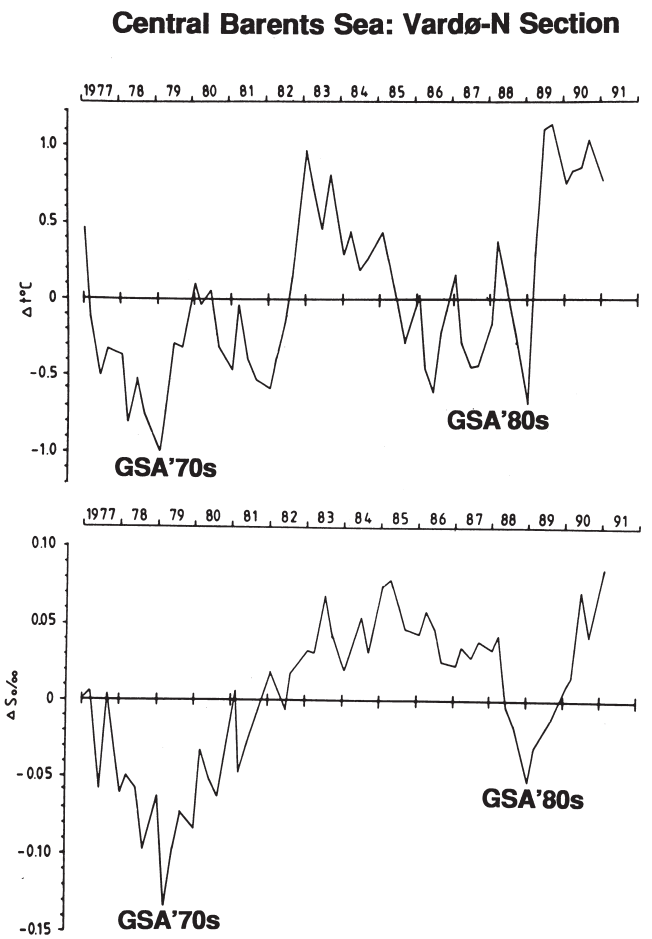

Fig. 26. Temperature (a) and salinity (b) anomalies in the 50–200 m layer on the Vardø-N section, central Barents Sea (Loeng et al., 1992, Fig. 3b).

Kola-N, southern Barents Sea (Fig. 27 (Loeng et al., 1992, Fig. 7b)). For this section we have only a temperature series for the 0–200 m layer and this shows a pronounced minimum in 1979 (GSA'70s) and an extended period of the decreasing temperature which reached a minimum in 1988–1989 (GSA'80s).

The three Barents Sea time series, which we have discussed above, have in common one peculiar feature: an extremely sharp, almost step-like return to the warmer (and saltier) conditions that occurred in 1989–1990, after the GSA'80s (Figs. 25–27). During this dramatic recovery, the temperature and salinity of the Barents Sea surface waters reached the highest values observed since 1977.

Fig. 28 (Korsbrekke et al., 1995, Fig. 4.2) presents a composite of three time series based on the data from winter surveys in the western, central, and eastern Barents Sea (salinity data for 1982 along Vardø-N section is missing (S. Mehl, 1997, personal communication)). Once again, the GSA'70s and GSA'80s are evident, especially in salinity.

3.14. West Spitsbergen Current

Sørkapp-W, West Spitsbergen Current, eastern Greenland Sea (Fig. 29 (Loeng et al., 1992, Fig. 4c)). The GSA'80s peaked first in the temperature (1986–1988), then in the salinity (1988). The GSA'70s had a similar T-S time lag: the temperature reached a minimum in or before 1978, while the salinity peaked in 1979.

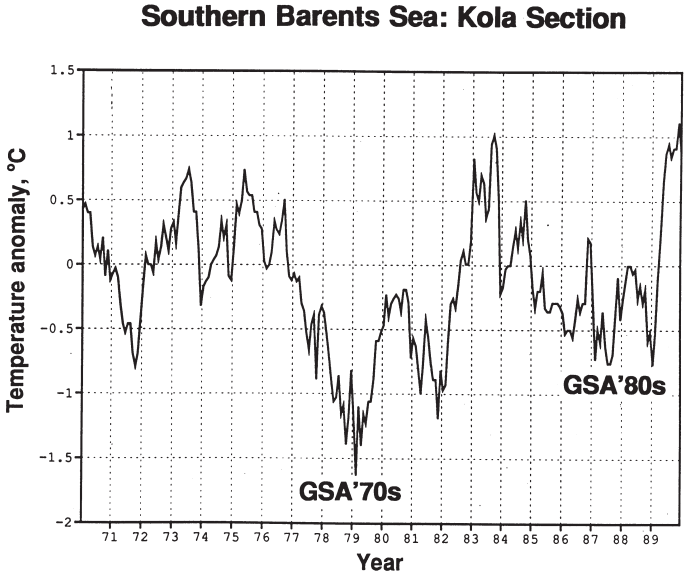

Fig. 27. Monthly temperature anomalies in the 0–200 m layer on the Kola section, southern Barents Sea (Loeng et al., 1992, Fig. 7b).

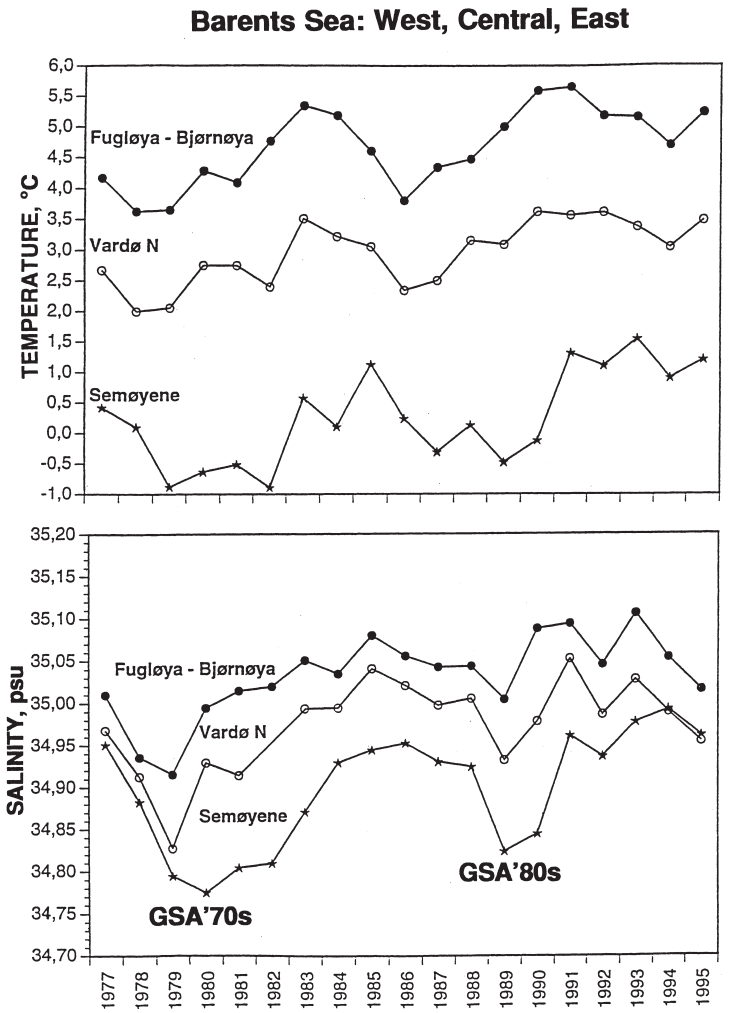

Fig. 28. Mean temperature (top) and salinity (bottom) in the 50–200 m depth layer during the winter surveys of 1977–1995 in the Barents Sea (Korsbrekke et al., 1995, Fig. 4.2) along Fugløya-Bjørnøya (Bear Island) section in March (upper curves), Vardø-N section in March (middle curves), and Semøyene (Sem Islands)-N section in January–February (bottom curves).

3.15. Return to the Iceland Sea

Iceland Sea (Fig. 30 (collated from Malmberg and Blindheim (1994), Figs 5a,b and Malmberg et al. (1996), Figs 5 and 7). Malmberg et al. (1990) have distinguished a "small anomaly" in the Arctic Intermediate Water *north* of Iceland in 1989–1990, when its core salinity was 34.92, which is significantly lower than 34.95 observed in 1987–1988. Malmberg et al. (1990) also related this anomaly to the low-salinity anomaly observed *south* of Iceland in 1985–1988 and (hypothetically) traced the

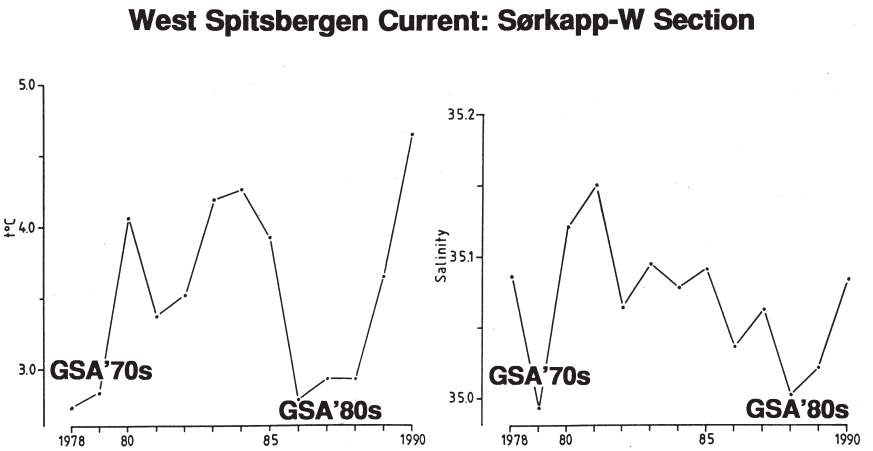

Fig. 29. Summer temperature (a) and salinity (b) in the 50–200 m layer on the Sørkapp-W section, West Spitsbergen Current (Loeng et al., 1992, Fig. 4c).

latter back to the low-salinity anomaly of 1975–1979 *north* of Iceland. Fig. 30 displays three time series from north and northeast of Iceland, with several low-salinity events (associated with invasions of Polar Water (Pol.) shown in the upper panel) being evident. The late 1960s event corresponds to the beginning of the GSA'70s; the late 1970s event(s) might signal the GSA'70s return from the south via the Irminger Current, then via the anticyclonic circulation around Iceland; the 1982 event might manifest the GSA'70s return from the north (from the East Greenland Current) via the East Icelandic Current; finally, the 1988–1990 event is apparently associated with the return of the next anomaly, the GSA'80s, either from the south (via the Irminger Current) or from the north (via the East Icelandic Current).

4. Discussion

4.1. Source: local versus remote

According to Dickson et al. (1988), the GSA'70s was indirectly caused by an intense, persistent high pressure anomaly cell established over Greenland in the 1960s (as documented by Dickson et al. (1975) who originally suggested this idea to explain the Greenland Sea GSA), resulting in abnormally strong northerly winds over the Greenland Sea that brought an increased amount of cold, fresh Polar water to Iceland. When surface salinities there decreased below a critical value of 34.7 (Malmberg, 1969), convective overturn ceased and ice started to form. Thus the cold, fresh anomaly was developed that was subsequently transported around the northern North Atlantic. Although Dickson et al. (1988) considered the Iceland Sea processes to be important in the formation of the GSA'70s, they unequivocally point to the Arctic Ocean as being the main source of the anomaly.

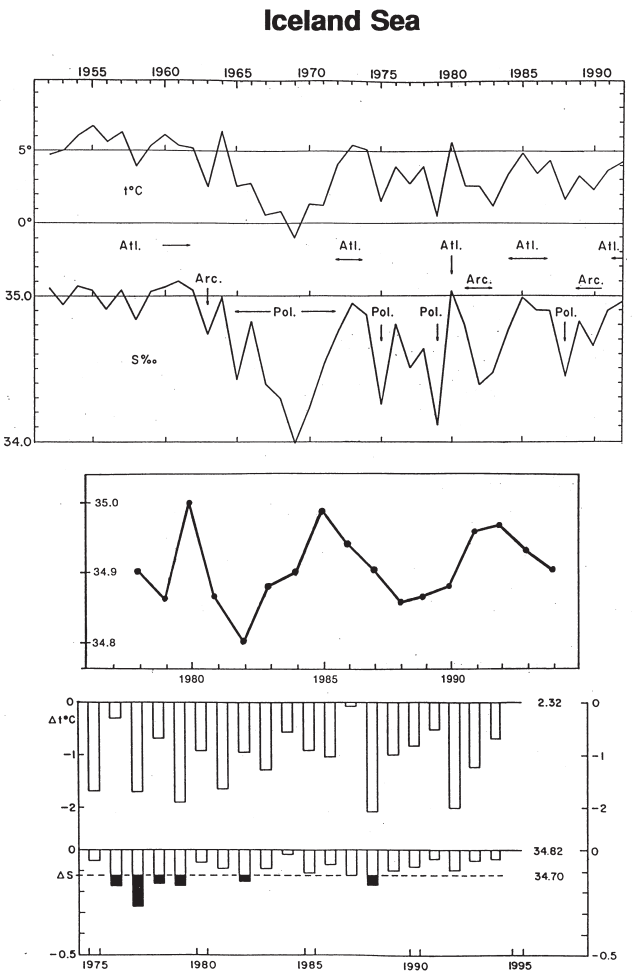

Fig. 30. Top: Temperature and salinity at 50 m in North Icelandic waters, May/June 1952–1992 (modified after Malmberg and Blindheim, 1994, Fig. 5a,b). Middle: Maximum salinity in the upper 300 m at Station S3 in North Icelandic waters, May/June 1978–1994 (modified after Malmberg et al., 1996, Fig. 7). Bottom: Anomaly of temperature and salinity at 25 m in the East Icelandic Current, spring 1975–1994 (modified after Malmberg et al., 1996, Fig. 5); the averages for the 1950–1958 period are shown to the right of the bar charts.

Aagaard and Carmack (1989) also viewed the Arctic Ocean as the feasible source of the GSA'70s and even stated that the anomaly *must* have had originated as a result of an increased fresh water discharge via Fram Strait (p.14,485). They claimed also that the suggested origin in the Arctic Ocean "can be contrasted with an origin north of Iceland, as hypothesized by Dickson et al. (1988)" (p.14,495), although both works are in reasonable agreement with regard to the main source of the GSA'70s.

The apparent "local versus remote" dilemma is resolved by Dickson (1995), p.312

as follows: The record extent of sea ice in the Greenland and Iceland Seas in the late 1960s (and, one might add, the record magnitude of the GSA'70s) was caused partly by remote forcing from the Arctic Ocean and partly by local preservation of the freshwater layer in the Iceland Sea, the latter being fundamental for the accumulation of the GSA'70s.

4.2. Salinity-sea ice link

Mysak and Manak (1989) noted that during its passage from the Greenland Sea to the Labrador Sea, the GSA'70s was accompanied by a large sea-ice extent anomaly, and proposed (*ibid*., p.400) that advection of negative salinity anomalies around the subpolar gyre could account for the apparent movement of positive ice anomalies. Exploring the Malmberg (1969) idea of surface freshwater enhancement of sea ice growth, Marsden et al. (1991) have shown that salinity anomalies actually lead sea ice anomalies (see also a discussion in Houghton (1996) who concurred with the above conclusion). The sea-ice propagation from the Greenland Sea into the Labrador Sea has been confirmed by Mysak et al. (1990), based on cross-correlation analysis of the 1953–84 ice data, with a notable exception, the large positive 1983 ice anomaly in the Labrador Sea, which had no counterpart in the Greenland Sea a few years earlier (Mysak et al., 1990, Fig. 3 and p.114). Actually, Mysak and Manak (1989), p.398 have already considered a hypothesis that the large positive 1972 ice anomaly in the Labrador Sea was "simply due to anomalous local atmospheric and oceanic conditions." They also suggested that severe ice conditions during winters 1983 and 1984 were due to anomalously strong northerly winds over the Labrador Sea, driven by a persistent high south of Hudson Bay, whose origin is supposedly associated with the 1982–83 ENSO event. Their Figs 18–19 clearly show that the 1983–84 ice anomaly in the Baffin Bay/Labrador Sea had not been preceded by a similar upstream anomaly in the Greenland Sea a few years earlier (see also Agnew (1993), Table 1). This conclusion is corroborated by the results of Chapman and Walsh (1993), Fig. 7, reproduced in Fig. 31, and of Parkinson and Cavalieri (1989), Figs 9 and 11, although the latter have obtained a weak maximum in 1979 in the Greenland Sea which, if significant at all, could be a precursor of the 1983–84 maximum in the Baffin Bay /Labrador Sea area. It is noteworthy that the GSA'80s sea ice extent anomaly in Davis Strait/Labrador Sea was even larger than the GSA'70s sea ice extent anomaly in the Greenland Sea ($40.7 \times 10^4 km^2$ in 1984 versus $33.4 \times 10^4 km^2$ in 1969, respectively, peak values, according to Table 1 from Agnew (1993)).

Thus the GSA'80s was apparently formed in the Baffin Bay /Labrador Sea region as a result of the extreme local atmospheric forcing of the early 1980s. The magnitude of this climatic anomaly was exceptional: At both Egedesminde and Godthåb, 1983 and 1984 were the coldest years on record since 1866, with annual air temperature anomalies of − 4.3°C and − 3.4°C in 1983, and − 4.3°C and − 3.7°C in 1984, respectively, below the 1946–60 reference period mean (Climatic Research Unit, 1985)(the Godthåb record is shown in Fig. 32 (Drinkwater, 1994, Fig. 5)).

The severity of the 1982–84 (and also 1972–74) ***ice conditions*** in this region can be further illustrated by *iceberg data* (Fig. 33) of the annual number of icebergs

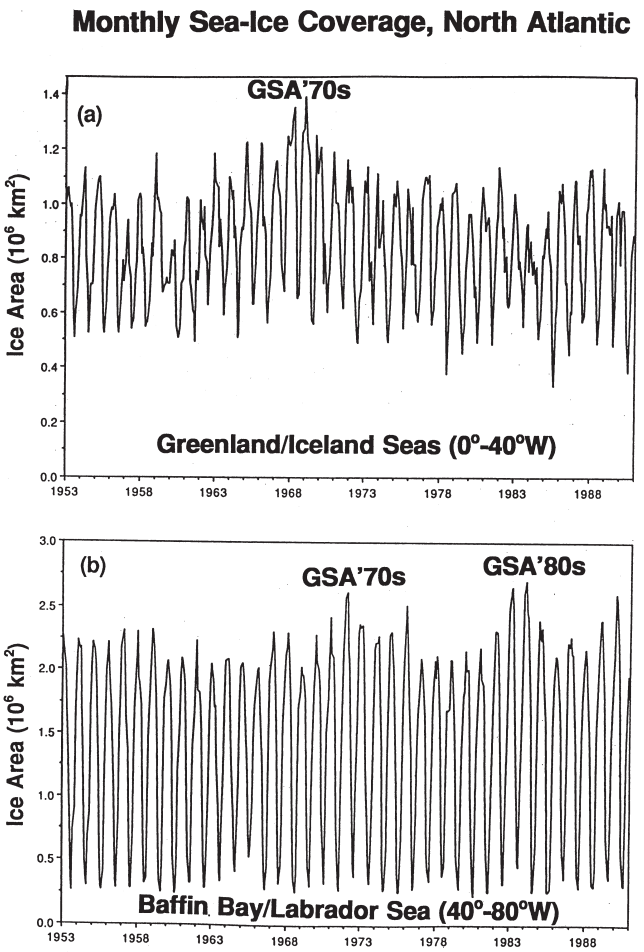

Fig. 31. End-of-month sea-ice coverage in longitudinal sectors containing (a) Greenland/Iceland Seas, GIS (0° – 40°W), and (b) Baffin Bay/Labrador Sea, BBLS (40° – 80°W) (modified after Chapman and Walsh, 1993, Fig. 7)). Note that, while the GSA'70s maximum in the BBLS has been preceeded by a maximum in the GIS, the GSA'80s maximum in the BBLS had no upstream precursor in the GIS.

passing the Grand Banks and crossing 48°N (Trivers, 1994). This number is a good index of general sea-ice severity because it correlates with sea-ice extent but is "relatively insensitive to iceberg production rates and to fluctuations in southerly iceberg fluxes in areas north of Baffin Island" (Marko et al., 1994, p.1335).

Mysak et al. (1990) proposed a ***negative feedback loop***, simplified by Mysak and Power (1992), which explains the GSA'70s origin by teleconnections with the western Arctic, particularly by large runoffs into the western Arctic during the mid-1960s. According to this scheme (Fig. 34), increased precipitation in northern Canada, by increasing the Mackenzie River runoff into the Beaufort Sea, leads to increased production of sea ice in the western Arctic Ocean. This pulse of sea ice is exported via

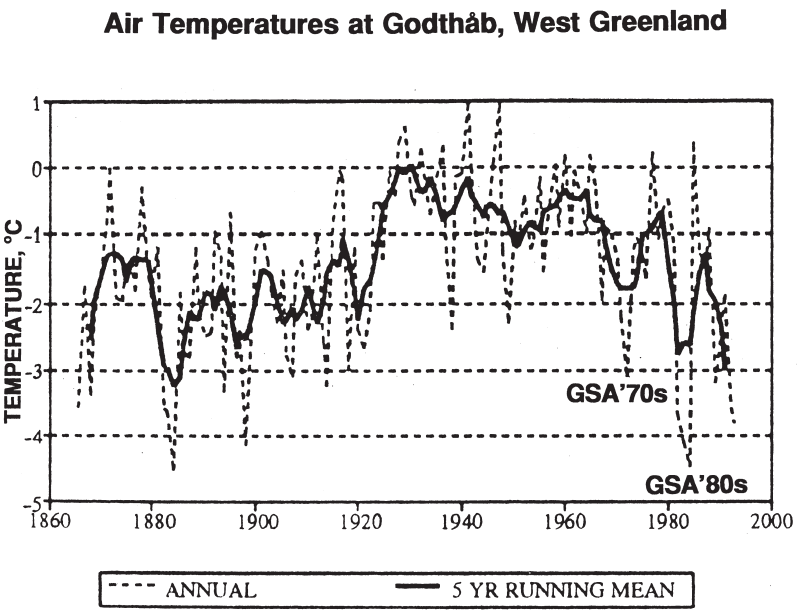

Fig. 32. Annual air temperatures at Godthåb, West Greenland (Drinkwater, 1994, Fig. 5).

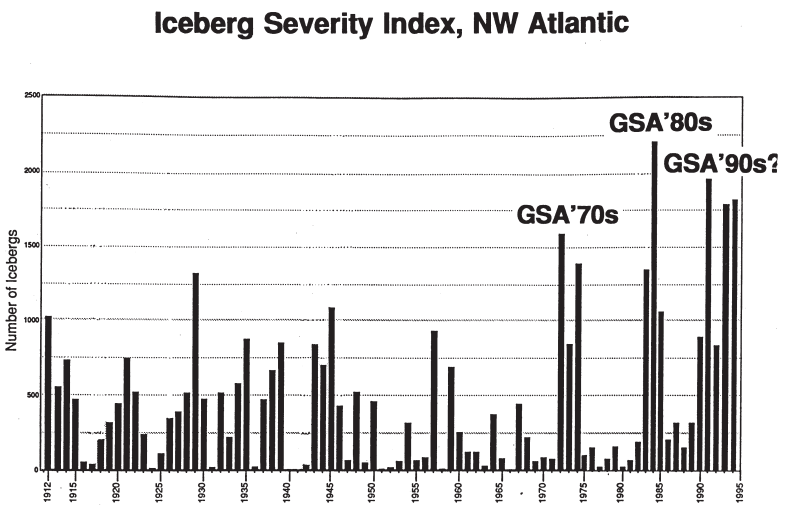

Fig. 33. Annual counts of icebergs crossing 48°N (modified after Trivers (1994), Fig. 1).

Fram Strait into the Greenland and Iceland Seas, where it melts, resulting in upper-layer freshening, stability enhancement, and suppression of convective overturn and of deep water formation; thus a new GSA is formed. A reduction in heat exchange of the upper layer with underlying warm Atlantic waters results in decreases in

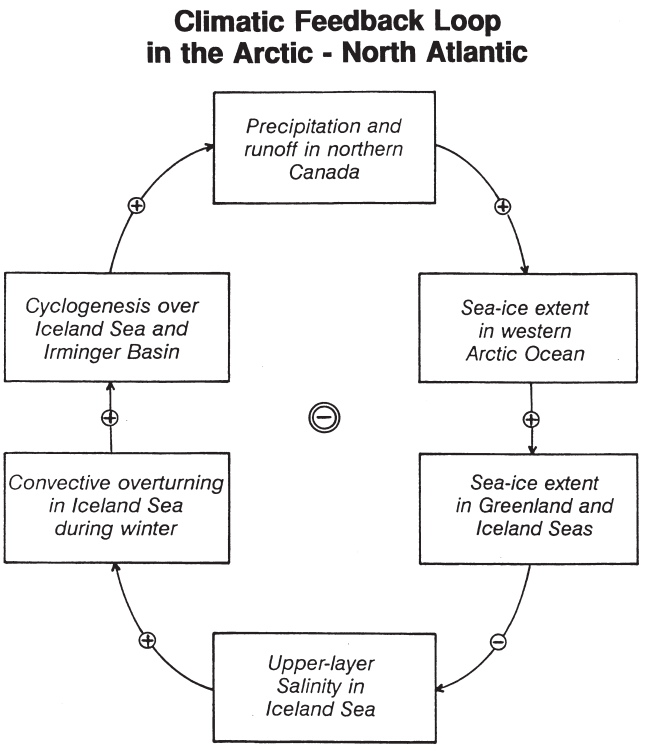

Fig. 34. Negative feedback loop linking the Arctic and subpolar North Atlantic (Power and Mysak, 1992, Fig. 1), a simplified version of the 10-component loop suggested by Mysak et al. (1990), Fig. 24, to account for Arctic/North Atlantic interdecadal climate oscillations.

ocean-to-atmosphere heat flux, cyclogenesis, and precipitation over northern North America, thus closing the loop.

The weakest links of the feedback loop are those related to the atmospheric hydrological cycle, i.e. cyclogenesis and precipitation, not to mention the relationship between precipitation and runoff, which is not necessarily linear. As shown by Bjornson et al. (1995), the main source for the Mackenzie basin precipitation fluctuations is the North Pacific, not Atlantic, as implied by the feedback loop. Mysak (1995) argues that the atmospheric link still can be considered operational thanks to results by Walsh et al. (1994). They studied water vapor fluxes across 70°N in 1973–90 and found that the maximum northward flux occurred around 10°E (Norwegian Sea) and the maximum southward flux around 260°E (Mackenzie Basin). However, to assert the validity of the suggested link in the case of the GSA'70s, "an interannual variability study of the water vapor fluxes from the Norwegian Sea to the Mackenzie basin, their convergence over the latter region and the observed precipitation there would have been carried out for those years just before, during, and just after the GSA" (Mysak, 1995, pp. 12–13).

The negative feedback loop discussed above was used by Mysak et al. (1990) to

predict another large positive sea ice extent anomaly in the Greenland sea in the late 1980s. Based on the winter data of 1987 and 1988, Mysak and Power (1991), pp. 88–89 claim the detection of such an anomaly. This, however, is in contradiction to the data in Agnew (1993), Table 1 which actually reveals there was a ***negative*** anomaly of $-4.4 \times 10^4 km^2$ in 1987 and only a very moderate positive anomaly of $8.4 \times 10^4 km^2$ in 1988 (compare with the massive GSA'70s anomaly which peaked at $33.4 \times 10^4 km^2$ in 1969 (Agnew (1993), Table 1)).

4.3. Remote forcing of GSAs and the Arctic Ocean fresh water budget

Passing the Labrador Coast, the GSA'70s had a salt deficit of 72×10^9 tons (Dickson et al., 1988). This fresh water excess of 2000 km^3 is equivalent to ~50% of the annual fresh water flux of the East Greenland Current through Fram Strait; the GSA'70s "can therefore be accounted for by a moderate perturbation of the outflow from the Arctic Ocean, for instance, a 2-year period of fresh water flux 25% above normal" (Aagaard and Carmack, 1989, p. 14495; a summary of the Fram Strait flux estimates is provided by Simonsen and Haugan (1996)). How likely is a perturbation of this magnitude and what mechanism(s) could account for it? To answer these questions, we should consider the freshwater budget of the Arctic Ocean.

The main positive components of the Arctic Ocean freshwater budget are river runoff, the Bering Strait inflow, and precipitation minus evaporation, (P-E), according to Aagaard and Carmack (1989), the primary reference on this subject until a recent work by P. Becker (1995). One advantage of Becker's work is his analysis of the ***interannual and long-term variability*** of river discharge and the Bering Strait inflow, features ignored by Aagaard and Carmack (1989). Using newly acquired Russian data to quantify the annual runoff discharge for the Arctic rivers for the years 1937–86 and the Bering Strait freshwater flux for 1941–87, Becker (1995) derived a mean annual river discharge of 2646 km^3/year, with a standard deviation of 150 km^3/year (for the 1973–87 period, when the Russian data overlap with the North American data)(Fig. 35), and a mean annual fresh water flux through the Bering Strait of 1829 km^3/year (0.058 Sv, ranging from -0.03 Sv to 0.12 Sv), for the 1941–1987 period (Fig. 36). The least known component of the Arctic Ocean fresh water budget is P-E; estimates vary between 400 km^3/year and 1400 km^3/year (Aagaard and Carmack, 1989). Variability of P-E is still unknown, although it might be estimated through water vapor flux convergence calculated from rawinsonde data. Using high-latitude rawinsonde data for 1973–1990, Walsh et al. (1994) have shown that the annual totals of the flux convergence are correlated with station-derived precipitation over the Mackenzie domain and with yearly variations of the Mackenzie discharge.

Table 3 summarizes estimates of main sources of fresh water input into the Arctic Ocean. Analysis of Table 3 shows that variations of positive components of the Arctic Ocean fresh water budget *per se* are too small to explain a large low-salinity anomaly of the GSA'70s' scale. Moreover, the residence times of fresh water inputs in the Arctic Ocean are several decades (Becker and Björk, 1996). Therefore, the

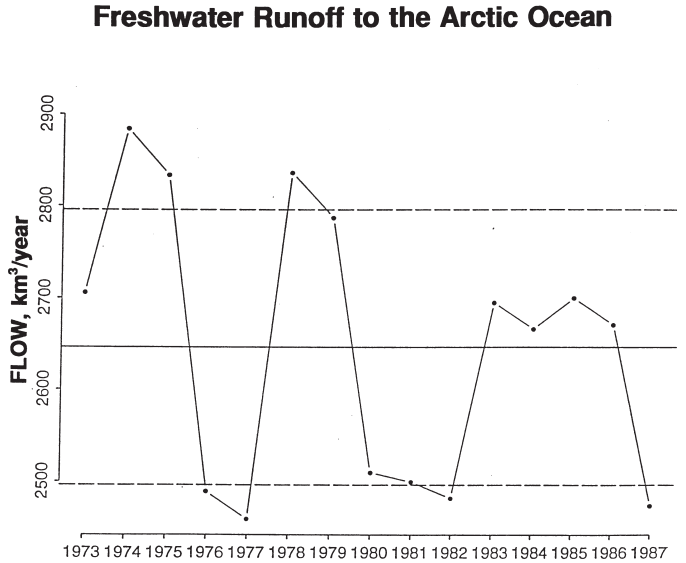

Fig. 35. Annual freshwater runoff to the Arctic Ocean derived from direct measurements of river discharge and an estimate of ungauged discharge (Becker, 1995, Fig. 12). The solid line is the mean, and the dashed lines are ± standard deviation from the mean.

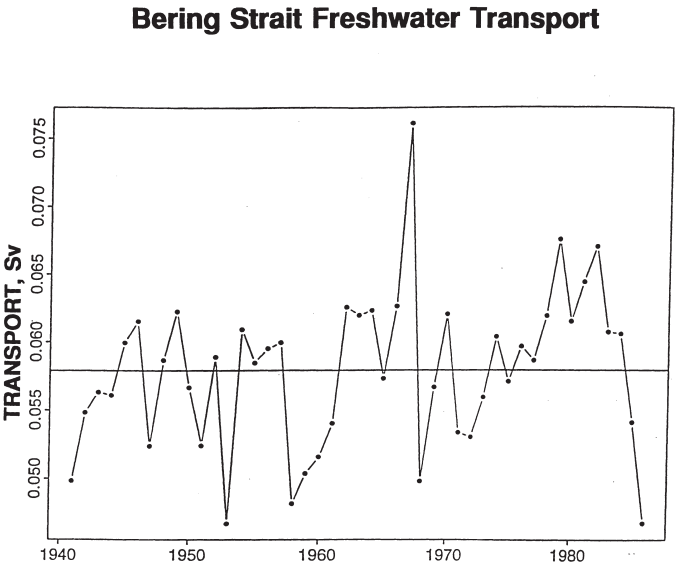

Fig. 36. Estimated annual mean freshwater transport through Bering Strait (Becker, 1995, Fig. 21). The horizontal line is the long-term mean of 0.058 Sv (1 Sv = 10^6 m^3/s = 31,536 km^3/year).

Table 3
Main sources of fresh water input into the Arctic Ocean (Notations: N/A, Not Available; σ, Standard Deviation)

Source	Mean Flux, km^3/yr	Variability	Time Period	Reference
River Runoff	3300	N/A	N/A	Aagaard and Carmack (1989)
	2646	σ = 150 km^3/yr	1973–1987	Becker (1995)
	1104	N/A	N/A	Steele et al. (1996)
Bering Strait	1670	N/A	N/A	Aagaard and Carmack (1989)
	1829	− 914 to 3658 km^3/yr	1941–1987	Becker (1995)
	1987	N/A	N/A	Steele et al. (1996)
Precipitation Less Evaporation, P-E	900	400 to 1400 km^3/yr	N/A	Aagaard and Carmack (1989)
	1652*	± 50%	1973–1990	Walsh et al. (1994)
	631	N/A	N/A	Steele et al. (1996)
Norwegian Coastal Current	250	N/A	N/A	Aagaard and Carmack (1989)

*Calculated from the 18-year annual mean moisture flux convergence of 17.3 cm/yr (Walsh et al., 1994) and the Arctic Ocean area of 9.55×10^6 km^2 (Aagaard and Carmack, 1989).

Arctic Ocean acts to smooth any interannual and multi-year (multi-annual) anomalies of fresh water input (Fig. 37) (Becker, 1995; Becker and Björk, 1996), and so Becker (1995) concluded that the only plausible cause of GSAs could be wind.

4.4. Arctic contribution I: northerly winds and Ellesmere pack

The dominant role of persistent wind anomalies in generating the GSA'70s has been postulated by Dickson et al. (1988), who emphasized the importance of sea level pressure (SLP) anomalies over the Greenland Sea. The concept of wind forcing has been supported and expanded by Walsh and Chapman (1990), who have shown that "the roots of the Great Salinity Anomaly can be traced to the atmospheric circulation not only locally (east of Greenland) but also over the Arctic Ocean" (*ibid*., p.1470). In particular, they showed that the SLP difference between southern Greenland (65°N, 40°W) and the Siberian coast (70°N, 150°E) reached its peak value for the 20th century in 1969 (Walsh and Chapman, 1990, Fig. 10), coinciding with the start of the GSA'70s. Moreover, Walsh and Chapman (1990) have shown that the SLP anomaly pattern of 1967–68 (their Fig. 4) should have contributed to an enhanced export from the Arctic Ocean of the thickest, oldest (hence less saline) sea ice from offshore of northern Canada and Greenland. Indeed, the thickness of multi-year pack ice north of Ellesmere Island exceeds 7 m (Bourke and Garrett, 1987, Fig. 5), and its average salinity can be as low as 2 (e.g., Thomas et al., 1996). Therefore an impact on the northern North Atlantic of an enhanced wind-forced export of the extremely thick, relatively fresh sea ice in late 1960s should be especially significant.

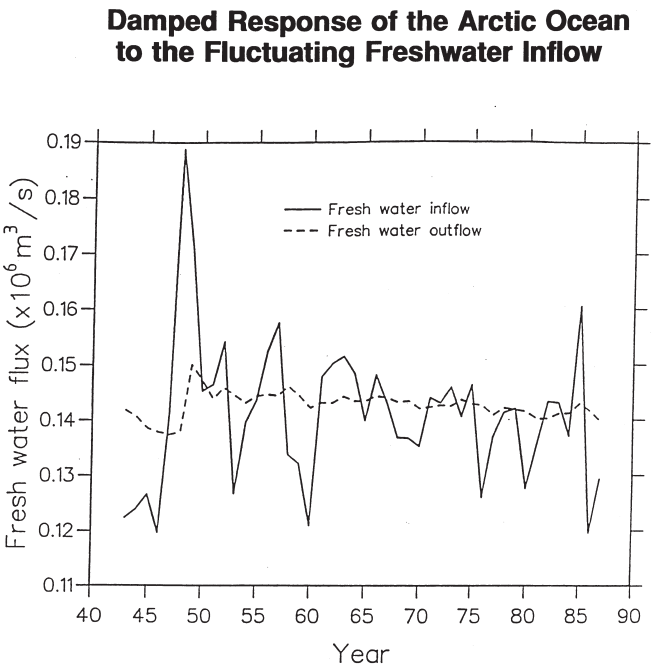

Fig. 37. Arctic Ocean freshwater inflow (rivers and Bering Strait) and model-simulated freshwater outflow (water plus ice), 1943–1987 (Becker, 1995, Fig. 36; Becker and Björk, 1996, Fig. 15).

The likelihood of a substantial ice export enhancement appears to be high: Thomas et al. (1996) have estimated that ice export via the Fram Strait ice export varies widely, from 1100 to 3000 km^3/year. Using a balance model, Steele et al. (1996), Fig. 10a, found that year-to-year changes in this ice export in the early 1980s amounted to nearly 0.04 Sv or 1261 km^3/yr. If such an anomaly were to be sustained for two years, it could cause a GSA comparable with the GSA'70s whose fresh water excess was about 2000 km^3 (Section 4.3). The most recent observations confirm that the interannual variability of the Fram Strait ice export is large enough to account for the GSA'70s (Aagaard et al., 1996).

The concepts of local versus remote forcing of the GSA'70s are complementary rather than mutually exclusive because "it appears that the Arctic component of the forcing provides a "remote boost" to the local forcing in the sense that the strongest oceanic impacts (e.g., a "Great Salinity Anomaly") will result when the phasing of ***both*** the local and the remote forcing is favorable. An enhanced outflow of Arctic ice ***without*** favorable local forcing east of Greenland will evidently not result in noteworthy anomalies of ocean temperature and salinity" (Walsh and Chapman, 1990, p.1471).

The above results have been corroborated by Serreze et al. (1992), who have shown that the mean winter SLP gradient between Ellesmere Island and the North Pole during 1966/67 to 1970/71 was persistently positive. The corresponding southward shift of anticyclonic activity, though modest, "may have contributed to an

anomalous pressure gradient north of Ellesmere Island and Greenland, increasing the contribution of multiyear ice to the Fram Strait ice outflow" (*ibid*., p.296).

The suggested scenario of wind forcing of the GSA'70s has been modelled by Häkkinen (1993). The model has reproduced large pulses of Fram Strait sea ice export, followed by large, persistent positive sea ice anomalies in the Greenland Sea. The model has also simulated the two large fresh anomalies in the Arctic Ocean, which entered the Greenland Sea in 1963–65 and in 1967–69. If these low-salinity anomalies coincided with large ice pulses from Fram Strait, as suggested by the model, this co-occurrence could have triggered the GSA'70s.

The crucial role of the Arctic Ocean freshwater outflow in generating advective anomalies in the North Atlantic was also demonstrated by Delworth et al. (1997) using a coupled ocean-atmosphere model. In a 2000-year integration, pronounced 40–80-year oscillations of temperature and salinity occur in the Greenland Sea, preceded by large-scale near-surface salinity anomalies in the Arctic, which appear to propagate via the East Greenland Current into the Labrador Sea and the central North Atlantic.

4.5. Local origin: Labrador Sea

The studies, reviewed above, emphasize the leading role of ***remote*** forcing of GSAs in the North Atlantic, such as the Arctic Ocean forcing, but largely ignore processes in marginal seas. Such processes, however, may be crucial for development of large-scale TS-anomalies in the North Atlantic. The Labrador Sea seems to be of particular importance because, as pointed out by Wohlleben and Weaver (1995), p.460a: "Recent modelling studies (Delworth et al., 1993; Weaver et al., 1994; Weisse et al., 1994) suggest that the source of interdecadal climate variability for the North Atlantic may well lie in the Labrador Sea."

For example, salinity-induced density perturbations (hence dynamic topography variations) observed in a fully coupled ocean-atmosphere model by Delworth et al. (1993) are largely confined to the Northwest Atlantic, particularly to the Labrador Sea. As shown by Deser and Blackmon (1993), the decadal variability in the sea ice extent in the Labrador Sea is closely linked to decadal variations in SST east of Newfoundland, with periods of positive sea ice extent anomalies in the Labrador Sea preceding by ~1–2 years periods of negative SST anomalies east of Newfoundland (Fig. 38, after Deser and Timlin, 1996, Fig. 3). The Labrador Sea might also play a major role in development of decadal-scale salinity anomalies in the North Atlantic, as shown by Weisse et al. (1994). They modelled the generation and propagation of such anomalies (with timescales of 10 to 40 years), applying the white noise freshwater flux forcing to the Labrador Sea *alone*, while the same forcing applied everywhere except the Labrador Sea did not excite any significant decadal variability in the North Atlantic. Their results imply that the Labrador Sea is the source of the decadal-scale variability observed over the entire North Atlantic, which is caused by variations in the local freshwater flux and "crucially depends on the relative isolation of the Labrador Sea in order for that basin to act as in integrator of the white noise time series of the freshwater flux" (Weisse et al., 1994, p.12420).

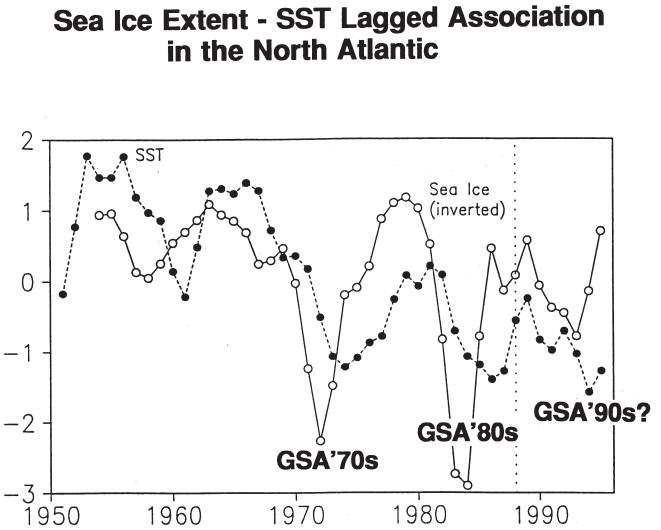

Fig. 38. Standardized anomalies of winter sea ice extent east of Newfoundland (46°–54°N, 55°–45°W, open circles) and SST in the subpolar North Atlantic (50°–60°N, solid circles) (modified after Deser and Timlin, 1996, Fig. 3). The vertical dotted line shows the last year of data presented in Deser and Blackmon (1993). The ice index has been inverted to expose association between high ice extent and low SST.

Using an idealized model of the North Atlantic, Weaver et al. (1994) have found the Labrador Sea to be the source of decadal (22 years) TS-variability. However, this variability is ***thermally*** driven and is insensitive to the freshwater flux (and wind forcing) used, contrary to the results of Weisse et al. (1994).

It should be noted that neither model contains an ice component although ice-ocean interactions alone can excite TS-variability (Yang and Neelin, 1993; Zhang et al., 1995).

Labrador Sea processes also play the dominant role in the interdecadal feedback loop (with a timescale of 21 years; Fig. 39, after Wohlleben and Weaver, 1995), similar to the one by Mysak et al. (1990) except that the new loop includes neither the intensified GIN Sea cyclogenesis nor increased Mackenzie River runoff to explain enhanced ice export via Fram Strait. Instead, Wohlleben and Weaver (1995) use the idea (suggested independently by Dickson (1995) and supported statistically) that subpolar SST anomalies over the North Atlantic (mainly, over the Labrador Sea) affect atmospheric sea level pressure anomalies over Greenland, and so result in the anomalous freshwater/sea ice transport from the Arctic Ocean via Fram Strait. These anomalies are advected into the Labrador Sea, suppressing convection and increasing meridional gradients across the North Atlantic Current; the intensified current transports increased amount of warm and salty water via the Irminger Current into the Labrador Sea, thus starting the second (reverse) part of the loop.

It should be noted also that the three major consecutive sea-ice anomalies of the early 1970s, 1980s and 1990s, in Hudson Bay, Baffin Bay and the Labrador Sea, are related to the three strong episodes of the **North Atlantic Oscillation** (NAO)

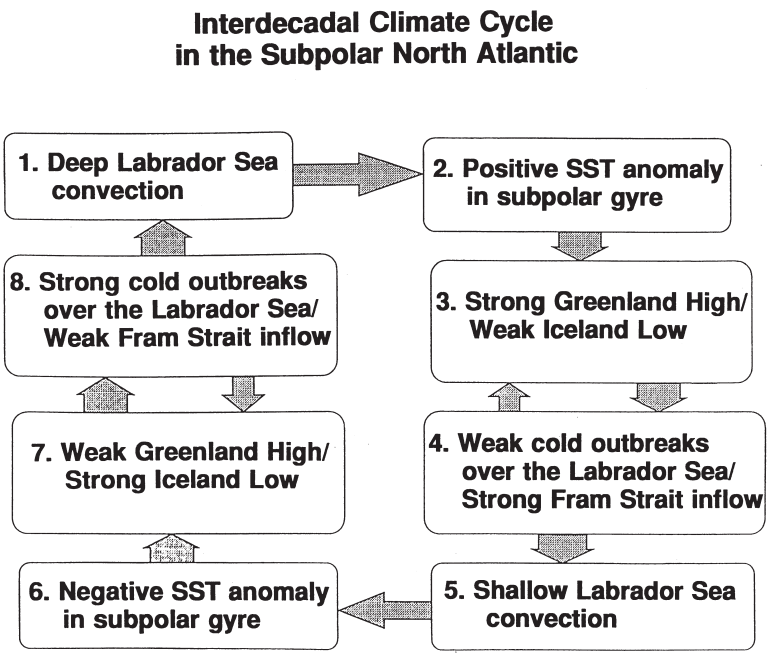

Fig. 39. Proposed interdecadal climate cycle for the subpolar North Atlantic (modified after Wohlleben and Weaver, 1995, Fig. 4).

and the **El-Niño-Southern Oscillation** (ENSO), based on cross-correlations between sea-ice extent, air temperature, the NAO index, and the Southern Oscillation index (Wang et al., 1994; Mysak et al., 1996). Using similar approaches, Drinkwater (1994) found that the Northwest Atlantic air temperatures (hence sea ice conditions) are linked to the large-scale atmospheric circulation pattern (characterized by the NAO index), while Prinsenberg et al. (1997) have shown the interannual variability of the sea ice extent along the Labrador and Newfoundland coasts is strongly correlated with large-scale North Atlantic atmospheric circulation anomalies described by the NAO index.

4.6. Arctic contribution II: Canadian Archipelago outflow

In Section 4.3–4.5 two different modes of the GSA formation are contrasted, remote and local, considered thus far as if they are mutually exclusive. In reality they can be combined: The local formation in the Labrador Sea might be greatly facilitated by an enhancement of freshwater outflow through the Canadian Archipelago (CA). We feel that the importance of the Arctic Ocean in remotely boosting the GSA formation via the CA has been overlooked in the past, being overshadowed by the perceived crucial role of the Fram Strait outflow (Section 4.3). As pointed out by Steele et al. (1996), p.20847, “most models neglect the flow through the Canadian Archipelago, or assume it is small”.

The freshwater flow from the Arctic Ocean through the CA into the Baffin Bay and Hudson Strait, and river discharge into Hudson Bay, are eventually integrated into the Labrador Current. Rudels (1986), p.174 has estimated the ***total*** Arctic surface water transport through the CA to be 0.7 Sv given S = 32.9 (the CA outflow is thus much fresher than the West Greenland Current, with S = 33.2), while other available estimates varied between 1.1 and 2.1 Sv (his Table 5). Rudels (1986), p.171–174 has also estimated the net ***ice export*** out of Baffin Bay to be 970 km^3/yr (with its salinity assumed to be 5). Aagaard and Carmack (1989) estimated the CA ***freshwater*** throughflow to be 920 km^3/yr on the average (assuming, however, its salinity to be 34.2, i.e. 1.3 higher than suggested by Rudels (1986)). These estimates seem rather conservative compared with the latest studies. Using a balance model, Steele et al. (1996) have estimated the CA ***freshwater*** flux to be 0.039 Sv, i.e. 1230 km^3/yr, or 34% of the total Arctic Ocean freshwater outflow. Ross (1992) has measured the Baffin Island Current ***total*** transport in Davis Strait to be 3.3 Sv, much larger than implied by the results of Rudels (1986) cited above. Mertz et al. (1993), Table 1 found that Baffin Bay and Hudson Strait are the largest contributors to the ***freshwater*** flux of the Labrador Current ($3–6 \times 10^4 m^3 s^{-1}$ and $3–10 \times 10^4 m^3 s^{-1}$, respectively, while the East Greenland Current contributes only $2.1 \times 10^4 m^3 s^{-1}$ and ice transport adds $1.9 \times 10^4 m^3 s^{-1}$). Loder et al. (1998), Table II, estimated the ***freshwater*** transport of the Baffin Island Current to be 120 milli-Sv, i.e. 3784 km^3/yr (based on the above results of Ross (1992) and Mertz et al. (1993)), whereas the East Greenland Current brings into the Labrador Sea only 29 milli-Sv (915 km^3/yr) of ***fresh water*** (based on the results of Clarke (1984b)). The ***freshwater*** transport of the Labrador Current through the Flemish Cap section has been estimated by Mertz et al. (1993) to be $1.7 \times 10^5 m^3 s^{-1}$, i.e. 0.17 Sv, which compares favorably with the mean ***freshwater*** transport of 0.13 ± 0.03 Sv, estimated by Petrie and Buckley (1996).

The above estimates show that:

1. The Labrador Current dominates in the total southward ***freshwater*** transport in the northern North Atlantic Ocean as noted by Mertz et al. (1993), pp. 293–294, so that significant long-term variations of the freshwater component of the Labrador Current are of great importance for the entire ocean;
2. The CA outflow appears to be a major contributor to the ***freshwater*** flux of the Labrador Current, so that substantial long-term fluctuations of the CA outflow might trigger (or, at least, facilitate) formation of GSA in the Labrador Sea.

The possibility of the CA freshwater flux variability being related to internal variability in the North Atlantic has been demonstrated by Weaver (1995) who used a coarse ocean general-circulation model to find out that if the CA freshwater flux from the Arctic Ocean into the Labrador Sea is sufficiently weak, 20-year internal oscillations develop under steady forcing.

4.7. Propagation of GSAs in the North Atlantic

The sequence of analogous events, the minima in salinity and temperature time series, observed all around the Subarctic gyre and into the Nordic Seas, clearly shows

the propagation of the GSA'80s to be qualitatively similar to the advection pattern of the 1970s anomaly. The advection speed of GSA'80s, however, was higher so that it took just 6 to 7 years for this anomaly to cover the distance between the Fylla Bank and the Barents Sea (Fig. 2), whereas the GSA'70s arrived in the Barents Sea about 8 to 10 years after it was observed at the Fylla Bank (Fig. 1). Comparison of these two patterns shows that this difference could be accounted for by the circulation of the Subarctic gyre apparently being more sluggish in the 1970s than in the 1980s. The GSA'70s reached OWS "C" about 4 to 6 years after passing by the Fylla Bank, whereas the GSA'80s has arrived in the vicinity of OWS "C" in early 1984 (Fig. 13), just 2 years after it had been observed at the Fylla Bank.

The intensity of the Subarctic gyre circulation can be evaluated using the Labrador gyre, its main component, whose major limbs are the West Greenland Current and the Labrador Current as a proxy. Because no systematic current measurements west of Greenland are available, the Labrador Current data have to be used to estimate the long-term variability of the Labrador (and Subarctic) gyre. The Labrador Current transport is largely determined by the density structure of the Labrador gyre, topography, and boundary flows (Tang et al., 1996). The gyre's density structure appears to be related to ***large-scale wind forcing***, while the local wind stress forcing plays a minor role (Myers et al., 1988, 1989; Reynaud et al., 1995; Tang et al., 1996). In particular, Myers et al. (1989) have found a strong negative correlation between the summer baroclinic transport in the West Greenland and Labrador Currents and the strength of the mid-latitude North Atlantic westerlies in the previous summer. The westerlies' interannual variability is governed mainly by the ***North Atlantic Oscillation (NAO)***, so that high NAO winters are associated with enhanced northerly flow across West Greenland and the Canadian Arctic (Hurrell, 1995). The winter NAO index exhibits pronounced ***decadal variability*** (Hurrell, 1995, Fig. 1a) related to the near-surface (0–400 m) temperature anomalies in the mid-latitude western North Atlantic (Molinari et al., 1997) and also probably associated with the GSA'70s, GSA'80s, and possibly GSA'90s (Mysak et al., 1996). The winter NAO index reveals also a very distinct ***multidecadal ascending trend*** (Hurrell, 1995, Fig. 1a), which might help explain the apparent ongoing intensification of the Subarctic gyre circulation and the faster advection of the GSA'80s compared with the GSA'70s noted above. If this explanation holds also for the GSA'90s, the latter should be transported even faster than the GSA'80s.

The GSAs propagate largely along the shelf-slope areas. The importance of these areas as conduits for advective anomalies has been stressed by Greatbatch and Peterson (1996). The advective factor (i.e. the impact of the TS-anomalies like GSA'70s and GSA'80s) is critically important (especially on the longer time scales, from interannual to decadal) even where other (local) factors are expected to be dominant, e.g. at Sta. 27 (Section 3.4) (Umoh et al., 1995).

Even though the deep water circulation is generally more sluggish compared with the surface circulation, the GSA signal might actually propagate much faster in the deep water layers of the Northwest Atlantic with intense western deep boundary currents once it passed through the Denmark Strait with the Overflow Water (Lazier, 1988, p.1251; Section 4.11).

4.8. Salt budget of GSAs

One of the most difficult problems related to the GSA life cycle is the quantification of their salt budgets. Dickson et al. (1988), pp. 138–143 were the first to try to answer one of basic questions: Is the GSA'70s salt deficit observed in the Northwest Atlantic sufficient to explain the subsequent freshening of the Northeast Atlantic? They estimated the salt deficit of the GSA'70s to be 72 gigatons (Gt) in the Labrador Current, decreasing to 47 Gt in the Faroe-Shetland Channel largely as a result of the North Atlantic Current branching to the north (Irminger Current) and to the southeast (toward Spain). Farther downstream, the Barents Sea branch carries away 16 Gt, leaving 24 Gt moving northward in the West Spitsbergen Current, which eventually splits into the 10-Gt Laptev Sea branch and the 13-Gt Greenland Sea branch.

This drastic downstream decrease from 72 Gt to 13 Gt does not mean, however, that the GSA was diluted underway; it reflects rather a partitioning of the Gulf Stream Extension system into several branches which eventually carry the bulk of the volume transport away from the Gulf Stream itself. Indeed, Dickson et al. (1988) assumed a ***constant*** salinity anomaly value $\Delta S = 0.1$ for their salt budget calculations throughout most of the GSA'70s journey around the northern North Atlantic save for (1) north of Iceland, where $\Delta S = 0.4$, and (2) the Labrador Current, where ΔS could be computed rigorously because of the availability of repeated salinity-depth sections across the current.

Salt budget histories of the GSA'70s and GSA'80s can be compared using the available time series described in Section 3. The comparison (for the ocean upper layer) is given in Table 4; the appropriate literature references are given in Fig. captions and in the text of Section 3.

Inspection of Table 4, as well as examination of original figures and data presented in Section 3, reveals that the GSA'80s was comparable with the GSA'70s as to their salt content because of similar magnitude and duration of the salinity anomalies. In the northwest and central North Atlantic, the GSA'80s was even more conspicuous in some places than was the GSA'70s (e.g. Labrador Sea and near OWS "Charlie"). In the northeast North Atlantic, however, the GSA'80s was weaker than the GSA'70s.

4.9. Recurrence of GSAs and their regularity; the GSA'90s

Within the framework of the advective hypothesis, one can envisage the following scenarios:

1. A GSA disappears after propagating around the North Atlantic.
2. A GSA returns to its origin and re-appears as the next GSA.

Another dilemma (which might be somehow related to the above one) can be stated as the problem of uniqueness of the GSA'70s: Are "we dealing with a unique, occasional, or regular (even cyclical) event" (Dickson, 1995, p.310)?

Dickson et al. (1988) argued that the GSA'70s could be advected repeatedly around the subpolar gyre. The recurrence of the GSA'70s was suggested also by

Table 4
Upper layer salinity anomalies of the 1970s and 1980s

Location	GSA'70s	GSA'80s	Fig.
West Greenland Current: Fylla Bank	max $\Delta S_0 = -0.6$	max $\Delta S_0 = -0.4$	Fig. 4
Central Labrador Sea	min $S_{0-250} = 34.52$	min $S_{0-250} = 34.33$	Fig. 6
Inshore Labrador Current: Sta.27	max $\Delta S_0 = -0.4$	max $\Delta S_0 = -0.6$	Fig. 8
North Atlantic Current: S9 Section, SE of OWS "C" ("Charlie")	min $S_{200} = 34.70$	min $S_{200} = 34.58$ (mainly, 34.62–34.71)	Fig. 13
OWS "C" ("Charlie")	min $S_{200} = 34.78$	min $S_{200} = 34.74$	Fig. 14
Irminger Current South of Iceland: Selvogsbanki Section	max $\Delta S_0 = -0.045$	max $\Delta S_0 = -0.045$	Fig. 15
Rockall Channel, Winter	max $\Delta S_0 = -0.12$	max $\Delta S_0 = -0.05$	Fig. 17
Faroe-Shetland Channel (North Atlantic Water)	min $S_0 = 35.26$	min $S_0 = 35.31$	Fig. 19
North Sea, Norwegian Coastal Current: Utsira	min $S_{100} = 34.54$	min $S_{100} = 34.66$	Fig. 21
Southern Norwegian Sea: Svinøy-NW Section, Summer	min $S_{50-200} = 35.10$	min $S_{50-200} = 35.18$	Fig. 23
Northern Norwegian Sea: Gimsøy-NW Section, Summer	min $S_{50-200} = 35.07$	min $S_{50-200} = 35.13$	Fig. 24
Western Barents Sea: Fugløya-Bjørnøya Section	max $\Delta S_{50-200} = -0.14$	max $\Delta S_{50-200} = -0.05$	Fig. 25
Western Barents Sea: Fugløya-Bjørnøya Section, March Surveys	min $S_{50-200} = 34.92$	min $S_{50-200} = 35.00$	Fig. 28
Central Barents Sea: Vardø-N Section	max $\Delta S_{50-200} = -0.13$	max $\Delta S_{50-200} = -0.05$	Fig. 26
Central Barents Sea: Vardø-N Section, March Surveys	min $S_{50-200} = 34.83$	min $S_{50-200} = 34.93$	Fig. 28
Eastern Barents Sea: Semøyene Section, January-February Surveys	min $S_{50-200} = 34.77$	min $S_{50-200} = 34.82$	Fig. 28
West Spitsbergen Current: Sørkapp-W Section, Summer	min $S_{50-200} = 34.99$	min $S_{50-200} = 35.00$	Fig. 29

Clarke (1984a) and Lazier (1988), among others. While repeated occurrence of the same anomaly is feasible, this seemingly did not happen with the GSA'70s, which arrived back to the Greenland Sea in 1981–1982 (Dickson et al., 1988) and in the Iceland Sea in 1981–1983 (Malmberg, 1986), i.e. too late to start the GSA'80s, which by that time was observed in the Labrador Sea.

Myers et al. (1989) has noted three distinct decadal-scale freshenings of the Labrador Sea around 1959, 1971, and 1984 associated with positive sea-ice extent anomalies in the Labrador Sea (Mysak and Manak, 1989). However, only one of these freshenings, GSA'70s, was correlated with a negative salinity anomaly north of Iceland (Dickson et al., 1988), therefore Myers et al. (1989), p.4, concluded: "The data do not support Dickson et al.'s hypothesis of a multiple passage of the fresh water pulse around the North Atlantic. They also suggest that the 1970's anomaly differed in character from the other anomalies."

Turrell and Shelton (1993) also considered a possibility of recurrence of the GSA'70s. They pointed to the reduced TS-characteristics of the Irminger Water in

the West Greenland area in 1976, attributed to the GSA'70s (Buch and Stein, 1989). The Irminger Water, however, is found here at the 400–600-m depth (Buch, 1984), so the Irminger Water anomaly cannot account for the ***upper*** layer anomaly off West Greenland. Turrell and Shelton (1993, p.68) also argued that the GSA'70s re-appeared first in North Icelandic waters, then west of Greenland (in 1982–1984) and concurred that the cold conditions west of Greenland in the early 1980s might be partially attributed to the increased "inflow of cold Arctic water from the East Greenland Current" (Buch and Stein, 1989, p.83). It should be noted, however, that Buch and Stein (1989) did not provide any data to support the idea of the enhanced inflow of East Greenland waters into the Labrador Sea in the early 1980s.

The advective hypothesis implies that a GSA could re-appear after passing around the Subarctic gyre. While the GSA path in the NW Atlantic seems to be well determined, apparently controlled by continental slope topography (East Greenland Current-West Greenland Current-Labrador Current-North Atlantic Current), there are at least ***two*** alternative routes whereby a GSA may recirculate. Firstly, the anomaly could follow the "great circle" via the Rockall Channel and the Faroe-Shetland Channel into the North Sea and the Norwegian Sea, then moving north with the West Spitsbergen Current, and eventually veering west to join the East Greenland Current in the western Greenland Sea (Route 1). Alternatively, it could shortcut the "great circle" and follow the "small circle" with the Irminger Current to the north then west to join the East Greenland Current in the western Irminger Sea (Route 2).

These two different closures (recirculations) would have different effects on a GSA. Following Route 1, a GSA would remain surface-intensified (e.g. numerous figures in Dickson and Blindheim (1984)), whereas following Route 2 (via the Irminger Current), a ***surface***-intensified GSA would become a ***subsurface*** one by the time it reaches the West Greenland Current, where the Irminger Current water is observed at intermediate depths (400–600 m, according to Buch (1984)).

The problem of recurrence of GSA has been revisited recently by Dickson (1995) who noted that "we have only inconclusive answers to its likely periodicity" (p.313) and admitted that the GSA might be "a more obvious, high-amplitude iteration of a regular event" (p.314). Notwithstanding the above reservations, Dickson (1995), p.316 concluded: "Although it contains periodic elements, the Great Salinity Anomaly [of the 1970s] is neither a periodic nor a frequently recurring phenomenon. One or possibly two such events are thought to have occurred during this century, and the event we observed in 1968–1982 was driven by a secular change in the winter pressure field at Greenland."

The recurrence of GSAs has been, however, corroborated recently by the results of climatological analysis of the most complete data base compiled by Yashayaev (1995, 1997) for the Labrador Sea and Newfoundland Basin. ***Three*** distinct low-salinity anomalies have been identified, associated with low-temperature anomalies, in the early 1970s, 1980s, and 1990s. Deser and Timlin (1996) also identified ***three*** positive sea ice extent anomalies east of Newfoundland in the early 1970s, 1980s, and 1990s each of which were followed after ~1–2 years by low-temperature anomalies in the subpolar North Atlantic (Fig. 38). The decadal periodicity of TS-anomalies in

the North Atlantic has been confirmed in the statistical study by Reverdin et al. (1997) who also point out that the most likely explanation appears to be advective.

The latest anomaly, GSA'90s, is also evident in the most recent data from the inshore Labrador Current (Fig. 8) (Drinkwater, 1994) and elsewhere on the Newfoundland Shelf (Colbourne et al., 1997). The origin of GSA'90s seems to be related to the severe winters of the early 1990s in the Baffin Bay/Labrador Sea area, when the negative air temperature monthly anomalies over West Greenland exceeded −10°C (Fig. 40); the winters of 1992 and 1993 at Godthåb were the coldest on record

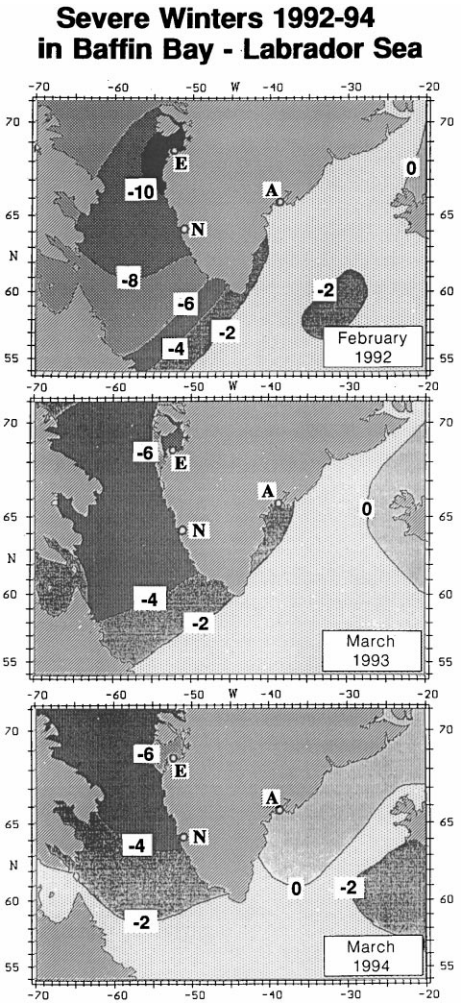

Fig. 40. Monthly mean air temperature anomalies (°C) over the Northwest Atlantic in February 1992 (top), March 1993 (middle) and March 1994 (bottom) relative to the 1961–90 climatic mean (modified after Stein, 1996a, Figs 4–6). E = Egedesminde, N = Nuuk (Godthåb), A = Angmagssalik.

since 1866 and thus anomaly persisted through until March 1994 (Climatic Research Unit, 1995a, b, 1996; Drinkwater, 1994; Stein, 1995a, b, 1996a, b).

4.10. Thermal anomalies and GSAs

As repeatedly noted and illustrated above, anomalous *salinity* events recorded from time series from around the North Atlantic are usually associated with *temperature* anomalies. The open ocean salinity anomalies could enter marginal seas and likely influence their thermal regime as shown by Becker and Pauly (1996) who found that the larger SST anomalies in the North Sea are related to salinity anomalies both in the Northeast Atlantic and in the North Sea itself. It is very interesting, therefore, to examine advection of individual large-scale *temperature* anomalies (the suitable temperature data are far more abundant than salinity data) which could be indicative of the propagation of the associated salinity anomalies. Using the COADS SST data in the North Atlantic for 1948–1992, Hansen and Bezdek (1996) have identified and tracked five cold anomaly features and nine warm anomaly features, with individual lifetimes of 3 to 10 years; "the long timescale of these extreme events and the continuity of their movements suggest a useful degree of predictability of SST based on persistence and propagation of features" (Ibid., p.8749). Most of the anomalies traveled around the Subarctic or Subtropical gyres, with the speed of 1–3 km/day, which is significantly less than the typical mean speed of the near-surface ocean circulation. Hansen and Bezdek (1996) have associated the cold SST anomaly C70 (see their Table 1) observed in 1970–1976, with the GSA'70s. The next cold SST anomaly to be observed in 1983–1986, C83, could be associated with the next low-S anomaly, the GSA'80s (D. V. Hansen, personal communication, 1996), notwithstanding two minor inconsistencies. First, our data clearly show that the GSA'80s propagated around the northern North Atlantic, while Hansen and Bezdek (1996) have found the associated C83 thermal anomaly to be stationary (the "nil" speed in their Table 1), although a careful examination of their Fig. 4 reveals a slow movement of C83 around the Subpolar gyre. Secondly, the GSA'80s has been traced through 1989, while C83 has been tracked only through 1986 because by that time the anomaly went into the GIN Sea, where Hansen and Bezdek (1996) could no longer identify it for their "field of view" was limited by 65°N.

4.11. Deep waters and GSAs

Lazier (1988), p.1249 pointed out that in the deep and near-bottom waters of the Labrador Sea the range of temperature variability over the 1962–1986 period and the magnitude of time series extrema ***increased*** with increasing density; the temperature extrema being evident on all the deep isopycnals. Because these deep waters originate from the Denmark Strait Overflow Water (DSOW), the deep water variability in the Labrador Sea should be associated with the upper water variability in the Iceland Sea. Thus the *surface*-intensified TS-anomalies in the Nordic Seas would translate into the *deep*-intensified TS-anomalies in the Labrador Sea and farther downstream be associated with the DSOW.

Once in the DSOW, the GSA signal in the Northwest Atlantic might sometimes propagate *faster* than the corresponding surface signal thanks to the intense, concentrated boundary currents which supply the Labrador Sea deep waters; these boundary currents would actually carry on the GSA signal faster than the ocean surface layer transport that is dominated by eddy diffusivity (Lazier, 1988, p.1251).

Aagaard and Carmack (1994), Fig. 2, proposed a new schematic to describe a relationship between freshwater supply from the Arctic and convective renewal rate in the North Atlantic, and suggested (ibid., pp. 7–8) that the GSA'70s caused the freshening and cooling of the North Atlantic deep water, which had first been described by Brewer et al. (1983) and further documented by Read and Gould (1992).

Häkkinen (1995) used a fully prognostic ice-ocean model to show that the Greenland Sea deep convection (hence deep water mass formation) is controlled by the Fram Strait ice export and/or by the local wind conditions in the Greenland Sea. She also showed that the changes in the salt content of the Greenland Gyre are determined by the advection of either fresh or salty anomalies produced either by Arctic outflows or by the shifts of the Polar Front.

Rudels (1995), p.297 pointed out that the GSA'70s inhibited the convective activity throughout the entire northern North Atlantic: "Then not only the production of Arctic Intermediate water in the Greenland and Icelandic Seas was shut off. The low salinity water also entered the Labrador Sea and closed down the formation of Labrador Sea deep water. Both the [Denmark Strait] overflow and the Labrador Sea contribution to the North Atlantic deep water were then reduced."

Curry and McCartney (1996) have shown that the time history of the convective activity in the Labrador Sea leaves its imprint on the Labrador Sea Water (LSW) characteristics. They point out (*ibid.*, pp. 27–28): "The convective events of the 1970s and late 1980s were preceded by a surface buildup of an extremely low salinity cap [GSA'70s and GSA'80s]... The downmixing of this fresh cap dramatically lowered the LSW core salinity." The LSW characteristics, especially its thickness, are found to be linked to the subtropical mid-depth warming/cooling pattern, with the subtropical basin-scale response lagging the subpolar signal by 5–7 years. Curry and McCartney (1996) have shown that the subtropical temperature response is dominated by the LSW thickness (i.e. by the volume of LSW available for mixing) rather than by the LSW temperature signal.

Dickson et al. (1996) have shown that the convective activity (hence the entire process of deep and intermediate water formation) in the Greenland, Labrador and northern Sargasso Seas underwent coordinated changes over the last several decades, some of them being related to variable horizontal exchange with the Arctic Ocean via Fram Strait, and propagation of GSA. They also argue that these in-phase changes (albeit of different sign) have been caused largely by "a direct impact of the shifting atmospheric circulation on the ocean" (Dickson et al., 1996, p.241).

4.12. Long-term variability and GSAs

Long-term variability of the ocean on variety of scales (decadal-to-centennial) might be of various kinds. Different mechanisms have been invoked to explain the observed long-term variability in the North Atlantic such as:

1. a ***shift*** in the ocean regime (Malmberg and Blindheim, 1984; Levitus, 1989a, b, c);
2. decadal and multi-decadal ***oscillations*** in the ocean-atmosphere system as indicated by statistical data analysis (Deser and Blackmon, 1993; Levitus et al., 1994; Levitus and Antonov, 1995; Levitus et al., 1995; Deser and Timlin, 1996; Reverdin et al., 1997) and modeling experiments (Weaver and Sarachik, 1991; Delworth et al., 1993, 1997; Holland et al., 1995);
3. a secular (century-scale) monotonous ***trend***(s), e.g. a cooling and freshening of the subpolar North Atlantic over the past several decades (Brewer et al., 1983; Levitus, 1989a, b, c; Read and Gould, 1992; Levitus and Antonov, 1995), which might have been initiated by the GSA'70s.

Although the relative importance of these factors is still unknown, it should be stressed that all these mechanisms are not mutually exclusive and hence all of them could be at work simultaneously. In other words, the ocean may be oscillating between two or more stable regimes; or undergoing a gradual, monotonous change (trend); it might be experiencing abrupt shifts from one state to another; or the ocean may be simultaneously exhibiting all of these modes of variability.

4.13. Ecological consequences of GSAs and their impact on fisheries

As it circulated around the North Atlantic, the GSA'70s "had direct and knock-on effects upon many trophic levels of the ecosystem" (Turrell and Shelton, 1993, p.68). For example, Cushing (1988) has shown that the GSA'70s adversely affected the spawning success of 11 of 15 stocks of fish, whose breeding grounds were traversed by the anomaly. However, the advected temperature and salinity anomalies are not *per se* necessarily the main direct cause of the adverse effect. For example, Hutchings and Myers (1994) found no effect of temperature and salinity on recruitment of northern cod. Instead, the anomalies might be signatures of profound changes in the ocean-scale current pattern, and it is the changing current pattern that is likely to affect the ecosystem, through north-south shifts of the Gulf Stream (Taylor, 1995) or quasi-meridional shifts of the North Subarctic Front associated with the northernmost branch of the North Atlantic Current (Belkin and Levitus, 1996). Influence of the GSA'70s on recruitment (e.g. Jakobsson, 1992) was felt even in the semi-enclosed North Sea (Svendsen et al., 1995), where in the late 1970s the entire ecosystem "changed overnight, probably caused by the entrance of ocean water with a different chemical composition" (Lindeboom et al., 1995, p.99).

The impact of GSAs on recruitment is, however, disputed by some researchers. For example, Mertz and Myers (1994), p.1, claim that "south of Greenland waters there were no significant temperature anomalies corresponding to the GSA['70s]". This conclusion contradicts to the results of other authors presented in Sections 3.2–3.5, and also to the results of Hansen and Bezdek (1996), p.8753, described in Section 4.10, who have traced a temperature anomaly (C70) associated with the GSA'70s. Mertz and Myers (1994), p.1, have also found that "the food chain coupling of environment to recruitment (climate to phytoplankton to zooplankton to fish) is not strong in the study region" [the northern Northwest Atlantic, from West Green-

land to the Grand Banks]. Further research is clearly warranted as to the ecological impact of GSAs, especially now that we have ***two*** thoroughly documented GSAs (of the 1970s and 1980s), and the third GSA (of the 1990s) might well be in progress.

4.14. Alternative explanations of GSAs

Once the advective hypothesis has been advanced to explain the GSA'70s, alternative hypotheses were put forward to account for the observed phenomena. For example, Ellett and MacDougall (1983); Dooley et al. (1984), and Martin et al. (1984) explained the temporal TS-variability west of Britain by a hypothetical large-scale eastward shift of water masses that may have resulted from a 300-km shift eastwards of the Polar Front. Unfortunately, there is no direct confirmation of such a shift having occurred.

Pollard and Pu (1985) suggested increased in situ surface moisture flux (i.e. increased excess of precipitation over evaporation) as the primary cause of local freshening. Facing the problem of explaining the source of the "extra" 1.4 m of fresh water they presumed had been added to the surface of the Northeast Atlantic, to account for the observed freshening Pollard and Pu (1985) insist that the excessive atmosphere-to-ocean freshwater flux needed had gone unnoticed because of the sparse observational network. Revisiting the hypothesis, Pollard et al. (1996), p.189, argue that "...there is no conflict between the various hypotheses put forward to explain the salinity anomalies... All these mechanisms contribute, with different balances in different years and at different places."

Furnes (1992) related the pronounced drop in the mid-1970s in temperature and salinity in the North Sea and Barents Sea (the latter also being associated with large sea-ice extent) to "a counterclockwise shift of the wind directions towards more southerly wind directions in the North Sea and northeasterly directions in the Barents Sea" (p.252). Hansen and Kristiansen (1994) noticed simultaneous salinity variations in water masses around Faroe Islands and concluded that the only mechanism which could explain this synchronisation is the changing dynamical balance of the three currents transporting these water masses, namely, the North Atlantic Current, the Continental Slope Current, and the East Icelandic Current. This synchronisation was also noticed by Turrell (1995) who concurred with the idea of a changing dynamic balance within the area as the main cause of the salinity changes in the Faroe-Shetland Channel.

Hansen and Kristiansen (1994), however, do not question the validity of the advective hypothesis in the Northwest and Northeast Atlantic, stressing that their objections are of rather local character, namely, they question the idea of "the salinity deficit in the Faroe-Shetland region mainly derived from the West Atlantic by advection" (*ibid*., p.12). They also note that the suggested dynamic change "may well involve a shift of the Polar Front south of Iceland, as suggested by Dooley et al. (1984), but does not necessarily do so, and must in any case be more widespread since it must involve also the East Icelandic Current and probably also regions in the eastern Atlantic south to about 40°N" (ibid., p.15). We feel that these ideas as well as the frontal shift hypothesis of Dooley et al. (1984) should be taken into account to rec-

oncile the large-scale advective explanation and some of the seemingly unexplainable phenomena occurring in the Central North Atlantic.

Another problem is a significant ***time lag between T and S extrema*** observed in time series around the North Atlantic (Section 3). What makes the problem even more difficult is that the ***sign*** of the time lag can be different in different places, for the same anomaly, be it GSA'70s or '80s. Thus the leading parameter may be either T or S or they can be synchronous. We have noticed, however, that in most cases T leads S, which could be explained as follows:

1. A negative air temperature anomaly causes surface cooling (negative T-anomaly);
2. The surface cooling (possibly combined with initial surface freshening from a remote source such as Fram Strait or the Canadian Archipelago) results in enhanced formation of sea ice;
3. The positive sea ice extent anomaly propagates downstream where the sea ice melt creates a negative salinity anomaly.

The time lag problem actually presents an unsurmountable obstacle not for the advective explanation, but for the frontal shift hypothesis because any temporal variability (in a fixed point) induced by frontal movements of a nearby front should be synchronous in T- and S-time series recorded at the fixed point since T and S are strongly correlated across oceanic fronts.

It should be stressed that the advective hypothesis advocated here is not the ***only*** possible explanation for the successions of similar events observed repeatedly around the northern North Atlantic, but rather it is the ***simplest*** mechanism that provides a coherent space-time pattern of large-scale decadal variability largely consistent with the available data. We refer the reader to the recent statistical study by Reverdin et al. (1997) which strongly corroborates the advective paradigm.

4.15. Two scenarios

In the advective framework, at least two scenarios are feasible of the GSA origin and propagation:

1. The GSA'70s was caused by enhanced ice export from the Arctic Basin via Fram Strait. The GSA'70s propagated around the North Atlantic, re-entered the East Greenland Current, and then emerged again as the GSA'80s and may well reappear once again as the GSA'90s given the roughly 10-year propagation time around the Subarctic gyre. This scenario implies the existence of yet unknown mechanism which reinforces the anomaly as it progresses. It also faces a problem. If there is a self-supporting mechanism, which accounts for the GSA maintenance, when and why does this mechanism break down, at times allowing a GSA to dissipate, as it apparently happened with the GSA of 1908–1910?
2. The second scenario envisages ***two*** main areas of GSA origin, Fram Strait and the Labrador Sea. As shown above, the GSA'70s was probably caused by an enhancement of Arctic fresh water export via Fram Strait, which was associated with a positive sea-ice extent anomaly propagating downstream from the Green-

land Sea to the Labrador Sea. In the 1980s, however, the situation was entirely different, there was no sea-ice excess in the Greenland Sea. However, in the Baffin Bay-Labrador Sea area, the winters of the early 1980s were extremely severe and the sea-ice extent reached the all-time high. We believe that it was this regional climatic situation in the Baffin Bay-Labrador Sea area in the early 1980s that was accountable for the origin of GSA'80s.

This hypothesis seems to be strongly corroborated by **the early 1990s data**, when, again, the winter conditions in the Baffin Bay /Labrador Sea area were extremely severe, with negative ***air temperature monthly anomalies*** up to – 10°C (Fig. 40) and large positive ***sea-ice extent anomalies*** (Stein, 1995a, b, 1996a, b; iceberg data in Fig. 33). This apparently leads to a fresh, cold anomaly (**GSA'90s**) in the West Greenland Current and in the Labrador Current (Drinkwater, 1994; Drinkwater et al., 1995; Colbourne et al., 1997), while the upstream atmospheric and oceanic conditions in the Greenland, Iceland and Irminger Seas were normal (Climatic Research Unit, 1995a, b, 1996; Climate Analysis Center, 1994; Stein, 1995a, b, 1996a, b). The dipolar structure in the air temperature anomaly field, i.e. the seesaw between the Labrador Sea and Greenland Sea during the winters of 1973, 1983, and 1992, has been noted also by Mysak et al. (1996). The ***annual SST anomaly*** for January–December 1993 in the Baffin Bay-Labrador Sea area exceeded – 3°C, being by far the world's largest SST anomaly of the year (Climate Analysis Center, 1994).

5. Summary and conclusions

Using all available published time series of temperature and salinity extended into the 1990s, we revisited the GSA'70s and documented the newly identified GSA'80s. Both propagated around the North Atlantic in a similar fashion. The advection mechanism, initially proposed to explain the observed sequence of events during the GSA'70s, apparently also holds true for the GSA'80s.

These two anomalies, however, seem to have had different origins. The GSA'70s was likely to have been triggered ***remotely***, by a freshwater/sea ice pulse from the Arctic Basin entering via Fram Strait. Consequently, the GSA'70s was accompanied by a large sea ice extent anomaly in the Greenland and Iceland Seas in the late 1960s, which was propagated downstream into the Labrador Sea in the early 1970s.

In contrast, the GSA'80s was probably formed ***locally***, in the Labrador Sea, largely as a result of the extremely severe winters of the early 1980s. The GSA'80s formation might have been facilitated by a likely contribution of the Arctic freshwater outflow via the Canadian Archipelago, supposedly enhanced as a result of intensification of northerlies observed during the event. This fresh, cold anomaly was also associated with a positive sea ice extent anomaly in the Labrador Sea, which, however, had no upstream precursor in the Greenland Sea, in contrast to the sea ice anomaly of the 1970s.

Data of the early 1990s seem to corroborate the above results. A new fresh, cold anomaly has been formed in the Labrador Sea during the harsh winters of the early

1990s, and was again accompanied by a large positive sea ice extent anomaly. These severe conditions were, however, mostly confined to the Labrador Sea and Baffin Bay, while the atmospheric and oceanic conditions in the Greenland, Iceland, and Irminger Seas were normal.

We thus arrive at two major conclusions which directly stem from the comparative study of the GSA'70s, GSA'80s, and, rudimentary, GSA'90s:

1. The GSAs are not necessarily caused solely by an enhanced export of freshwater and sea ice from the Arctic Basin via Fram Strait.
2. The Labrador Sea/Baffin Bay area can play a key role in the formation of GSAs, as well as in propagation of the GSAs formed upstream.

There are two modes of the GSA origin in the North Atlantic, ***remote*** (resulting from an enhanced Arctic Ocean freshwater export) and ***local*** (resulting from the effects of severe winters in the Labrador Sea/Baffin Bay area). Both modes should be taken into account in attempts to model decadal variability of the coupled ocean-ice-atmosphere system in the North Atlantic/Arctic Basin.

Long-term observations in fixed locations thus provide indispensable information about decadal-scale variations of the circulation pattern and its intensity. Compilation of data from the monitoring of further events similar to the "Great Salinity Anomalies" of 1970s and 1980s should allow the multidecadal variability of the ocean circulation and climate to be better studied, modeled and eventually understood.

6. Acknowledgements

A synthesis of this kind would be impossible without close collaboration with, and contributions from, scores of colleagues studying various parts of the most diverse and wonderfully complex megabasin in the world, the northern North Atlantic. Many colleagues generously and unselfishly shared with us their latest findings and ideas. We extend our most sincere gratitude to Thorkild Aarup, Gerd Becker, Peter Becker, Manfred Bersch, Johann Blindheim, Eric Buch, Ad Corten, Robert Dickson, Harry Dooley, Ken Drinkwater, David Ellett, Tor Gammelsrød, Bogi Hansen, Donald Hansen, James Helbig, David Holland, Robert Houghton, Jeffrey Hutchings, Sigbjorn Mehl, Gordon Mertz, Ransom Myers, John Lazier, John Loder, Harald Loeng, Lawrence Mysak, Raymond Pollard, Gilles Reverdin, Tom Rossby, Bert Rudels, Michael Steele, Manfred Stein, Einar Svendsen, Arnold Taylor, Bill Turrell, Andrew Weaver, and Igor Yashayaev. We are also gratefully acknowledged to two anonymous reviewers whose thoughtful comments significantly contributed to improvement of the manuscript. This study was completed while Igor Belkin and John Antonov held, respectively, Senior Research Associateship and Research Associateship with Ocean Climate Laboratory of the NODC, NOAA, awarded by the National Research Council (NRC). The constant support by the NRC and the NOAA Climate and Global Change Program is greatly appreciated.

7. References

Aagaard, K., & Carmack, E.C. (1989). The role of sea ice and other fresh water in the Arctic circulation. *Journal of Geophysical Research, 94*, 14485–14498.

Aagaard, K., & Carmack, E. C. (1994). The Arctic Ocean and climate: A perspective. In O. M. Johannessen, R. D. Muench, & J. E. Overland (Eds.), *The Polar Oceans and Their Role in Shaping the Global Environment: The Nansen Centennial Volume*. AGU, Washington, D.C., pp. 5–20.

Aagaard, K., Roach, A. T., Moritz, R. E., & Schweiger, A. J. (1996). Ice export from the Arctic Ocean, 1991–1994. In A.-M. Wilburn (Ed.), The Atlantic Climate Change Program, *Proceedings From the Principal Investigators Meeting*, May 14-16, 1996. WHOI, Woods Hole, MA, pp. 1–5.

Agnew, T. (1993). Simultaneous winter sea-ice and atmospheric circulation anomaly patterns. *Atmosphere-Ocean, 31*, 259–280.

Arhan, M., Colin De Verdiere, A., & Memery, L. (1994). The eastern boundary of the subtropical North Atlantic. *Journal of Physical Oceanography, 24*, 1295–1316.

Baranov, E.I. (1991). Circulation and water transports in the North Atlantic (in Russian). Trudy Gosudarstvennogo Okeanograficheskogo Instituta. *Proceedings of the State Oceanographic Institute Moscow, 202*, 45–65.

Becker, G., & Dooley, H. (1995). The 1989-1991 high-salinity anomaly in the North Sea and adjacent areas. *Ocean Challenge, 6*, 52–57.

Becker, G., & Pauly, M. (1996). Sea surface temperature changes in the North Sea and their causes. *ICES Journal of Marine Science, 53*, 887–898.

Becker, P. (1995). The effect of Arctic river hydrological cycles on Arctic Ocean circulation. Ph.D. Thesis, Old Dominion University, Norfolk, VA, xi + 203 pp.

Becker, P., & Björk, G. (1996). Residence times in the upper Arctic Ocean. *Journal of Geophysical Research, 101*, 28377–28396.

Belkin, I.M., & Levitus, S. (1996). Temporal variability of the Subarctic Front near the Charlie-Gibbs Fracture Zone. *Journal of Geophysical Research, 101*, 28317–28324.

Bjarni Sæmundsson GSP Group. (1991). S.-A. Malmberg (Ed.), Greenland Sea Project 1987–1991, ICES C.M. 1991/C:36, 22 pp.

Bjornson, H., Mysak, L.A., & Brown, R.D. (1995). On the interannual variability of precipitation and runoff in the Mackenzie drainage basin. *Climate Dynamics, 12*, 67–76.

Bourke, R.H., & Garrett, R.P. (1987). Sea ice thickness distribution in the Arctic Ocean. *Cold Regions Science and Technology, 13*, 259–280.

Brewer, P.G., Broecker, W.S., Jenkins, W.J., Rhines, P.B., Rooth, C.G., Swift, J.H., Takahashi, T., & Williams, R.T. (1983). A climatic freshening of the deep Atlantic north of 50°N over the past 20 years. *Science, 222*, 1237–1239.

Buch, E. (1982). Review of oceanographic conditions in Subareas 0 and 1 during the 1970-1979 decade. *NAFO Scientific Council Studies, 5*, 43–50.

Buch, E. (1984). Variations in temperature and salinity of West Greenland waters, 1970-1982. *NAFO Scientific Council Studies, 7*, 39–43.

Buch, E. (1985). Seasonal and year to year variations of West Greenland waters in recent years. *Rit Fiskideildar, 9*, 141–151.

Buch, E., & Stein, M. (1987). Time series of temperature and salinity at the Fylla Bank Section, West Greenland. ICES C.M. 1987/C:4, 22 pp.

Buch, E., & Stein, M. (1989). Environmental conditions off West Greenland, 1980-85. *Journal of the Northwest Atlantic Fisheries Science, 9*, 81–89.

Chapman, W.L., & Walsh, J.E. (1993). Recent variations of sea ice and air temperature in high latitudes. *Bulletin of the American Meteorological Society, 74*, 33–47.

Clarke, R. A. (1984a). Changes in the western North Atlantic during the decade beginning in 1965. ICES C.M. 1984/Gen:17, Mini-Symp., 11 pp.

Clarke, R.A. (1984b). Transport through the Cape Farewell-Flemish Cap section. *Rapp. P.-V. Reun. Conseil International pour l'Exploration de la Mer, 185*, 120–130.

Climate Analysis Center. (1994). Halpert, M. S., Bell, G. D., Kousky, V. E., & Ropelewski, C. F. (Eds.),

Fifth Annual Climate Assessment: 1993. National Meteorological Center, National Weather Service, NOAA, Camp Springs, MD, 111 pp.

Climatic Research Unit, University of East Anglia. (1985). Arctic regions surface temperature anomalies [year 1984]. *Climate Monitor*, *13*(5), 150.

Climatic Research Unit, University of East Anglia. (1995a). Arctic regions surface air temperature anomalies [December 1991 to December 1992]. *Climate Monitor*, *21*(1–5), 85–92.

Climatic Research Unit, University of East Anglia. (1995b). Arctic regions surface air temperature anomalies [December 1992 to December 1993]. *Climate Monitor*, *22*(1–5), 91–98.

Climatic Research Unit, University of East Anglia. (1996). Arctic regions surface air temperature anomalies [December 1993 to May 1994]. *Climate Monitor*, *23*(1–2), 69–72.

Colbourne, E., De Young, B., Narayanan, S., & Helbig, J. (1997). Comparison of hydrography and circulation on the Newfoundland Shelf during 1990-1993 with the long-term mean. *Canadian Journal of Fisheries and Aquatic Sciences*, *54*(Suppl.1), 68–80.

Corten, A., & Van De Kamp, G. (1996). Variation in the abundance of southern fish species in the southern North Sea in relation to hydrography and wind. *ICES Journal of Marine Science*, *53*(6), 1113–1119.

Curry, R. G., & McCartney, M. S. (1996). Links between subtropical mid-depth warming/cooling patterns and variations in convection intensity in the subpolar Labrador Sea. In A.-M. Wilburn (Ed.), The Atlantic Climate Change Program, *Proceedings From the Principal Investigators Meeting*, May 14–16, 1996, WHOI, Woods Hole, MA, pp. 27–35.

Cushing, D. H. (1988). The northerly wind. In B. J. Rothschild (Ed.), *Toward a Theory on Biological-Physical Interactions in the World Ocean*. Kluwer Academic Publishers, Dordrecht etc., pp. 235–244.

Danielssen, D.S., Svendsen, E., & Ostrowski, M. (1996). Long-term hydrographic variation in the Skagerrak based on the section Torungen-Hirtshals. *ICES Journal of Marine Science*, *53*(6), 917–925.

Delworth, T., Manabe, S., & Stouffer, R.J. (1993). Interdecadal variations of the thermohaline circulation in a coupled ocean-atmosphere model. *Journal of Climate*, *6*(11), 1993–2011.

Delworth, T., Manabe, S., & Stouffer, R.J. (1997). Multidecadal climate variability in the Greenland Sea and surrounding regions: a coupled model simulation. *Geophysical Research Letters*, *24*(3), 257–260.

Deser, C., & Blackmon, M.L. (1993). Surface climate variations over the North Atlantic Ocean during winter: 1900-1989. *Journal of Climate*, *6*(9), 1743–1753.

Deser, C., & Timlin, M. S. (1996). Decadal variations in sea ice and sea surface temperature in the subpolar North Atlantic. In A.-M. Wilburn (Ed.), The Atlantic Climate Change Program, *Proceedings From the Principal Investigators Meeting*, May 14–16, 1996, WHOI, Woods Hole, MA, pp. 36–40.

Dickson, R. R. (1995). The local, regional, and global significance of exchanges through the Denmark Strait and Irminger Sea. In D. G. Martinson, K. Bryan, M. Ghil, M. M. Hall, T. M. Karl, E. S. Sarachik, S. Sorooshian, & L. D. Talley (Eds.), Natural Climate Variability on Decade-to-Century Time Scales. National Academy Press, Washington, D.C., pp. 305–317.

Dickson, R.R., & Blindheim, J. (1984). On the abnormal hydrographic conditions in the European Arctic during the 1970s. Rapports et Procès-Verbaux des Réunions. *Conseil International pour l'Exploration de la Mer*, *185*, 201–213.

Dickson, R.R., Lamb, H.H., Malmberg, S.-A., & Colebrook, J.M. (1975). Climatic reversal in northern North Atlantic. *Nature*, *256*(5517), 479–482.

Dickson, R.R., Meincke, J., Malmberg, S.-A., & Lee, A.J. (1988). The "Great Salinity Anomaly" in the northern North Atlantic, 1968-1982. *Progress in Oceanography*, *20*(2), 103–151.

Dickson, R., Lazier, J., Meincke, J., Rhines, P., & Swift, J. (1996). Long-term coordinated changes in the convective activity of the North Atlantic. *Progress in Oceanography*, *38*(3), 241–295.

Dietrich, G., Kalle, K., Krauss, W., & Siedler, G. (1975). Allgemeine Meereskunde. Bornträger, Berlin, 593 pp.

Dooley, H. D. (1992). Data archeology at ICES. In: Proceedings of the Ocean Climate Data Workshop, February 18–21, 1992, compiled by James Churgin, Goddard Space Flight Center, Greenbelt, MA, pp. 173–185.

Dooley, H.D., Martin, J.H.A., & Ellett, D.J. (1984). Abnormal hydrographic conditions in the Northeast Atlantic during the 1970s.Rapports et Procès-Verbaux des Réunions. *Conseil International pour lExploration de la Mer*, *185*, 179–187.

Drinkwater, K. F. (1994). Climate and oceanographic variability in the Northwest Atlantic during the 1980s and early 1990s. NAFO SCR Doc. 94/71, 39 pp.

Drinkwater, K. F., Colbourne, E., & Gilbert, D. (1995). Overview of environmental conditions in the Northwest Atlantic in 1994. NAFO SCR Doc. 95/43, 60 pp.

Ellett, D.J. (1979). Hydrographic conditions in the Rockall Channel, January-March 1977. *Annales Biologiques, 34*, 56–58.

Ellett, D. J. (1980). Long-term water-mass in the North-eastern Atlantic, ICES C.M., 1980/C:9, 12 pp.

Ellett, D.J. (1982). Long-term water-mass changes to the west of Britain. Time Series of Ocean Measurements. *World Climate Programme Report WCP-, 21*, 245–254.

Ellett, D.J. (1994). Salinity variations west of Scotland. *NERC News, January, 1994*, 15–18.

Ellett, D.J. (1995). Physical oceanography of the Rockall Trough. *Ocean Challenge, 6*(1), 18–23.

Ellett, D.J., & Blindheim, J. (1992). Climate and hydrographic variability in the ICES area during the 1980s. *ICES Marine Science Symposia, 195*, 11–31.

Ellett, D. J., & Jones, S. R. (1994). Surface temperature and salinity time-series from the Rockall Channel, 1948–1992. Fisheries Research Data Report No. 36, MAFF Direct. Fish. Res., Lowestoft, 24 pp.

Ellett, D.J., & MacDougall, N. (1983). Some monitoring results from west of Britain. *IOC Technical Series Rept, 24*, 21–25.

Ellett, D. J., & Turrell, W. R. (1992). Increased salinity levels in the NE Atlantic. ICES C.M. 1992/C:20, 12 pp.

Farrelly, B., Gammelsrød, T., Golmen, L.-G., & Sjøberg, B. (1985). Hydrographic conditions in the Fram Strait during summer 1982. *Polar Research, 3*(2), 227–238.

Furnes, G.K. (1992). Climatic variations of oceanographic processes in the north European seas: a review of the 1970s and 1980s. *Continental Shelf Research, 12*(2–3), 235–256.

Gammelsrød, T., & Holm, A. (1984). Variations of temperature and salinity at station M (66°N, 2°E) since 1948. Rapports et Procès-Verbaux des Réunions. *Conseil International pour lExploration de la Mer, 185*, 188–200.

Gammelsrød, T., Østerhus, S., & Godøy, Ø. (1992). Decadal variations of ocean climate in the Norwegian Sea observed at Ocean Station "Mike" (66°N, 2°E). *ICES Marine Science Symposia, 195*, 68–75.

Greatbatch, R.J., & Peterson, K.A. (1996). Interdecadal variability and oceanic thermohaline adjustment. *Journal of Geophysical Research, 101*(C9), 20467–20482.

Häkkinen, S. (1993). An Arctic source for the Great Salinity Anomaly: A simulation of the Arctic ice-ocean system for 1955-1975. *Journal of Geophysical Research, 98*(C9), 16397–16410.

Häkkinen, S. (1995). Simulated interannual variability of the Greenland Sea deep water formation and its connection to surface forcing. *Journal of Geophysical Research, 100*(C3), 4761–4770.

Hansen, B., & Kristiansen, R. (1994). Long-term changes in the Atlantic water flowing past the Faroe Islands. ICES C.M. 1994/S:4, 16 pp.

Hansen, D.V., & Bezdek, H.F. (1996). On the nature of decadal anomalies in North Atlantic sea surface temperature. *Journal of Geophysical Research, 101*(C4), 8749–8758.

Heath, M.R., Henderson, E.W., Slesser, G., & Woodward, E.M.S. (1991). High salinity in the North Sea. *Nature, 352*(6331), 116.

Holland, W.R., Capotondi, A., & Holland, M.M. (1995). Advances in ocean modeling for climate change research. *Reviews of Geophysics, 33*(Suppl.), 1411–1424.

Hopkins, T.S. (1991). The GIN Sea-A synthesis of its physical oceanography and literature review 1972-1985. *Earth-Science Review, 30*(3–4), 175–318.

Houghton, R.W. (1996). Subsurface quasi-decadal fluctuations in the North Atlantic. *Journal of Climate, 9*(6), 1363–1373.

Hovgård, H., & Buch, E. (1990). Fluctuation in the cod biomass of the West Greenland sea ecosystem in relation to climate. In K. Sherman, L. M. Alexander, & B. D. Gold, (Eds.), Large Marine Ecosystems: Patterns, Processes, and Yields. AAAS, Washington, D.C., pp. 36–43.

Hurrell, J.W. (1995). Decadal trends in the North Atlantic Oscillation: Regional temperatures and precipitation. *Science, 269*(5224), 676–679.

Hutchings, J.A., & Myers, R.A. (1994). What can be learned from the collapse of a renewable resource? Atlantic cod, Gadus morhua, of Newfoundland and Labrador. *Canadian Journal of Fisheries and Aquatic Sciences, 51*(9), 2126–2146.

ICES [International Council for the Exploration of the Sea]. (1997). Inventory of long (> 20 years) time series of oceanographic, meteorological, fisheries and astronomical observations and model results. ICES Shelf Seas Oceanography Working Group, 16 pp.

Jakobsson, J. (1992). Recent variability in the fisheries of the North Atlantic. *ICES Marine Science Symposia*, *195*, 291–315.

Keeley, J.R. (1982). Temperature and salinity anomalies along the Flemish Cap section in the 1970s. *NAFO Scientific Council Studies*, *5*, 87–94.

Korsbrekke, K., Mehl, S., Nakken, O., & Sunnanå, K. (1995). Bunnfiskundersøkelser i Barentshavet vinteren 1995 (Investigations on demersal fish in the Barents Sea winter 1995). Fisken og Havet, No. 13, 86 pp. (in Norwegian).

Krauss, W. (1986). The North Atlantic Current. *Journal of Geophysical Research*, *91*(C4), 5061–5074.

Krauss, W. (1995). Currents and mixing in the Irminger Sea and in the Iceland Basin. *Journal of Geophysical Research*, *100*(C6), 10851–10871.

Kushnir, Y. (1994). Interdecadal variations in North Atlantic sea surface temperature and associated atmospheric conditions. *Journal of Climate*, *7*(1), 141–157.

Lappo, S.S., Alekseev, G.V., & Efimov, V.V. (1995). On oceanological results of the program Sections. Izvestiya, Russian Academy of Sciences. *Atmospheric and Oceanic Physics, Engl. Transl.*, *31*(3), 373–384.

Lazier, J.R.N. (1980). Oceanographic conditions at Ocean Weather Ship BRAVO 1964-1974. *Atmosphere-Ocean*, *18*(3), 227–238.

Lazier, J.R.N. (1988). Temperature and salinity changes in the deep Labrador Sea, 1962-1986. *Deep-Sea Research*, *35*(8), 1247–1253.

Lazier, J.R.N. (1994). Observations in the Northwest Corner of the North Atlantic Current. *Journal of Physical Oceanography*, *24*(7), 1449–1463.

Lazier, J. R. N. (1995). The salinity decrease in the Labrador Sea over the past thirty years. In D. G. Martinson, K. Bryan, M. Ghil, M. M. Hall, T. M. Karl, E. S. Sarachik, S. Sorooshian, & L. D. Talley (Eds.), Natural Climate Variability on Decade-to-Century Time Scales. National Academy Press, Washington, D.C., pp. 295–302; discussion: pp. 302–303; color plate: p.331.

Levitus, S. (1989). Interpentadal variability of temperature and salinity at intermediate depths of the North Atlantic Ocean, 1970-1974 versus 1955-1959. *Journal of Geophysical Research*, *94*(C5), 6091–6131.

Levitus, S. (1989). Interpentadal variability of salinity in the upper 150 m of the North Atlantic Ocean, 1970-1974 versus 1955-1959. *Journal of Geophysical Research*, *94*(C7), 9679–9685.

Levitus, S. (1989). Interpentadal variability of temperature and salinity in the deep North Atlantic, 1970-1974 versus 1955-1959. *Journal of Geophysical Research*, *94*(C11), 16125–16131.

Levitus, S., & Antonov, J.I. (1995). Observational evidence of interannual to decadal-scale variability of the subsurface temperature-salinity structure of the World Ocean. *Climatic Change*, *31*(2–4), 495–514.

Levitus, S., Antonov, J.I., & Boyer, T.P. (1994). Interannual variability of temperature at a depth of 125 meters in the North Atlantic Ocean. *Science*, *266*(5182), 96–99.

Levitus, S., Antonov, J., Zhou, Z., Dooley, H., Teretschenkov, V., Selemenov, K., & Michaels, A. F. (1995). Observational evidence of decadal-scale variability of the North Atlantic Ocean. In D. G. Martinson, K. Bryan, M. Ghil, M. M. Hall, T. M. Karl, E. S. Sarachik, S. Sorooshian, & L. D. Talley (Eds.), Natural Climate Variability on Decade-to-Century Time Scales. National Academy Press, Washington, D.C., pp. 318–324; discussion: pp. 324–327.

Lindeboom, H., Van Raaphorst, W., Beukema, J., Cadée, G., & Swennen, C. (1995). (Sudden) changes in the North Sea and Wadden Sea: Oceanic influences underestimated? Deutsche Hydrographische Zeitschrift, 47. *Suppl.*, *2*, 87–100.

Loder, J. W., Petrie, B., & Gawarkiewicz, G. (1998). The coastal ocean off northeastern North America: A large-scale view. In A. R. Robinson, & K. Brink (Eds.), *The Sea: The Global Coastal Ocean*, Volume 11: Regional Studies and Syntheses. John Wiley and Sons, Inc., New York, pp. 105–133.

Loeng, H., Blindheim, J., Ådlandsvik, B., & Ottersen, G. (1992). Climatic variability in the Norwegian and Barents Seas. *ICES Marine Science Symposia*, *195*, 52–61.

Malmberg, S.-A. (1969). Hydrographic changes in the waters between Iceland and Jan Mayen in the last decade. *Jökull*, *19*, 30–43.

Malmberg, S.-A. (1973). Astand sjavar milli Islands og Jan Mayen, 1950-72. *Aegir*, *66*, 146–148.

Malmberg, S.-A. (1984a). A note on the seventies anomaly in Icelandic waters. ICES C.M. 1984/Gen:14, 15 pp.

Malmberg, S.-A. (1984). Hydrographic conditions in the East Icelandic Current and sea ice in North Icelandic waters, 1970-1980.Rapports et Procès-Verbaux des Réunions. *Conseil International pour l'Exploration de la Mer*, *185*, 170–178.

Malmberg, S.-A. (1985). The water masses between Iceland and Greenland. *Rit Fiskideildar*, *9*, 127–140.

Malmberg, S.-A. (1986). The ecological impact of the East Greenland Current on the North Icelandic waters. In S. Skreslet (Ed.), *The Role of Freshwater Outflow in Coastal Marine Ecosystems*. Springer-Verlag, Berlin etc., pp. 389–404.

Malmberg, S.-A., & Blindheim, J. (1993). Climate, cod and capelin in northern waters. ICES Climate, Cod, and Capelin Symposium, No. 20, 20 pp.

Malmberg, S.-A., & Blindheim, J. (1994). Climate, cod, and capelin in northern waters. *ICES Marine Science Symposia*, *198*, 297–310.

Malmberg, S.-A., & Kristmannsson, S.S. (1992). Hydrographic conditions in Icelandic waters, 1980-1989. *ICES Marine Science Symposia*, *195*, 76–92.

Malmberg, S.-A., & Svansson, A. (1982). Variations in the physical marine environment in relation to climate. ICES C.M. 1982/Gen:4, 44 pp.

Malmberg, S.-A., Kristmannsson, S. S., & Buch, E. (1990). Greenland Sea Project in the western part of the Iceland Sea from Jan Mayen to the Denmark Strait. ICES C.M. 1990/C:27, 14 pp.

Malmberg, S.-A., Valdimarsson, H., & Mortensen, J. (1994). Long time series in Icelandic waters. ICES C.M. 1994/S:8, 17 pp.

Malmberg, S.-A., Valdimarsson, H., & Mortensen, J. (1996). Long time series in Icelandic waters in relation to physical variability in the northern North Atlantic. *NAFO Scientific Council Studies*, *24*, 69–80.

Marko, J.R., Fissel, D.B., Wadhams, P., Kelly, P.M., & Brown, R.D. (1994). Iceberg severity off Eastern North America: Its relationship to sea ice variability and climate change. *Journal of Climate*, *7*(9), 1335–1351.

Marsden, R.F., Mysak, L.A., & Myers, R.A. (1991). Evidence for stability enhancement of sea ice in the Greenland and Labrador Seas. *Journal of Geophysical Research*, *96*(C3), 4783–4789.

Martin, J. H. A. (1976). Long-term changes in the Faroe-Shetland Channel associated with intrusions of Iceland-Faroe Ridge water during the period 1955–1975. ICES C.M.1976/C:22, 11 pp.

Martin, J.H.A. (1993). Norwegian Sea intermediate water in the Faroe-Shetland Channel. *ICES Journal of Marine Science*, *50*(2), 195–201.

Martin, J. H. A., Dooley, H. D., & Shearer, W. (1984). Ideas on the origin and biological consequences of the 1970's salinity anomaly. ICES C.M. 1984/Gen:18.

Meincke, J. (1986). Convection in the oceanic waters west of Britain. *Proceedings of the Royal Society of Edinburgh*, *88B*, 127–139.

Mertz, G., & Myers, R.A. (1994). The ecological impact of the Great Salinity Anomaly in the northern North-west Atlantic. *Fisheries Oceanography*, *3*(1), 1–14.

Mertz, G., Narayanan, S., & Helbig, J. (1993). The freshwater transport of the Labrador Current. *Atmosphere-Ocean*, *31*(2), 281–295.

Molinari, R.L., Mayer, D.A., Festa, J.F., & Bezdek, H.F. (1997). Multiyear variability in the near-surface temperature structure of the midlatitude western North Atlantic Ocean. *Journal of Geophysical Research*, *102*(C2), 3267–3278.

Myers, R. A., Akenhead, S. A., & Drinkwater, K. F. (1988). The North Atlantic Oscillation and the ocean climate of the Newfoundland Shelf, NAFO SCR Doc. 88/65, 22 pp.

Myers, R.A., Akenhead, S.A., & Drinkwater, K. (1990). The influence of Hudson Bay runoff and ice-melt on the salinity of the inner Newfoundland Shelf. *Atmosphere-Ocean*, *28*(2), 241–256.

Myers, R. A., Helbig, J., & Holland, D. (1989). Seasonal and interannual variability of the Labrador Current and West Greenland Current. ICES C.M. 1989/C:16, 10 pp.

Myers, R. A., Mertz, G., & Helbig, J. A. (1990b). Long period changes in the salinity of Labrador Sea Water. ICES C.M. 1990/C:21, 8 pp.

Mysak, L. A. (1995). Interdecadal climate variability at northern high latitudes: Observations and models.

Universite Catholique de Louvain, Institut d'Astronomie et de Geophysique Georges Lemaitre, Contribution No. 78, 24 pp.

Mysak, L.A., & Manak, D.K. (1989). Arctic sea-ice extent and anomalies, 1953-1984. *Atmosphere-Ocean*, *27*(2), 376–405.

Mysak, L.A., & Power, S.B. (1991). Greenland sea ice and salinity anomalies and interdecadal climate variability. *Climatological Bulletin*, *25*(2), 81–91.

Mysak, L.A., & Power, S.B. (1992). Sea-ice anomalies in the western Arctic and Greenland-Iceland Sea and their relation to an interdecadal climate cycle. *Climatological Bulletin*, *26*(3), 147–176.

Mysak, L.A., Manak, D.K., & Marsden, R.F. (1990). Sea-ice anomalies observed in the Greenland and Labrador Seas during 1901-1984 and their relation to an interdecadal Arctic climate cycle. *Climate Dynamics*, *5*(2), 111–133.

Mysak, L.A., Ingram, R.G., Wang, J., & Van Der Baaren, A. (1996). The anomalous sea-ice extent in Hudson Bay, Baffin Bay and the Labrador Sea during three simultaneous NAO and ENSO episodes. *Atmosphere-Ocean*, *34*(2), 313–343.

Narayanan, S., Prinsenberg, S., & Smith, P.C. (1996). Current meter observations from the Labrador and Newfoundland shelves and comparisons with barotropic model predictions and IIP surface currents. *Atmosphere-Ocean*, *34*(1), 227–255.

Otto, L., & Van Aken, H.M. (1996). Surface circulation in the northeast Atlantic as observed with drifters. *Deep-Sea Research*, *43*(4), 467–499.

Otto, L., Zimmerman, J.T.F., Furnes, G.K., Mork, M., Saetre, R., & Becker, G. (1990). Review of the physical oceanography of the North Sea. *Netherlands Journal of Sea Research*, *26*(2–4), 161–238.

Parkinson, C.L., & Cavalieri, D.J. (1989). Arctic sea ice 1973-1987: Seasonal, regional, and interannual variability. *Journal of Geophysical Research*, *94*(C10), 14499–14523.

Petrie, B., & Buckley, J. (1996). Volume and freshwater transport of the Labrador Current in Flemish Pass. *Journal of Geophysical Research*, *101*(C12), 28335–28342.

Petrie, B., Loder, J.W., Lazier, J., & Akenhead, S. (1992). Temperature and salinity variability on the eastern Newfoundland Shelf: The residual field. *Atmosphere-Ocean*, *30*(1), 120–139.

Pollard, R.T., & Pu, S. (1985). Structure and circulation of the upper Atlantic Ocean northeast of the Azores. *Progress in Oceanography*, *14*(1–4), 443–462.

Pollard, R.T., Griffiths, M.J., Cunningham, S.A., Read, J.F., Perez, F.F., & Rios, A.F. (1996). Vivaldi 1991-A study of the formation, circulation and ventilation of Eastern North Atlantic Central Water. *Progress in Oceanography*, *37*(2), 167–192.

Power, S.B., & Mysak, L.A. (1992). On the interannual variability of Arctic sea-level pressure and sea ice. *Atmosphere-Ocean*, *30*(4), 551–577.

Prinsenberg, S.J., Peterson, I.K., Narayanan, S., & Umoh, J.U. (1997). Interaction between atmosphere, ice cover, and ocean off Labrador and Newfoundland from 1962 to 1992. *Canadian Journal of Fisheries and Aquatic Sciences*, *54*(Suppl.1), 30–39.

Read, J.F., & Gould, W.J. (1992). Cooling and freshening of the subpolar North Atlantic Ocean since the 1960s. *Nature*, *360*(6399), 55–57.

Reverdin, G., Cayan, D., & Kushnir, Y. (1997). Decadal variability of hydrography in the upper northern North Atlantic in 1948-1990. *Journal of Geophysical Research*, *102*(C4), 8505–8531.

Reverdin, G., Cayan, D., Dooley, H.D., Ellett, D.J., Levitus, S., Du Penhoat, Y., & Dessier, A. (1994). Surface salinity of the North Atlantic: Can we reconstruct its fluctuations over the last one hundred years? *Progress in Oceanography*, *33*(4), 303–346.

Reynaud, T.H., Weaver, A.J., & Greatbatch, R.J. (1995). Summer mean circulation of the northwestern Atlantic Ocean. *Journal of Geophysical Research*, *100*(C1), 779–816.

Ross, C. K. (1992). Moored current meter measurements across Davis Strait. NAFO SCR Doc. 92/70, 20 pp.

Rudels, B. (1986). The outflow of polar water through the Arctic Archipelago and the oceanographic conditions in Baffin Bay. *Polar Research*, *4*(2), 161–180.

Rudels, B. (1995). The thermohaline circulation of the Arctic Ocean and the Greenland Sea. *Phil. Trans. R. Soc. Lond. A*, *352*, 287–299.

Serreze, M.C., Maslanik, J.A., Barry, R.G., & Demaria, T.L. (1992). Winter atmospheric circulation in the

Arctic Basin and possible relationships to the Great Salinity Anomaly in the northern North Atlantic. *Geophysical Research Letter*, *19*(3), 293–296.
Simonsen, K., & Haugan, P.M. (1996). Heat budget of the Arctic Mediterranean and sea surface heat flux parameterizations for the Nordic Seas. *Journal of Geophysical Research*, *101*(C3), 6553–6576.
Steele, M., Thomas, D., Rothrock, D., & Martin, S. (1996). A simple model study of the Arctic Ocean freshwater balance. *Journal of Geophysical Research*, *101*(C9), 20833–20848.
Stein, M. (1988). List of NAFO standard oceanographic sections and stations. NAFO SCR Doc. 88/01, Ser. No. N1432, 13 pp.
Stein, M. (1995). Climatic conditions around Greenland-1992. *NAFO Scientific Council Studies*, *22*, 33–41.
Stein, M. (1995). Climatic conditions around Greenland-1993. *NAFO Scientific Council Studies*, *22*, 43–49.
Stein, M. (1996). Environmental overview of the Northern Atlantic area-with focus on Greenland. *NAFO Scientific Council Studies*, *24*, 29–39.
Stein, M. (1996b). Climatic conditions around Greenland-1995. NAFO SCR Doc. 96/15, 15 pp.
Svendsen, E., & Danielssen, D. (1995). Volume and nutrient transports in the northern North Sea and climate variability in the Skagerrak. NOWESP 2nd Annual Report, pp. 201–210.
Svendsen, E., & Magnusson, A.K. (1992). Climatic variability in the North Sea. *ICES Marine Science Symposia*, *195*, 144–158.
Svendsen, E., Aglen, A., Iversen, S. A., Skagen, D. W., & Smestad, O. (1995). Influence of climate on recruitment and migration of fish stocks in the North Sea. In R. J. Beamish (Ed.), Climate Change and Northern Fish Populations. Canadian Special Publication of Fisheries and Aquatic Sciences, *121*, pp. 641–653.
Tang, C.C.L., Gui, Q., & Peterson, I.K. (1996). Modeling the mean circulation of the Labrador Sea and the adjacent shelves. *Journal of Physical Oceanography*, *26*(10), 1989–2010.
Taylor, A.H. (1983). Fluctuations in the surface temperature and surface salinity of the North-East Atlantic at frequencies of one cycle per year and below. *Journal of Climatology*, *3*(3), 253–269.
Taylor, A.H. (1995). North-South shifts of the Gulf Stream and their climatic connection with the abundance of zooplankton in the UK and its surrounding seas. *ICES Journal of Marine Science*, *52*(3–4), 711–721.
Taylor, A.H., & Stephens, J.A. (1980). Seasonal and year-to-year variations in surface salinity at the nine North Atlantic Ocean Weather Stations. *Oceanologica Acta*, *3*(4), 421–430.
Thomas, D., Martin, S., Rothrock, D., & Steele, M. (1996). Assimilating satellite concentration data into an Arctic sea ice mass balance model, 1979-1985. *Journal of Geophysical Research*, *101*(C9), 20849–20868.
Trites, R.W. (1982). Overview of oceanographic conditions in NAFO Subareas 2, 3 and 4 during the 1970-79 decade. *NAFO Scientific Council Studies*, *5*, 51–78.
Trites, R.W., & Drinkwater, K.F. (1990). Overview of environmental conditions in the Northwest Atlantic in 1988. *NAFO Scientific Council Studies*, *14*, 7–20.
Trivers, G. (1994). International Ice Patrol's iceberg season severity. Report of the International Ice Patrol in the North Atlantic, Bulletin No. 80, Appendix C, 49–59. U.S. Coast Guard CG-188-49.
Turrell, W.R. (1992). The East Shetland Atlantic Inflow. *ICES Marine Science Symposia*, *195*, 127–143.
Turrell, W.R. (1992). New hypotheses concerning the circulation of the northern North Sea and its relation to North Sea fish stock recruitment. *ICES Journal of Marine Science*, *49*(1), 107–123.
Turrell, W.R. (1995). A century of hydrographic observations in the Faroe-Shetland Channel. *Ocean Challenge*, *6*(1), 58–63.
Turrell, W. R., & Shelton, R. G. J. (1993). Climatic change in the north-eastern Atlantic and its impacts on the salmon stocks. In D. Mills (Ed), *Salmon at Sea and New Enhancement Strategies*, *1*. Blackwell Scientific, Oxford, pp. 40–78.
Turrell, W.R., Slesser, G., Payne, R., Adams, R.D., & Gillibrand, P.A. (1996). Hydrography of the East Shetland Basin in relation to decadal North Sea variability. *ICES Journal of Marine Science*, *53*(6), 899–916.
Umoh, J.U., Loder, J.W., & Petrie, B. (1995). The role of air-sea fluxes in annual and interannual ocean temperature variability on the eastern Newfoundland Shelf. *Atmosphere-Ocean*, *33*(3), 531–568.

Walsh, J.E., & Chapman, W.L. (1990). Arctic contribution to upper-ocean variability in the North Atlantic. *Journal of Climate*, *3*(12), 1462–1473.

Walsh, J.E., Zhou, X., Portis, D., & Serreze, M.C. (1994). Atmospheric contribution to hydrologic variations in the Arctic. *Atmosphere-Ocean*, *32*(4), 733–755.

Walsh, M., & Martin, J. H. A. (1986). Recent changes in distribution and migration of the western mackerel stock in relation to hydrographic changes. ICES C.M. 1986/H:17.

Wang, J., Mysak, L.A., & Ingram, R.G. (1994). Interannual variability of sea-ice cover in Hudson Bay, Baffin Bay and the Labrador Sea. *Atmosphere-Ocean*, *32*(2), 421–447.

Weaver, A. J. (1995). Decadal-to-millennial internal oceanic variability in coarse-resolution ocean general-circulation models. In D. G. Martinson, K. Bryan, M. Ghil, M. M. Hall, T. M. Karl, E. S. Sarachik, S. Sorooshian, & L. D. Talley (Eds.), Natural Climate Variability on Decade-to-Century Time Scales. National Academy Press, Washington, D.C., pp. 365–381.

Weaver, A.J., & Hughes, T.M.C. (1992). Stability and variability of the termohaline circulation and its link to climate. *Trends in Physical Oceanography*, *1*, 15–70.

Weaver, A.J., & Sarachik, E.S. (1991). Evidence for decadal variability in an ocean general circulation model: An advective mechanism. *Atmosphere-Ocean*, *29*(2), 197–231.

Weaver, A.J., Aura, S.M., & Myers, P.G. (1994). Interdecadal variability in an idealized model of the North Atlantic. *Journal of Geophysical Research*, *99*(C6), 12423–12441.

Weisse, R., Mikolajewicz, U., & Maier-Reimer, E. (1994). Decadal variability of the North Atlantic in an ocean general circulation model. *Journal of Geophysical Research*, *99*(C6), 12411–12421.

Wohlleben, T.M.H., & Weaver, A.J. (1995). Interdecadal climate variability in the subpolar North Atlantic. *Climate Dynamics*, *11*(8), 459–467.

Worthington, L. V. (1976). On the North Atlantic circulation, The Johns Hopkins University Press, Baltimore and London, 110 pp.

Yang, J., & Neelin, J.D. (1993). Sea ice interactions with thermohaline circulation. *Geophysical Research Letters*, *20*(2), 217–220.

Yashayaev, I. M. (1995). Annual and interannual variability of temperature and salinity in the Newfoundland Basin. In: The Abstracts of the XXI General Assembly of the IAPSO, August 5–12, 1995, Honolulu, HA, p.51.

Yashayaev, I. M. (1997). Computer atlas of the Newfoundland Basin and the Labrador Sea. In: The Abstracts of the Fifth Scientific Meeting of The Oceanography Society, April 1–4, 1997, Seattle, WA, p.36.

Zhang, S., Lin, C.A., & Greatbatch, R.J. (1995). A decadal oscillation in an ocean model coupled with a thermodynamic sea ice mode. *Journal of Marine Research*, *53*(1), 79–106.